

N71-14759



THE PENNSYLVANIA
STATE UNIVERSITY

IONOSPHERIC RESEARCH

Scientific Report No. 355

ON THE CONSTRUCTION AND USE OF THE
PENN STATE MKI IONOSPHERIC MODEL

by

J. S. Nisbet

May 1, 1970

IONOSPHERE RESEARCH LABORATORY



CASE FILE
COPY

University Park, Pennsylvania NASA Grant NGL 39-009-003

Ionospheric Research

NASA Grant NGL 39-009-003

Scientific Report

"On the Construction and Use of the
Penn State MK1 Ionospheric Model"

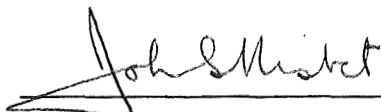
by

J. S. Nisbet

May 1, 1970

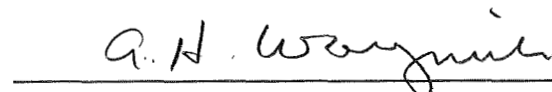
Scientific Report No. 355

Submitted by:



John S. Nisbet, Professor of Electrical Engineering
Project Supervisor

Approved by:



A. H. Waynick, Director
Ionosphere Research Laboratory

Ionosphere Research Laboratory
The Pennsylvania State University
University Park, Pennsylvania

ABSTRACT

The parameters controlling the development of a simple model of the E and F regions of the ionosphere are discussed. Uses of such models in scientific investigations and engineering applications are given.

A computer model is described which will provide estimates of the electron and ion densities in middle latitudes as a function of latitude, longitude, altitude, season, time and solar activity. Statistical parameters for mid latitude blanketing sporadic E are presented. An analytic expression is used for the CIRA 1965 neutral atmospheric models. The F_1 region is treated using a photoequilibrium model with three ionic constituents and 62 ionizing radiation groups. The F_2 layer uses theoretical models arranged to fit boundary conditions of $N_m F_2$, $H_m F_2$ and the electron density at 1000 km. Values of $N_m F_2$ are obtained using the CCIR Report 340 atlas of ionospheric characteristics. The mid-latitude sporadic E layer is treated by presenting three parameters of the layer, the probability of observing sporadic E with a blanketing frequency greater than 0.5 MHz, the average peak electron density when sporadic E is observed and the standard deviation assuming log normal distributions for the peak electron density.

The restrictions on the model and the availability of data on suitable boundary conditions are discussed. Suggestions for further development of models of the ionosphere are given.

ACKNOWLEDGMENTS

This work was supported by NASA under grant NGL 39-009-003. A major portion of the initial comparison of the theoretical model with observations was done using data from the Arecibo Observatory. The Arecibo Observatory is operated by Cornell University with the support of the Advanced Research Projects Agency and the National Science Foundation under contract with the Air Force Office of Scientific Research.

The computer programming was under the direction of Mr. R. Divany. The author is grateful for valuable suggestions from Dr. K. Rawer, Dr. S. A. Bowhill, and other members of COSPAR Working Group IV panel 4B on the International Reference Ionosphere.

TABLE OF CONTENTS

Abstract	i
Acknowledgements	II
List of Figures	IV
1. INTRODUCTION	1
2. THE NEUTRAL ATMOSPHERIC MODELS.	3
3. SOLAR FLUX AND ABSORPTION	8
4. REACTIONS AND REACTION RATES	15
5. MODEL FOR THE UPPER F REGION	17
5.1 Electron density at the F2 peak	18
5.2 Altitude of the F2 peak	19
5.3 The electron temperature at the peak	27
5.4 Model for the upper F-region	35
5.5 Nighttime F region	36
6. MODELS FOR THE MIDLATITUDE SPORADIC E	40
7. COMPARISONS OF THE MODEL WITH DATA	46
Conclusions	68
References	71
Appendix - Fortran Program	76

LIST OF FIGURES

	Page
Fig. 1: Comparison of CIRA with P.S. U. Mkl neutral atmospheric densities	7
Fig. 2: World map of $\sin x$	22
Fig. 3: Model values of $H_m F_2$ summer solstice $\bar{S}_{10.7}=100$	28
Fig. 4: Model values of $H_m F_2$ winter solstice $\bar{S}_{10.7}=100$	29
Fig. 5: Model values of $H_m F_2$ equinox $\bar{S}_{10.7}=100$	30
Fig. 6: Model values of $H_m F_2$ equinox $\bar{S}_{10.7}=200$	31
Fig. 7: Model of average energy \bar{E} per photoelectron given to ambient electrons	33
Fig. 8: Local noon model boundary conditions at 1000 Km	37
Fig. 9: Local midnight model boundary conditions at 1000 Km	38
Fig. 10: Six month average mid-winter and mid-summer probability of sporadic E with $f_b E_s > 0.5\text{MHz}$, $\bar{S}_{10.7}=100$	44
Fig. 11: Electron densities for Grand Bahama Island, March 1959, $\bar{S}_{10.7} = 220$	47
Fig. 12: Electron densities for St. Johns, Newfoundland, March 1959, $\bar{S}_{10.7} = 220$	48
Fig. 13: Electron densities for Grand Bahama Island, March 1961, $\bar{S}_{10.7} = 103$	49
Fig. 14: Electron densities for St. Johns, Newfoundland, March 1961, $\bar{S}_{10.7} = 103$	50
Fig. 15: Electron densities for Grand Bahama Island, December 1960, $\bar{S}_{10.7} = 141$	52

- Fig. 16: Electron densities for St. Johns, Newfoundland, May 1960,
 $\bar{S}_{10.7} = 161$ 53
- Fig. 17: Electron densities for St. Johns, Newfoundland, November
 1960, $\bar{S}_{10.7} = 146$ 54
- Fig. 18: Electron densities for Grand Bahama Island, December 1960,
 $\bar{S}_{10.7} = 141$ 55
- Fig. 19: Comparison of Arecibo data with two models for F2 region
 peak electron density 56
- Fig. 20: Plasma frequency Millstone Hill, July 1964, $\bar{S}_{10.7} = 68$. . . 59
- Fig. 21: Plasma frequency Millstone Hill, November 1964, $\bar{S}_{10.7} =$
 73 60
- Fig. 22: Plasma frequency, Nancay, March 12, 1967, $\bar{S}_{10.7} =$
 135.9 61
- Fig. 23: Plasma frequency, Arecibo Observatory, June 26,
 1968, $S_{10.7} = 141.40$ 62
- Fig. 24: Plasma frequency, Arecibo Observatory, December 14,
 1968, $S_{10.7} = 135.7/138.6$ 63
- Fig. 25: Six month running average of $f_b E_s$ during 1958-1965; d
 indicates December of each year 65
- Fig. 26: Six month running averages of P1, P2, P3, P4, P5, and
 P6 during 1958-1965; curves refer to the average P values
 in the post-midnight period of 01-04 hours. In the observed
 data P1 curve for Port Stanley is not shown because it is
 not reliable. 66
- Fig. 27: Six month running averages of P1, P2, P3, P4, P5 and P6
 (top to bottom in that order) during 1958-1965); curves refer
 to the average P values in the afternoon 13-16 hours 67

1. Introduction

A sufficiently complete and accurate model of the ionosphere would appear to have many applications. While our understanding of all the processes involved is still far from complete and the complexities of a program incorporating all those effects that are understood to be important would tax the largest computer, it would appear that at least a start at the development of a simplified model could be made that would be of use for many applications. The Penn State Mk I Ionospheric Model is an initial attempt along these lines. It is intended to be used to determine the feasibility of models of this type and to investigate what additional parameters are required for a more precise formulation.

One of the main uses of a model would be in theoretical analysis. Frequently in the calculation of an effect such as, for example, the transport of photoelectrons from a conjugate region, it is necessary to assume a model of the electron density in that region. It is often quite difficult to find the data on which a suitable model can be based, especially if, as is common, the region is not located close to a station at which routine ionospheric measurements are made. Such analysis may require the profiles at a given point or as in, for example, studies of the damping of neutral atmospheric winds, the density distributions over large geographical areas. In planning observations or experiments, it is frequently important or convenient to have an estimate of what the range of ionospheric conditions is likely to be some time in the future to ensure that instrument ranges are optimal or adequate. In the comparison of observations from different locations and different times, it is often important to be able to distinguish effects due to altitude, location or time.

The above applications can be satisfied with a comparatively simple ionospheric model. Variations from day to day are quite large in the F_2 region on days that appear similar on a basis of solar or magnetic activity as has been shown for example by Doupnik and Nisbet (1968) so that minor variations from the average profile are likely to be less than variations from day to day.

A much greater level of sophistication is required in a model designed to be used to study the theoretical behavior of the F region itself. Such models of the global morphology of the region would be of great value in separating true anomalies i.e. differences between actual behavior and theoretical predictions and effects produced by well understood mechanisms such as the variations in solar zenith angle or less well understood effects such as electric fields or neutral air motions. Relatively simple models may still be of considerable use if care is taken in their application. It has been shown, for example, that the altitude of the peak is, as would be expected from theoretical analysis quite well correlated with the ion velocities. Good global models of $N_m F_2$ and $H_m F_2$ could be of considerable use in sorting out the effects of transport on the F region for comparison with theoretical models based on electric field systems and neutral winds.

Once ionospheric models have been developed and verified they should be of considerable use in making predictions of propagation conditions for radio transmission for the more sophisticated applications in which a complete profile is required such as mode studies and for the estimation of refractive corrections in tracking navigational satellites.

2. The neutral atmospheric models

There is a considerable advantage in using a standard model such as the CIRA 1965 atmospheric models as a basis for the production and loss calculations. These models, unfortunately, are in tabular form and it was decided that the problems of storage and interpolating would be large while the computer time necessary to develop them from the defining equations would be prohibitive. Stein and Walker (1965) showed that the densities in the upper atmosphere could be fitted quite accurately using a rather simple temperature function due to Bates (1959).

$$T(z) = T_{\infty} - (T_{\infty} - T_0) \exp(-\tau z)$$

Where z is the geopotential altitude.

T_{∞} is the exospheric temperature.

T_0 is the temperature at the lower boundary.

and τ is a variable which controls the temperature gradient at the lower boundary.

Once the temperature profile and the densities at the lower boundary are determined and it is assumed that each constituent is in diffusion equilibrium, the densities of each of the constituents as a function of altitude may be calculated. The density of the i th constituents n_i is given by

$$n_i(z) = n_i(z=0) \left[\frac{T_{\infty}}{T_0} (\exp \tau z - 1) + 1 \right]^{-(1 + \gamma_i)} \exp(\tau z)$$

Where $\gamma_i = \frac{m_i g_0}{\tau k T_{\infty}}$

m_i is the mass of the i th constituent

g_0 is the acceleration due to gravity at 120 km

k is the Boltzman's constant

In the MK 1 model, the following relation has been employed

$$T_0 = 355K$$

$$T_\infty = \sum_0^5 C_n \cos \frac{2\pi n H_L}{24} + \sum_1^5 S_n \sin \frac{2\pi n H_L}{24}$$

$$\tau = \sum_0^5 A_n \cos \frac{2\pi n H_L}{24} + \sum_1^5 B_n \sin \frac{2\pi n H_L}{24}$$

where values for the coefficients are as given in Table 1 as functions of F . The CIRA (1965) models can be reproduced using for F the values of 10.7 cm flux associated with the CIRA tables.

To allow for the semi-annual variation the following relation is used in the Penn State Mark I model program

$$F = \bar{S} \left[1 + (.115 + .0411 \sin (2\pi \frac{D-172}{365})) \sin (4\pi \frac{D-80}{365}) - .0882 \right]$$

where \bar{S} is the estimated average unadjusted 2800 MHz solar flux in units of $10^{-22} \text{ W m}^{-2} \text{ Hz}^{-1}$.

TABLE 1

Coefficients for the Neutral Density Model

A0 =	2.210156E - 02 - 1.970030E - 05*F	C0 =	5.443538E + 02 + 4.328897E + 00*F
A1 =	6.712358E - 03 - 1.181107E - 05*F	C1 =	-1.179819E + 02 - 6.495360E - 01*F
A2 =	2.748180E - 04 + 3.390522E - 07*F	C2 =	3.115091E + 01 - 4.766818E - 02*F
A3 =	-5.663477E - 04 + 8.669016E - 07*F	C3 =	4.069323E + 00 + 4.154682E - 02*F
A4 =	-4.652258E - 05 + 2.322930E - 07*F	C4 =	-6.389061E + 00 + 1.415760E - 02*F
A5 =	8.984354E - 05 - 1.128157E - 07*F	C5 =	1.045482E + 00 - 1.995652E - 02*F
B1 =	-3.407398E - 03 + 1.900959E - 05*F	S1 =	-1.138663E + 01 - 7.298749E - 01*F
B2 =	-5.428597E - 04 + 4.101313E - 06*F	S2 =	1.359668E + 01 + 2.815729E - 03*F
B3 =	-2.518983E - 04 - 5.341112E - 07*F	S3 =	9.859158E - 01 + 8.138881E - 02*F
B4 =	-1.380845E - 04 + 2.075324E - 07*F	S4 =	7.061132E - 01 - 1.151708E - 02*F
B5 =	1.358994E - 04 + 3.931811E - 07*F	S5 =	-2.925315E - 01 - 4.625236E - 02*F

The boundary conditions at 120 km are those of CIRA (1965)

$$n(\text{N}_2) \text{ 120 km} = 4.0 \times 10^{11} \text{ cm}^{-3}$$

$$n(\text{O}_2) \text{ 120 km} = 7.5 \times 10^{10} \text{ cm}^{-3}$$

$$n(\text{O}) \text{ 120 km} = 7.6 \times 10^{10} \text{ cm}^{-3}$$

Figure 1 shows the atomic oxygen and molecular nitrogen densities given by the MK1 model compared with those from the CIRA (1965) model for 4 hours and 14 hours with a 2800 MHz solar flux of $150 \times 10^{-22} \text{ W m}^{-2} \text{ Hz}^{-1}$ corresponding to $F = 150$.

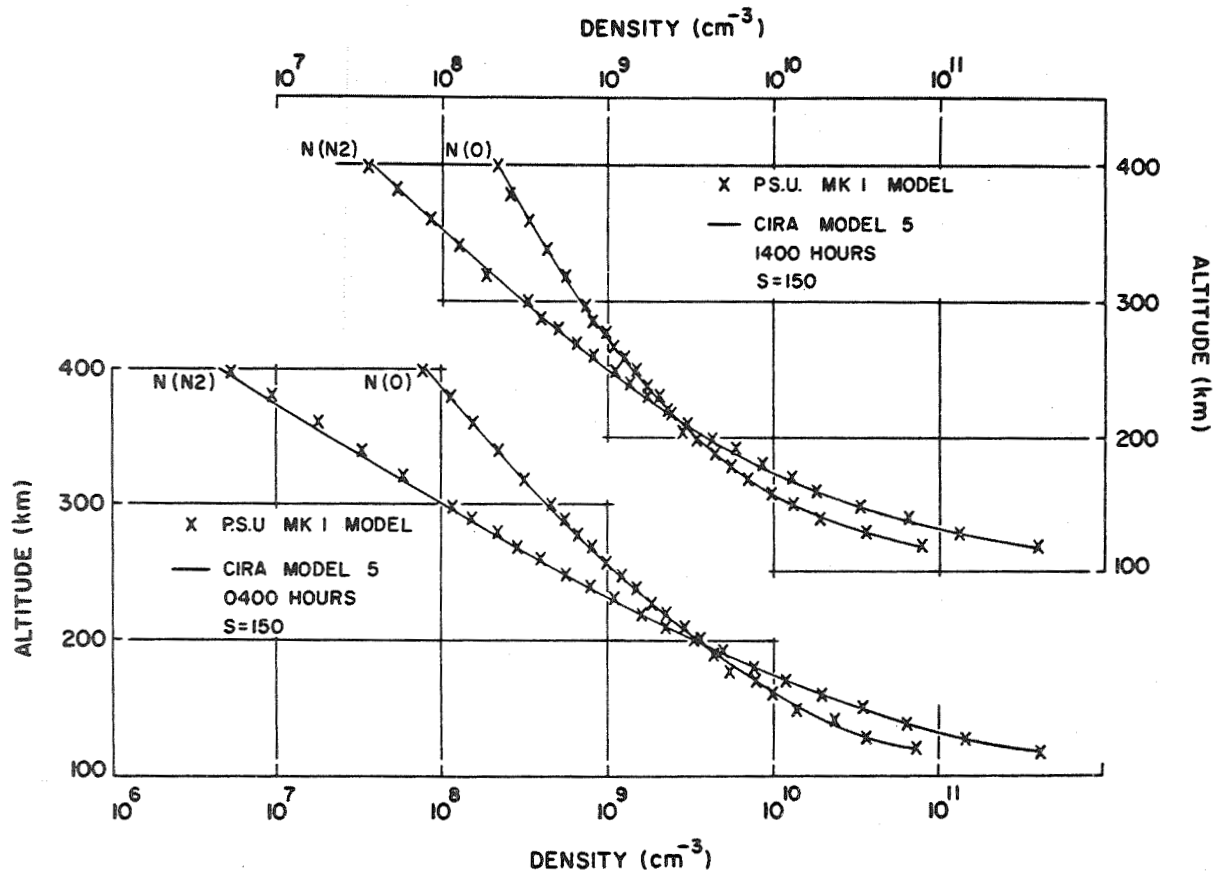


Figure 1 Comparison of CIRA with P.S. U. Mk 1 neutral atmospheric densities.

3. Solar flux and absorption model

The neutral atmosphere sub-program calculates the densities of the neutral N₂, O₂ and O and the neutral temperature at each altitude. The column content CN of a species is given to a good approximation at all times by the product of the local scale height and the local number density. In the present program it is assumed that the column content along the solar direction is given by the product of the neutral column content and the secant of the solar zenith angle. This is a decreasingly accurate approximation as the zenith angle approaches 90°, however, it was concluded that with the present program which uses equilibrium ionospheric models the additional complexity of using more accurate methods of calculations such as those described by Swider (1964) was probably not justified.

The intensity of the radiation at each wavelength group and altitude is assumed to be given by

$$I_i(N) = I_{i\infty} \exp \left(- \sum_M CN_{MN} \sec \chi C_{Mi} \right)$$

where

$I_{i\infty}$ is the incident extraterrestrial flux of wavelength group i

$I_i(N)$ is the intensity of the wavelength group i at the altitude with index N

CN_{MN} is the vertical column content of neutral species M above altitude with index N

C_{Mi} is the absorption cross section of species M at wavelength group i

and χ is the local solar zenith angle.

where

$$\sec \chi = 1 / \left(\sin g \sin \delta + \cos g \cos \delta \cos \left(\frac{2\pi (HL - 12)}{24} \right) \right)$$

where

HL is the local solar time in decimal hours
g is the geographic latitude
 δ is the solar declination

In this program it has been assumed that

$$\delta = - .40915 \cos \frac{2\pi (D + 8)}{365.25}$$

where D is the day number.

The production of ions from species M at altitude index N is then given by

$$\text{PROD (M, N)} = \text{DEN(M, N)} \sum_i I_i (N) \text{CP(M, i)}$$

where

PROD (M, N) is the production of ions from species M
at altitude of index N
DEN (M, N) is the density of neutral species M
 $I_i (N)$ is the intensity of the i th radiation group
CP (M, i) is the ionization cross section for the neutral
species M for radiation group i

It is a comparatively simple matter to use any desired number of wavelength groups in a program of this type. The number of lines included controls to some extent the program storage requirements. In the present program it was decided to use the 62 relevant wavelength groups given by Hinteregger et al (1965). Modifications have been made to these data to take account of more recent measurements of Hinteregger (1967), Manson (1967, 1968) and of the variation with solar activity

based on Hall et al (1969). The values of solar flux and the absorption and ionization cross sections adopted are given in Table 2.

It should be noted that a reasonable representation of the ionospheric electron densities can be obtained with a much smaller number of wavelength groups. One solar flux program has been used which gives quite satisfactory agreement with the electron density data available with only six groups.

TABLE 2

Assumed Photon Fluxes and Absorption and Ionization Cross Sections

Wavelength $\overset{\circ}{\text{A}}$	Photon Flux cm^{-2}	Absorption Cross Sections 10^{-18} cm^2			Ionization Cross Sections 10^{-18} cm^2		
		O	O2	N ₂	O	O2	N ₂
1025.7	.310 \sqrt{S}	0.0	1.6	0.0	0.0	0.9	0.0
991.5	.0459 \sqrt{S}	0.0	1.9	1.40	0.0	0.76	0.0
1027-990	1.5	0.0	1.9	0.23	0.0	0.76	0.0
977.0	.459 \sqrt{S}	0.0	4.0	2.6	0.0	1.6	0.0
972.5	.0746 \sqrt{S}	0.0	40.0	250.0	0.0	18.0	0.0
990-950	0.6	0.0	8.25	1.65	0.0	4.15	0.0
949.7	.0402 \sqrt{S}	0.0	5.9	4.25	0.0	3.0	0.0
937.8	.0230 \sqrt{S}	0.0	5.2	5.35	0.0	2.9	0.0
950-920	0.7	0.0	7.0	3.4	0.0	4.2	0.0
920-911	0.8	0.0	7.4	3.8	0.0	4.8	0.0
911-890	4.0	4.7	9.3	4.35	4.7	7.9	0.0
890-860	3.8	4.9	8.9	4.95	4.9	6.2	0.0
860-840	1.8	5.0	11.7	4.95	5.0	5.3	0.0
832-835	0.65	5.3	13.5	11.1	5.3	5.4	0.0
840-810	1.6	5.3	26.0	3.35	5.3	9.1	0.0
810-796	0.7	6.1	40.0	6.75	6.1	14.0	0.0
790.1	.00474 S	6.1	33.0	28.0	6.1	13.4	14.0

TABLE 2
(cont'd)

787.7	.00369 S	6.1	28.0	9.7	6.1	11.2	4.9
780.3	.00211 S	11.0	33.0	13.8	11.0	16.8	7.6
796-780	0.5	6.1	28.0	26.0	6.1	13.9	14.3
770.4	.00422 S	8.5	20.0	13.8	8.5	10.2	8.3
765.1	.00303 S	8.5	25.0	71.0	8.5	13.9	49.0
780-760	0.6	8.5	22.0	24.0	8.5	11.2	14.5
760-740	0.4	8.5	22.0	25.0	8.5	13.0	17.7
740-732	0.15	14.5	41.0	25.0	14.5	29.0	17.4
703.8	.00264 S	13.0	33.0	26.0	13.0	23.0	23.0
732-700	0.35	14.0	35.0	22.0	14.0	25.0	20.0
700-665	0.7	14.0	27.0	27.0	14.0	22.0	24.0
665-630	.0402 \sqrt{S}	14.0	33.0	26.0	14.0	31.0	25.0
629.7-625	.138 \sqrt{S}	14.0	35.0	23.0	14.0	33.0	23.0
630-600	.0918 \sqrt{S}	14.0	39.0	22.0	14.0	37.0	22.0
584.3	.008 \sqrt{S}	13.0	29.0	23.0	13.0	28.0	21.0
600-580	.0287 \sqrt{S}	12.9	27.0	23.0	12.9	25.0	21.0
580-540	.0918 \sqrt{S}	13.0	30.0	26.0	13.0	26.0	22.0
540-510	.0574 \sqrt{S}	13.0	29.0	26.0	13.0	26.0	23.0
510-500	.0574 \sqrt{S}	13.0	28.0	25.0	13.0	25.0	22.0
500-480	.0689 \sqrt{S}	12.9	27.0	25.0	12.9	24.0	21.0

TABLE 2
(cont'd)

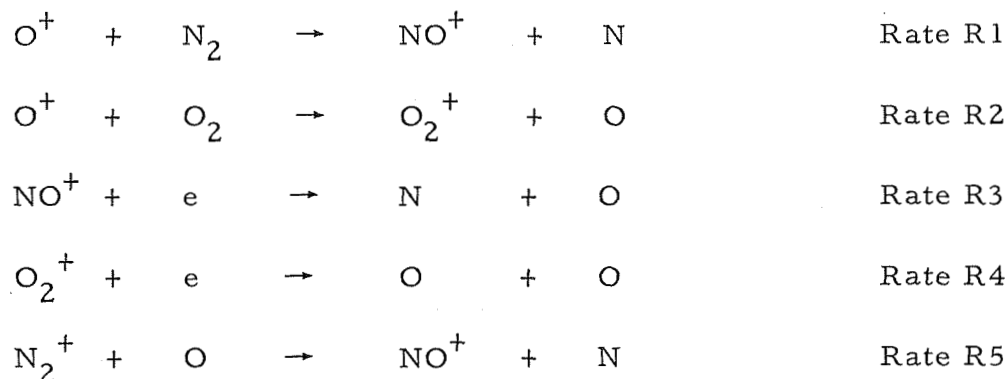
460-435	.0402 \sqrt{S}	10.5	25.0	22.0	10.5	23.0	19.8
435-400	.0689 \sqrt{S}	12.5	24.0	20.0	12.5	24.0	20.0
400-370	.0459 \sqrt{S}	11.1	23.0	18.5	11.1	23.0	18.5
368.1	.00527 \sqrt{S}	10.3	22.0	16.5	10.3	22.0	16.5
370-355	.0803 \sqrt{S}	10.0	22.0	16.5	10.0	22.0	16.5
355-340	.0689 \sqrt{S}	9.3	22.0	15.5	9.3	22.0	15.5
340-325	.0459 \sqrt{S}	8.7	21.0	14.6	8.7	21.0	14.6
325-310	.0459 \sqrt{S}	8.1	20.0	13.4	8.1	20.0	13.4
303.8	.459 \sqrt{S}	9.8	19.5	12.0	9.8	19.5	12.0
310-280	.0918 \sqrt{S}	9.2	18.7	12.0	9.2	18.7	12.0
280-260	8.68 x 10 ⁻⁵ S ²	8.0	16.0	10.7	8.0	16.0	10.7
257-256.3	5.21 x 10 ⁻⁵ S ²	7.2	14.4	9.8	7.2	14.4	9.8
260-240	6.94 x 10 ⁻⁵ S ²	6.7	13.4	9.7	6.7	13.4	9.7
240-220	6.94 x 10 ⁻⁵ S ²	5.6	11.2	8.3	5.6	11.2	8.3
220-205	5.21 x 10 ⁻⁵ S ²	4.7	9.4	7.2	4.7	9.4	7.2
205-190	2.78 x 10 ⁻⁴ S ²	4.0	8.0	6.0	4.0	8.0	6.0
190-180	3.82 x 10 ⁻⁴ S ²	3.4	6.8	4.7	3.4	6.8	4.7
180-165	5.55 x 10 ⁻⁴ S ²	2.9	5.7	3.9	2.9	5.7	3.9
165-138	6.94 x 10 ⁻⁵ S ²	2.1	4.2	2.8	2.1	4.2	2.8
138-103	1.08 x 10 ⁻⁵ S ²	1.1	2.2	1.75	1.1	2.2	1.75

TABLE 2
(cont'd)

103-83	$2.44 \times 10^{-5} S^2$	0.7	1.4	0.8	0.7	1.4	0.8
83-62	$2.44 \times 10^{-5} S^2$	0.4	0.8	0.6	0.4	0.8	0.6
62-41	$1.37 \times 10^{-5} S^2$	0.22	0.44	0.25	0.22	0.44	0.25
41-31	$4.57 \times 10^{-6} S^2$	0.1	0.2	0.07	0.1	0.2	0.07

4. Reactions and reaction rates

It will be assumed that the predominating reactions in the normal E and F regions are



Current rates for R5 are approximately two orders of magnitude larger than those for R1, Fite (1969). As the production rates for N_2^+ ions and O^+ ions and the neutral N_2 and O densities are comparable it will be assumed that reaction rate R5 is sufficiently large that the N_2^+ ion density can be neglected and the NO^+ production rate increased by the rate of ionization of N_2 .

With these assumptions it can be shown that under photoequilibrium conditions when transport is neglected

$$\begin{aligned}
 n(\text{O}^+) &= \frac{\text{PROD}(\text{O})}{\text{R1 } n(\text{N}_2) + \text{R2 } n(\text{O}_2)} \\
 N_e &= \frac{1}{2} \left\{ n(\text{O}^+) + \left[n(\text{O}^+)^2 + 4 \left(\frac{n(\text{O}^+) \text{R1 } n(\text{N}_2) + \text{PROD}(\text{N}_2)}{\text{R3}} \right. \right. \right. \\
 &\quad \left. \left. \left. + \frac{n(\text{O}^+) \text{R2 } n(\text{O}_2) + \text{PROD}(\text{O}_2)}{\text{R4}} \right) \right] \right\}^{1/2} \\
 n(\text{NO}^+) &= \frac{\text{R1 } n(\text{N}_2) N(\text{O}^+) + \text{PROD}(\text{N}_2)}{N_e \text{R3}}
 \end{aligned}$$

$$N(O_2^+) = \frac{R2 \ n(O_2) \ n(O^+) + \text{PROD}(O_2)}{N_e \ R4}$$

Rates for the dissociative recombination of NO^+ have been taken from Weller and Biondi (1968) as

$$R3(z) = \frac{1.44 \times 10^{-4}}{T(z)} \quad \text{cm}^3 \text{sec}^{-1},$$

and for O_2^+ from Kasner and Biondi (1967) as

$$R4(z) = \frac{6.6 \times 10^{-5}}{T(z)} \quad \text{cm}^3 \text{sec}^{-1},$$

It should, however, be borne in mind that these reaction rates are for equal electron and neutral temperatures and that they may be in error in the upper F1 region where the electron temperature may be much larger than the neutral temperature.

Fite (1969) has summarized positive reaction rates including those for the atomic oxygen ion charge exchange reactions with N_2 and O_2 . He gives the following values

$$\begin{aligned} R1 &= 2 \pm 1 \times 10^{-12} \quad \text{cm}^3 \text{sec}^{-1}, \\ R2 &= 2 \pm 1 \times 10^{-11} \quad \text{cm}^3 \text{sec}^{-1}, \end{aligned}$$

As discussed previously it was decided for the sake of simplicity to base the current model on static calculations for the electron density and to take account of dynamic effects and motions produced by winds and electric fields by specifying as boundary values the peak altitude for the F2 region. When this is done with a static model of the type chosen only the ratio of $R1$ and $R2$ remains to be specified. For the current model it was assumed that $R2$ was ten times $R1$ and $R1$ was found from the solution of the F region continuity equation under equilibrium conditions as discussed by Nisbet (1963).

5. Model for the upper F region

In the F region up to an altitude of about 180 km it may be reasonable to assume that the electron density is primarily controlled by the local production and loss of ionization. It may also be assumed that the time constants involved are sufficiently short that the assumption of photoequilibrium is unlikely to greatly increase the percentage error in a model with a 1 hour resolution given the existing knowledge of the solar flux, cross sections and neutral densities. Above 180 km this approximation becomes increasingly inaccurate until about two scale heights above the maximum the profile is almost entirely controlled by diffusion and gravity. In this intervening region around the peak electron density the following effects are important

1. Production and recombination
2. Diffusion
3. Electric fields
4. Neutral wind motions
5. Time dependence terms in the continuity equation
6. The electron, ion and neutral temperatures

The situation is further complicated by the coupling which exists between the equations controlling the electron densities and the electron and ion temperatures. It will be desirable in the future to develop models consistent with all the above parameters. It did not seem possible at the present time to specify the electric fields or neutral wind system sufficiently accurately to make a useful ionospheric model and the advantages in simplicity and computing time in using an equilibrium rather than a dynamic model are very great. It was therefore decided to use a static model but to set as boundary conditions empirical data on the altitude and electron density at the F2 maximum.

The models adopted are those of Nisbet (1963). These express the equilibrium solutions of the F region continuity equation in terms of exponential series. Account is taken of the attenuation of the ionizing radiation by absorption, a scale height for the ionic species different from that for the neutral gases controlling the diffusion and the molecular species controlling the recombination, and a non-divergent vertical flux of ions. Matching the empirical model peak altitudes and densities is accomplished by adjusting the assumed reaction rates R1 and R2 and the vertical flux.

5.1 Electron density at the F2 peak

The C. C. I. R. Atlas of Ionospheric Characteristics, C. C. I. R. (1967) includes the coefficients of the numerical mapping functions for the F2 layer critical frequency $f_o F_2$ at two levels of solar activity corresponding to twelve month smoothed mean values of the Zurich monthly sunspot numbers of 0 and 100 for each month of the year. These data are based on vertical incidence ionospheric soundings for all available stations for the years 1954 through 1958.

For the PennState Mk I ionospheric model it was desired to use the 2800 MHz solar flux as the index controlling the solar activity rather than the Zurich sunspot number because it has been used for the CIRA (1965) neutral models. Our calculations indicated that the peak electron density is approximately linearly related to the decimetric solar flux. The CCIR models assume a linear relation between $f_o F_2$ and R_z . To determine the interpolation formula for solar activity calculations were made for several stations of the peak electron density as a function of 2800 MHz solar flux for the years 1959 to 1962. In this way the values $60 \times 10^{-22} \text{ W m}^{-2} \text{ Hz}^{-1}$ and $136 \times 10^{-22} \text{ W m}^{-2} \text{ Hz}^{-1}$ were obtained for the two

models to give the interpolation formula.

$$N_m F_2 = 1.24 \times 10^4 \frac{f_{100}^2 (\bar{S} - 60) + f_o^2 (136 - \bar{S})}{76} \text{ cm}^{-3}$$

where

f_o is the predicted $f_o F_2$ for $R = 0$ in MHz

f_{100} is the predicted $f_o F_2$ for $R = 100$ in MHz

5.2 Altitude of the F₂ peak

The data used for the calculations of the altitude of the peak of the F₂ layer were profiles reduced from ionograms. The stations used are given in table 3. Data for Grand Bahamas, Puerto Rico, Ft. Monmouth, White Sands and St. Johns were made available by J. W. Wright. Data for Panama, Talara and Huancayo were taken from Schmerling (1958a, b, c, 1959a, b, 1960a, b). The data from Huancayo were supplemented by some incoherent scatter measurements at Jicamara reported by Farley (1966). In the case of Panama and Talara for which only high solar activity data was available the approximation was made that the height of the maximum remained at a constant pressure level throughout the solar cycle.

The above data are obviously insufficient to provide the twelve sets of 975 coefficients given in the C. C. I. R. model for the peak density.

TABLE 3

Data Used for Model of $N_m F_2$

<u>Station</u>	<u>Data</u>	<u>Lat.</u>	<u>Long.</u>	<u>sin x</u>
Grand Bahamas	March 1959 to Feb. 1962	26.6N	78.2W	0.74120
Puerto Rico	April 1959 to Feb. 1962	18.5N	67.2W	0.67664
Ft. Monmouth	Feb. 1959 to Feb. 1962	40.4N	74.1W	0.81948
White Sands	March 1959 to Jan. 1962	32.3N	106.5W	0.75123
St. Johns	March 1959 to April 1961	47.6N	52.7W	0.83668
Panama	July 1957 to Dec. 1958	9.4N	75.0W	0.55638
Talara	July 1957 to Dec. 1958	4.6N	75.0W	0.22282
Huancayo	July 1957 to Dec. 1958	12.0S	75.0W	0.01351

It was decided to use as the latitude variable the sin of x the modified dip. This parameter was used as the main latitude variable in the C. C. I. R. (1967) model.

$$\sin x = \sin \arctan \left(\frac{I}{\sqrt{\cos \lambda}} \right)$$

where

I is the magnetic dip

λ is the geographic latitude

A world map of values of $\sin x$ is given as figure 2.

From an examination of the seasonal variation of the peak altitude it appeared that the predominant seasonal change was sinusoidal with a period of one year and a maximum or minimum at the December solstice. The data for each station for the winter months November, December and January and the summer months May, June and July were all grouped together. As with the exception of Huancayo, all the stations included in the data are in the northern hemisphere it was assumed that conditions are the same for similar local seasons in the northern and southern hemisphere at the same unadjusted solar flux.

For each station a linear least squares fit was first made to the peak altitude at each hour as a function of the 2800 MHz solar flux and values obtained for values of \bar{S} of 100 and 200 for local winter and local

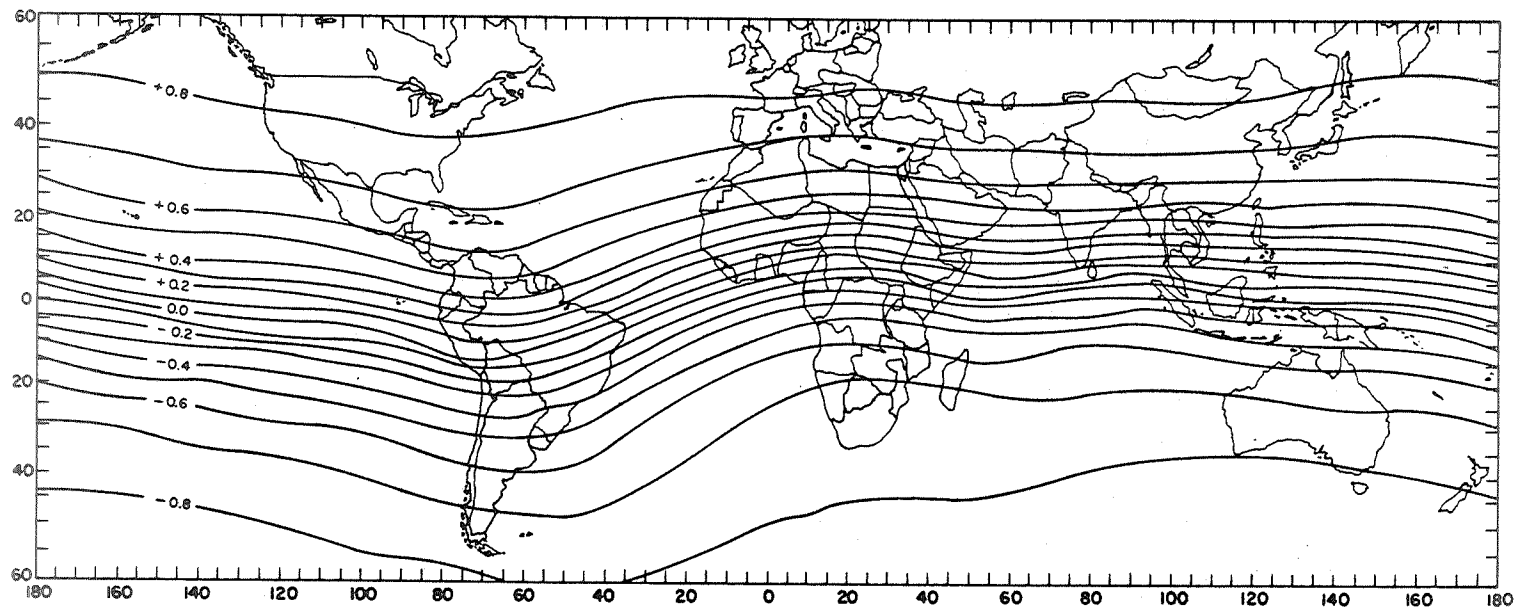


Figure 2 World map of $\sin x$.

TABLE 4

COEFFICIENTS FOR $H_m F^2$ $S_{10.7} = 100$ SUMMER

n/m	<u>a</u>				
	0	1	2	3	4
0	3.1705E 2	3.3274E 2	-1.1897E 3	1.2287E 3	-3.7186E 2
1	-3.6066E 0	3.1859E 1	-1.0750E 3	2.8063E 3	-1.7593E 3
2	1.1881E 1	8.9212E 1	-6.3058E 2	1.0757E 3	-5.4713E 2
3	-6.3852E 0	1.3781E 2	-7.5412E 2	1.1718E 3	-5.4878E 2
4	-8.9576E-1	6.8596E 1	-4.5622E 2	8.5637E 2	-4.6784E 2
5	3.3496E 0	-1.0212E 2	5.2297E 2	-8.0599E 2	3.8070E 2
6	1.9793E 0	-9.8264E 1	5.0090E 2	-8.2938E 2	4.2491E 2
			<u>b</u>		
1	-5.9241E 1	-1.1160E 2	7.2859E 2	-8.1400E 2	2.5632E 2
2	-2.0142E 1	4.3541E 1	2.6204E 2	-6.1047E 2	3.2624E 2
3	-2.3830E 0	-5.3660E 0	3.0777E 1	-1.0719E 2	8.4173E 1
4	2.2423E 0	3.5550E 1	-2.5423E 2	3.9297E 2	-1.7622E 2
5	4.3970E 0	4.4893E 1	-2.4352E 2	3.8097E 2	-1.8680E 2
6	1.9734E-1	-2.7897E 1	2.2773E 2	-4.1116E 2	2.1052E 2

TABLE 4

(cont'd)

 $S_{10.7} = 100$ WINTER

n/m	<u>a</u>				
	0	1	2	3	4
0	3.1998E 2	9.8526E 0	4.5898E 2	-1.1754E 3	6.9513E 2
1	-2.6843E 1	1.7413E 2	-1.5135E 3	3.3457E 3	-1.9785E 3
2	-1.1297E 1	3.0140E 1	-1.3842E 2	4.4889E 2	-3.2998E 2
3	-9.7099E 0	-3.2377E 1	1.1502E 2	-1.4196E 2	6.8595E 1
4	6.7014E 0	-7.9243E 1	3.4751E 2	-5.4850E 2	2.7280E 2
5	3.4791E 0	9.0675E 0	4.8381E 1	-1.5807E 2	9.6815E 1
6	-3.8361E 0	1.0170E 2	-4.2008E 2	5.7780E 2	-2.5517E 2
			<u>b</u>		
1	-3.7190E 1	-3.5619E 2	1.5680E 3	-1.9977E 3	8.2192E 2
2	-2.5507E 0	4.9054E 1	-4.1015E 2	8.2698E 2	-4.6277E 2
3	-1.1507E 0	1.4445E 2	-6.1789E 2	8.4686E 2	-3.7146E 2
4	2.7301E 0	7.3172E 0	5.0862E 1	-2.4468E 2	1.8395E 2
5	5.0311E 0	-5.6539E 0	1.3707E 2	-3.5340E 2	2.1697E 2
6	1.5232E 0	-3.9023E 1	1.9591E 2	-3.1092E 2	1.5232E 2

TABLE 4
(cont'd)

$S_{10.7} = 200$ WINTER

n/m	<u>a</u>				
	0	1	2	3	4
0	3.8608E 2	1.0519E 2	1.8570E 2	-9.8738E 2	6.5984E 2
1	-3.3678E 1	6.7720E 1	-1.0551E 3	2.7560E 3	-1.7334E 3
2	-1.7639E 1	7.0142E 1	-3.0989E 2	7.1349E 2	-4.5618E 2
3	-1.5911E 1	-1.4335E 1	-4.4358E 1	1.8003E 2	-1.0532E 2
4	1.0060E 1	-6.9187E 1	2.3776E 2	-3.7643E 2	1.9788E 2
5	3.7396E 0	5.7202E 1	-1.7353E 2	1.7804E 2	-6.5560E 1
6	-6.1503E 0	1.4982E 2	-6.5065E 2	9.5417E 2	-4.4719E 2

b

1	-5.3310E 1	-5.0337E 2	2.1753E 3	-2.7381E 3	1.1182E 3
2	-5.3819E 0	2.3231E 1	-3.0603E 2	6.9896E 2	-4.1035E 2
3	-2.6952E 0	2.0964E 2	-8.0779E 2	1.0446E 3	-4.4335E 2
4	2.0211E 0	7.4877E 1	-3.0404E 2	3.4287E 2	-1.1538E 2
5	6.4624E 0	1.9698E 1	6.0566E 1	-3.0155E 2	2.1516E 2
6	1.3950E 0	-5.3858E 1	2.9350E 2	-4.7603E 2	2.3455E 2

summer. These values were then fitted to a sixth degree Fourier series in the local time

$$H_m F_2 = a_0 + \sum_{n=1,6} a_n \cos \frac{2\pi HL}{24} + b_n \sin \frac{2\pi HL}{24}$$

Each of the a's and b's was then fitted to a power series expansion in terms of $\sin x$.

$$H_m F_2 = \sum_{m=0,4} \left(a_{0m} + \sum_{n=1,6} a_{nm} \cos \frac{2\pi HL}{24} + b_{nm} \sin \frac{2\pi HL}{24} \right) \sin^m x$$

Table 4 shows the coefficients used in the model. The winter and summer values of $H_m F_2$ were then calculated using an interpolation formula based on a linear variation with the 2800 MHz solar flux

$$H = .01 \left[(\bar{S} - 100) H_{200} + (200 - \bar{S}) H_{100} \right]$$

the value for the day was then calculated

$$H = H_W \left(.5 + 0.565 \cos \frac{2\pi (D + 8)}{365.25} \right) + H_S \left(.5 - 0.565 \cos \frac{2\pi (D + 8)}{365.25} \right)$$

Figures 3, 4 and 5 show model values of $H_m F_2$ for summer and winter solstice and equinox conditions for $\bar{S} = 100$. Figure 6 shows the equinox values for $\bar{S} = 200$.

5.3 The electron temperature at the peak.

Nisbet (1968) has described a method of calculating the photo-electron number densities in the F region as a function of altitude and energy. In the course of this work it was discovered that the average energy per photoelectron \bar{E} given to the ambient electrons by the photoelectrons

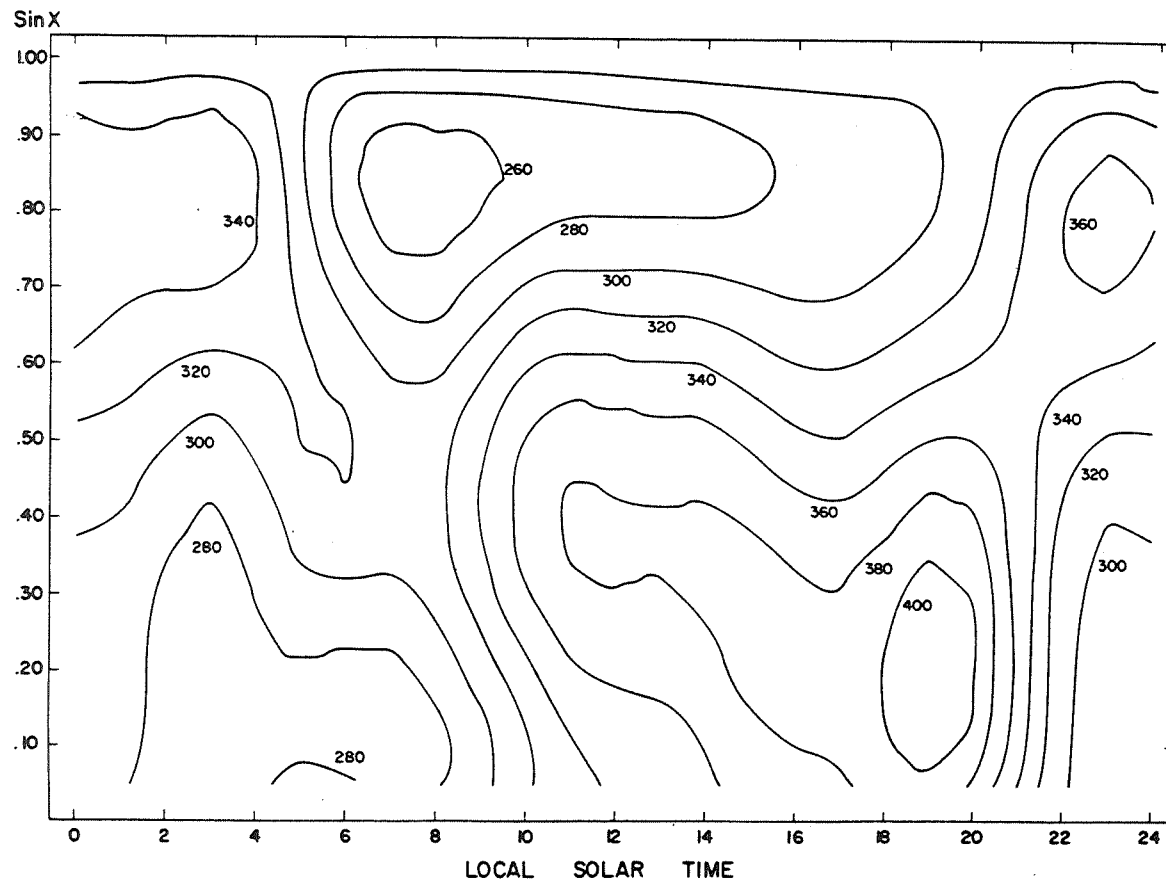


Figure 3 Model values of $H_m F_2$ summer solstice $\bar{S}_{10.7} = 100$.

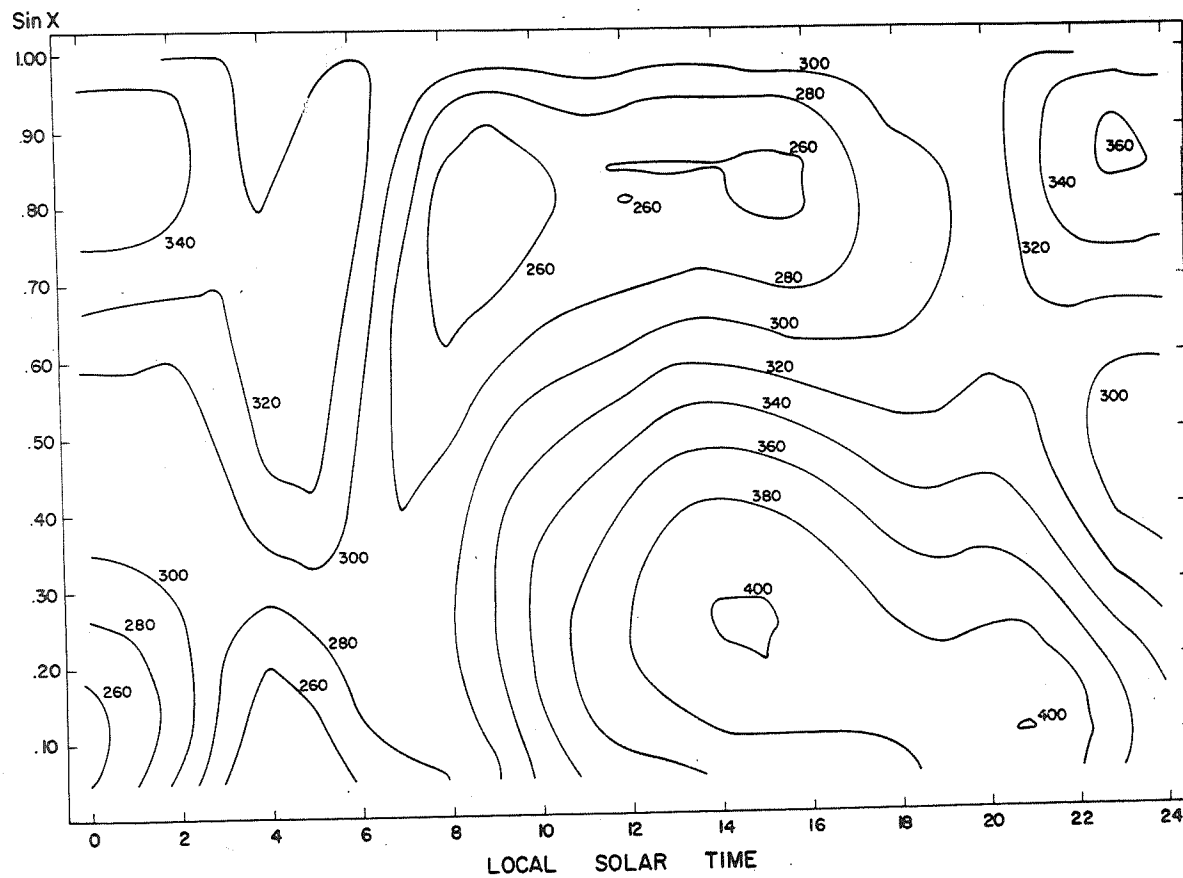


Figure 4 Model values of $H_m F_2$ winter solstice $\bar{S}_{10.7} = 100$.

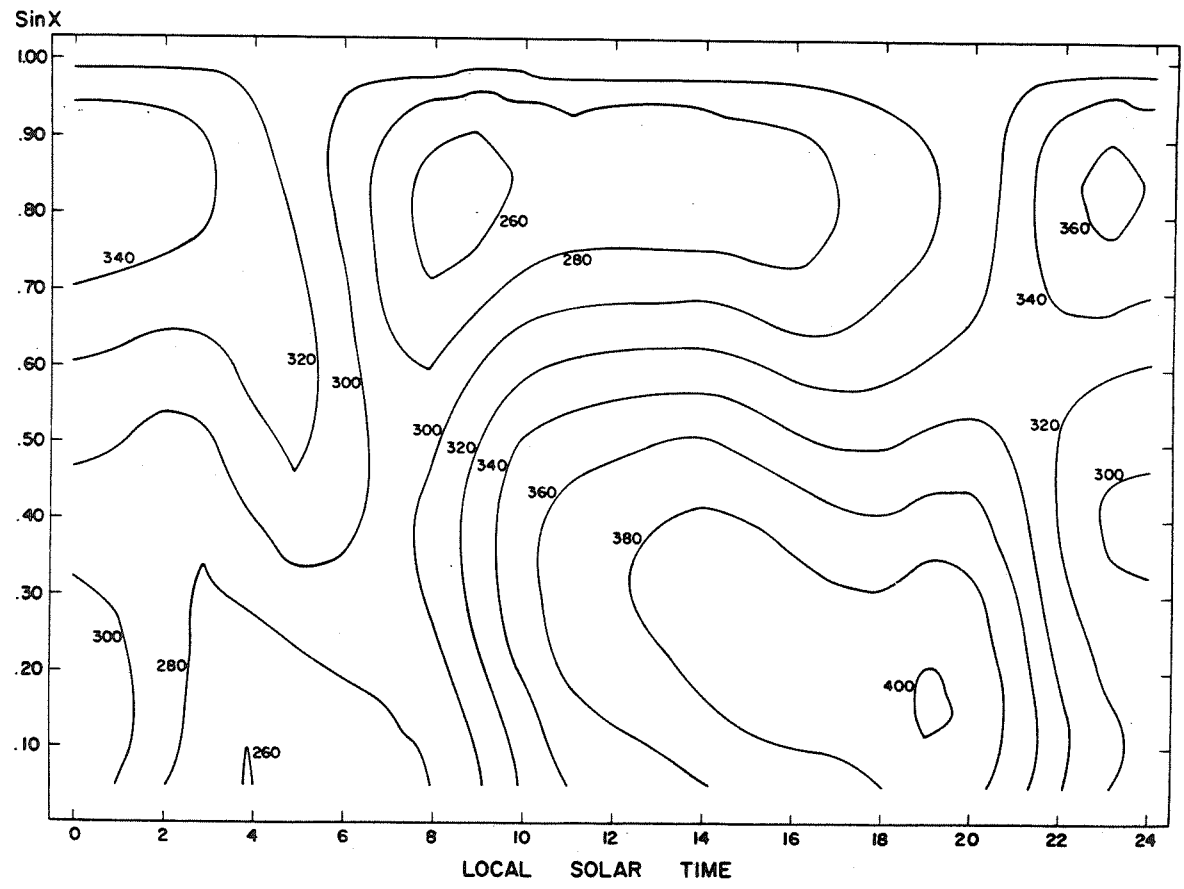


Figure 5 Model values of $H_m F_2$ equinox $\bar{S}_{10.7} = 100$.

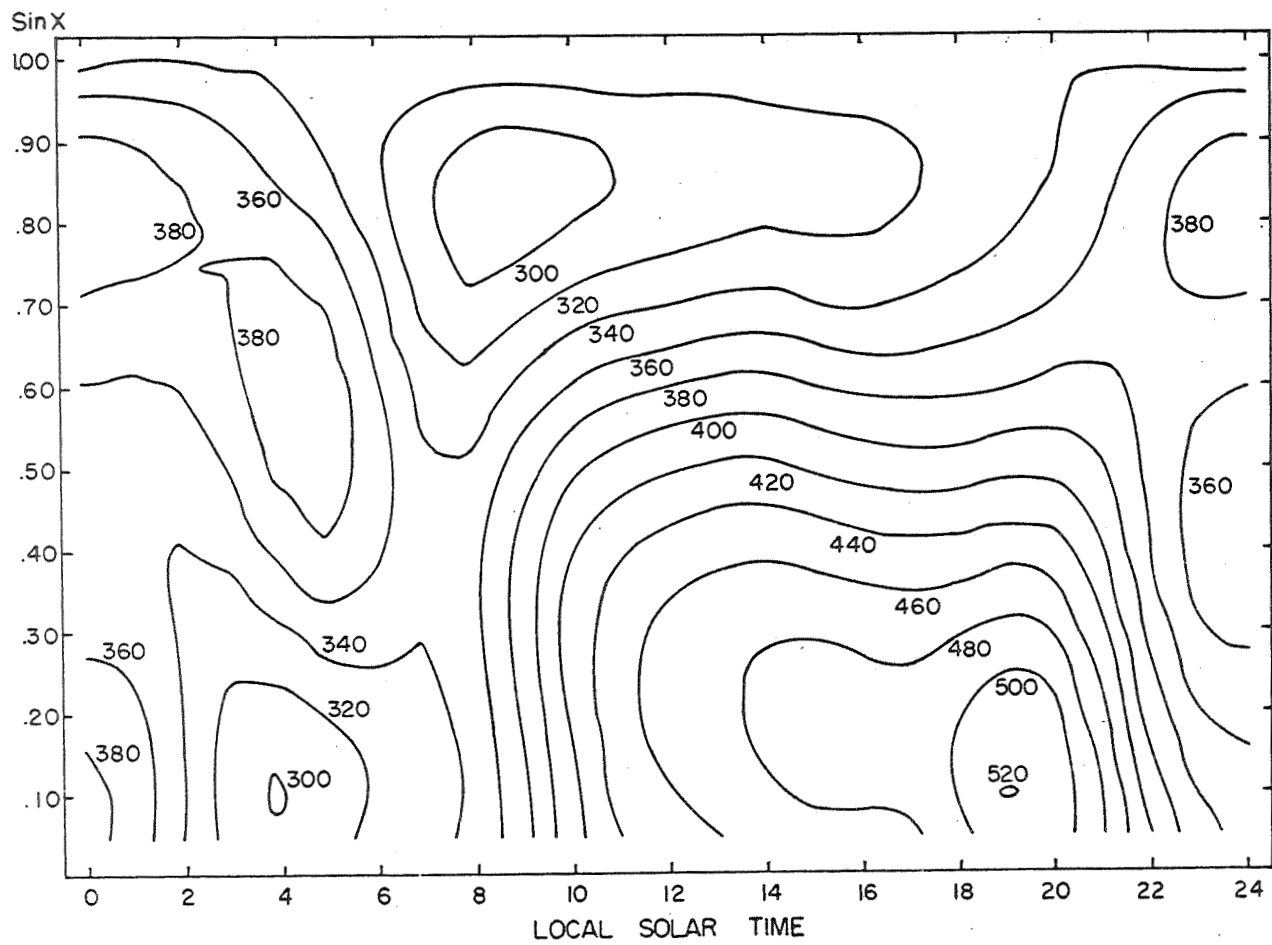


Figure 6 Model values of $H_m F_2$ equinox $\bar{S}_{10.7} = 200$.

was a relatively invariant function of the ratio of the ambient electron density to the sum of the neutral densities over a wide range of ionosphere conditions at altitude ranges where non local heating is not significant. This appears reasonable as the average energy per photoelectron given to the ambient electrons depends on the ratio of the losses to the ambient electrons to the losses to neutral particles. The neutral species considered each have different loss rates and photoelectron production spectra, but as the above ratio is very altitude dependent, partial compensation is provided in that a given ratio is normally encountered in a limited range of pressure and hence in a limited range of relative concentrations of the three major constituents. The photoelectron production spectrum changes with solar activity; however, the lower energy photoelectrons are more effective in heating the ambient electrons so that \bar{E} does not seem to be greatly affected. The relation used in the present model is due to Swartz (1969) and is shown in Figure 7

$$\begin{aligned} \bar{E} &= -15.287875 - 9.92974304 \ell - 0.12446207 \ell^2 \\ &+ 0.34853088 \ell^3 + 0.051060516 \ell^4 + 0.0027944732 \ell^5 \\ &+ 0.000054252519 \ell^6 \end{aligned}$$

where

$$\ell = \log_e \left(\frac{N_e}{n(O) + n(N_2) + n(O_2)} \right)$$

The heat input to the ambient electrons at the peak is then given by the average energy per photoelectron given to the ambient electrons multiplied by the total ion production rate.

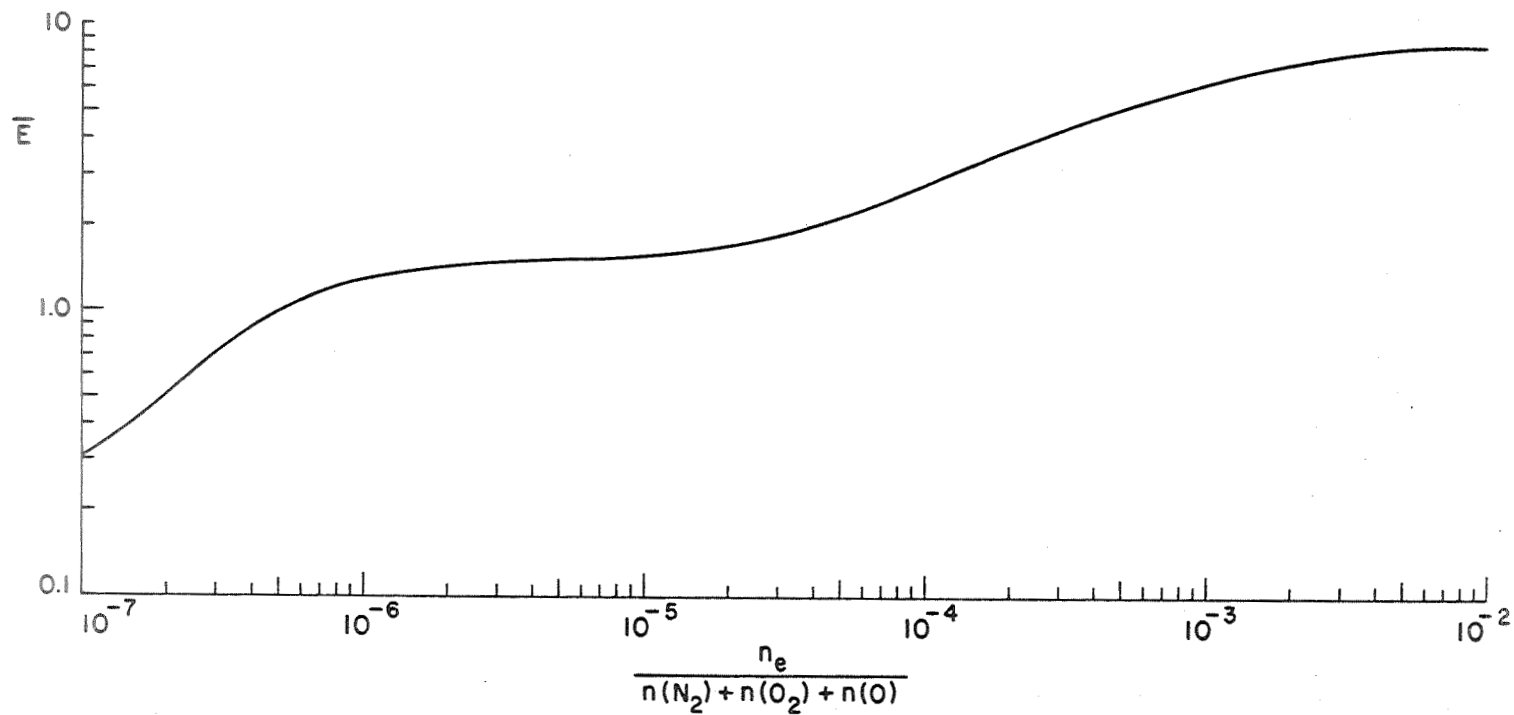


Figure 7 Model of average energy \bar{E} per photoelectron given to ambient electrons.

$$Q = \bar{E} \sum_M \text{PROD (M)}$$

This heat input is then equated to the various energy loss processes for the ambient electrons and the electron temperature at the peak determined using an iterative procedure. The equations used for the various loss processes are as follows:

Electron to ion loss

$$Q_{ei} = 3.2 \times 10^{-8} N_e^2 T_e^{3/2} (T_e - T) \log_e \left[\frac{12.42 T_e^{3/2} T^{1/2}}{(N_e (T_e - T))^{1/2}} \right] \text{ ev cm}^{-3}$$

Rotational loss to N₂

$$R_{N_2} = \frac{2.9 \times 10^{-14} N_e n(N_2) (T_e - T)}{T_e^{0.5}} \text{ ev cm}^{-3}$$

Vibrational loss to N₂

$$V_{N_2} = N_e n(N_2) (T_e - T) (3.0271 + 1.4793 \times 10^{-3} T) (-2.1529 \times 10^{-12} T_e^{-1} + 5.7891 \times 10^{-15} - 4.7555 \times 10^{-18} T_e + 1.327 \times 10^{-21} T_e^2) \text{ ev cm}^{-3}$$

Rotational loss to O₂

$$R_{O_2} = \frac{6.9 \times 10^{-14} N_e n(O_2) (T_e - T)}{T_e^{0.5}} \text{ ev cm}^{-3}$$

Vibrational loss to O₂

$$V_{O_2} = N_e n(O_2) (1.39 \times 10^{-12} - 6.98 \times 10^{-15} T_e + 8.29 \times 10^{-18} T_e^2) \text{ ev cm}^{-3}$$

Fine structure loss to O

$$F_O = 3.4 \times 10^{-12} N_e n(O) \frac{(T_e - T)}{T} (1 - 7 \times 10^{-5} T_e) \text{ ev cm}^{-3}$$

5.4 Model for the upper F region

In the region above the peak diffusion plays the dominant role in determining the electron density profile along a field line. The situation is complicated by the change in the mean ionic mass from that of oxygen to that of hydrogen and by the electron and ion temperature gradients. The equations for the temperatures and densities are coupled and most programs developed to solve the system of equations use an iterative approach in which the temperature and density equations are solved successively. In the present program an extremely simple model has been employed. In this model it is assumed that the electron and ion temperatures remain constant above the peak, and the proton density is chosen to make the

electron densities at 1000 km agree with empirical boundary conditions. The model provides a smooth transition between densities empirically chosen at 1000 km and the densities and scale heights in the region of the peak. As the proton scale height is so large its serious underestimation due to the assumptions of the model does not cause large errors in the electron density profiles up to 1250 km.

Figures 8 and 9 show the assumed boundary values of the electron density at 1000 km for winter and summer for two levels of solar activity. The data on which these estimates were based was taken from Brace et al (1967), Chan and Colin (1969), Matuura and Ondoh (1969), and Jelly and Petrie (1969).

5.5 Nighttime F region

Little information on nighttime ionization sources at middle latitudes is available. Based on measurements by Young et al (1968) on 10 August 1967 three lines have been included Lyman β , He I and He II. For lack of better information, it has been assumed that at night the intensities of these lines are 0.3%, 0.1% and 0.1% of their daytime magnitude at noon.

For the upper F region a simple empirical formula was employed. Below the peak at altitudes when the following formula exceeded the photoequilibrium density the electron density was assumed to be,

$$N_e = 1.32019 N_m F_2 \left[\exp(0.5 (Z_m - Z)/H - 0.277778 \exp(1.8 (Z_m - Z)/H)) \right]$$

above the peak it was assumed that

$$N_e = 1.32019 N_m F_2 \left[\exp(0.5 (Z_m - Z)/H - 0.277778 \exp(1.8 (Z_m - Z)/H)) \left[1 - \rho + \rho \exp(15(Z_m - Z)/16H) \right]^{1/2} \right]$$

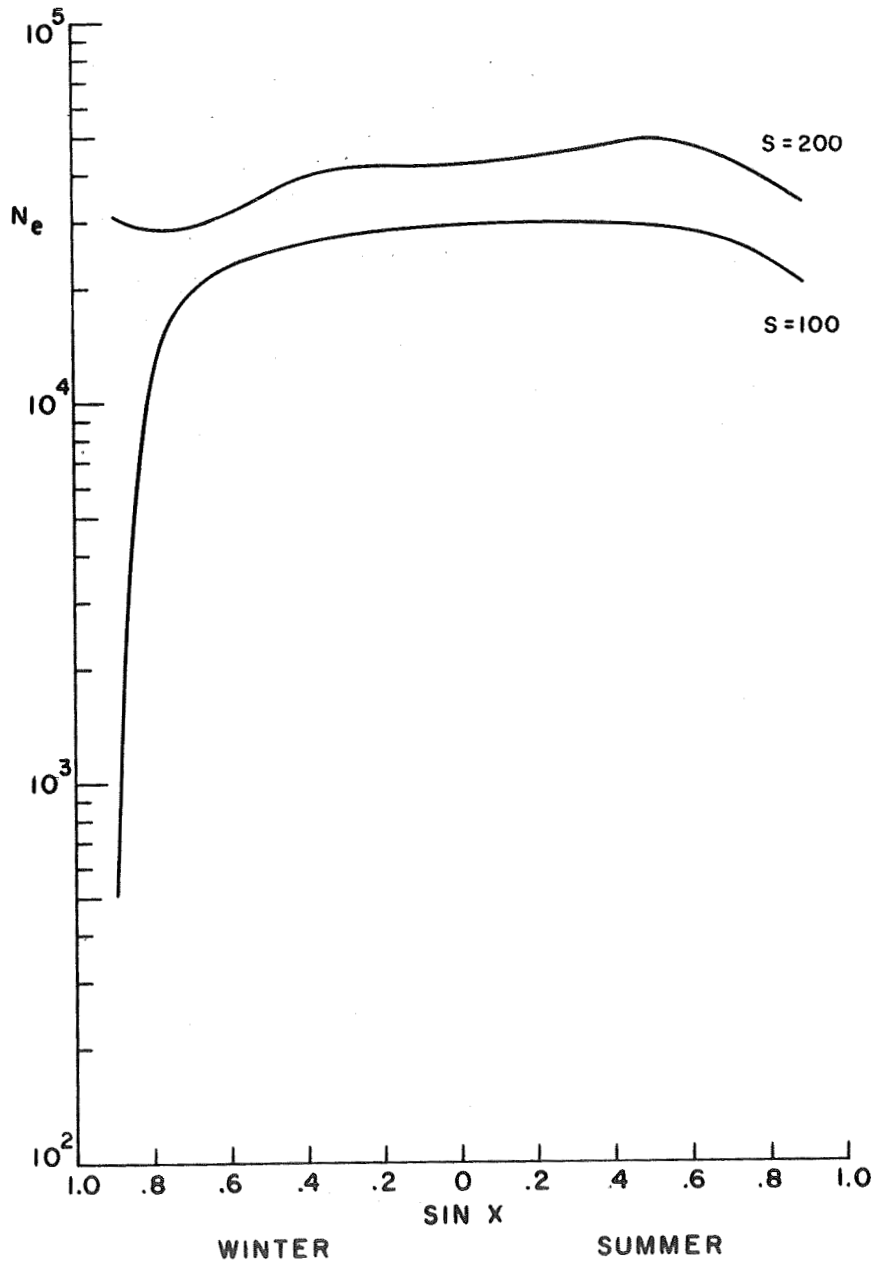


Figure 8 Local noon model boundary conditions at 1000 Km.

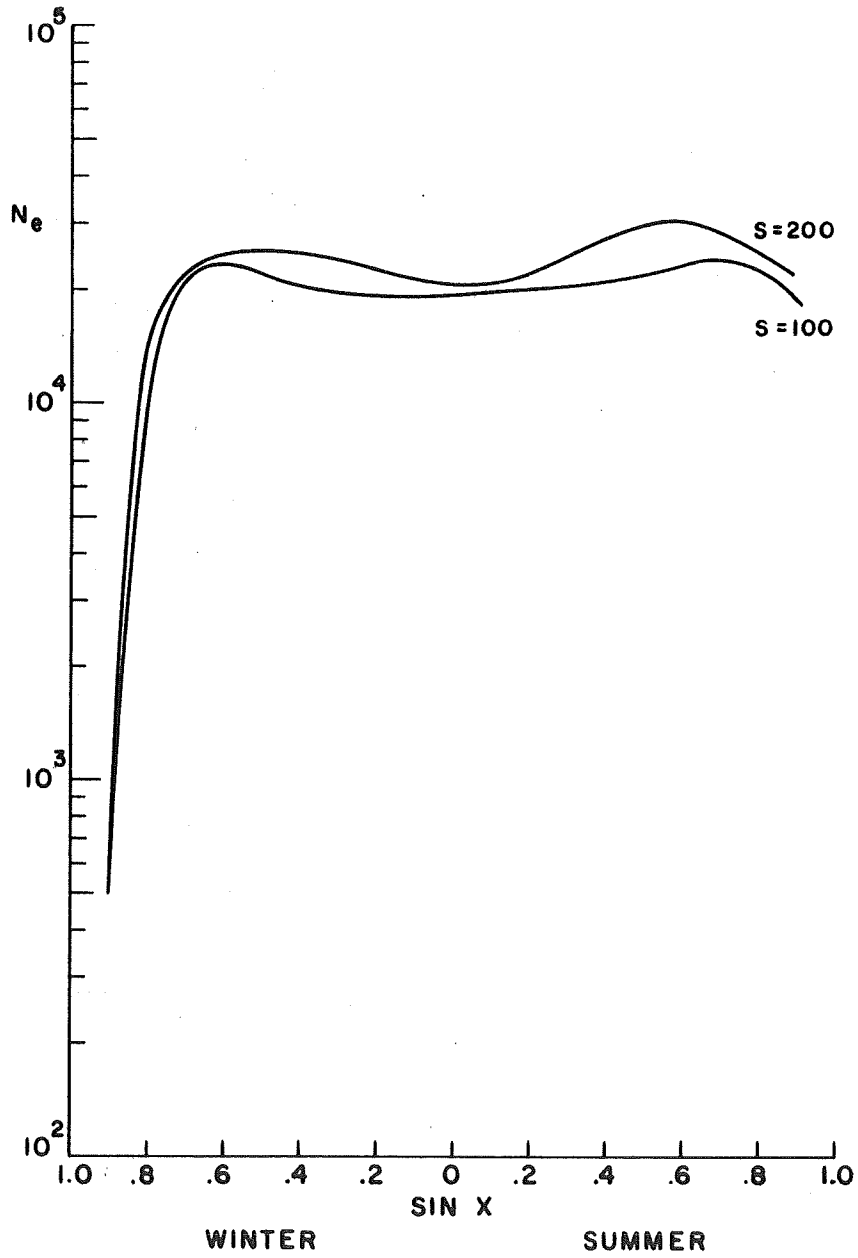


Figure 9 Local midnight model boundary conditions at 1000 Km.

where

Z_m is the geopotential altitude of the peak

Z is the geopotential altitude at which the density is being calculated

H is the local scale height of atomic oxygen

and

$$\rho = \left(\frac{N_{1000}}{N_{mF_2}} \right)^2 \exp((Z - Z_m)/16H)$$

where

N_{1000} is the boundary value electron density at 1000 km

and

N_{mF_2} is the electron density at the maximum.

6. Models for midlatitude sporadic E

Because it was desired to give an example of the way in which statistical information as well as estimated mean models could be included it was decided to make an initial attempt at including one of the most variable ionospheric phenomena, midlatitude sporadic E, in the models. This also seemed appropriate because of its interest for aeronomy and radio propagation.

It was decided that the smallest number of statistical parameters possible should be included in the model. These were chosen to be the probability of occurrence, the mean electron density when it was observed and the standard deviation of the distribution about this mean electron density. In the absence of other information it was decided to assume that the distribution of the densities was log normal.

The data used in this analysis were taken from Reddy and Matsushita (1968) and were thus based on measurements of blanketing sporadic E for the years 1958 through 1965 for six stations. Matsushita (1966) suggested that the blanketing frequency $f_b E_s$ represents the plasma frequency of the E_s layer corresponding to M_1 type sporadic E. This assumption appears to be consistent with rocket measurements according to Reddy and Rao (1968). The six stations employed by Reddy and Matsushita were Adak, Kokobunji, Grand Bahama Island, Talara, Rarotonga, and Port Stanley. The data used consisted of plots of six and twelve month running averages of $f_b E_s$ over four periods 09-12 hours, 13-16 hours, 21-00 hours and 01-04 hours and of the percentage occurrence of $f_b E_s \geq 0.5, 2.0, 3.0, 4.0, 5.0$ and 6.0 MHz.

The limited number of stations and times is obviously insufficient to provide more than a very minimal model of the diurnal, seasonal,

solar cycle, and geographical variation of even mid latitude blanketing sporadic E. It was hoped that the attempt to provide such models might at least indicate some of the possibilities, difficulties and methods of data analysis that might prove helpful in developing later and more accurate models.

Because of the difference in the data parameters used in the model and those given by Reddy and Matsushita, a rather involved data processing technique was used which involved several simplifying assumptions. The most obvious variation in sporadic E densities and probabilities appeared to be the annual variation with a maximum in local summer and a minimum in local winter. It was assumed that this variation could be represented by the fundamental Fourier coefficient with a maximum or a minimum on January 1st depending on the hemisphere. Winter and summer values of each parameter were read for each year from 1958 through 1965 and these were fitted to linear relations with the 2800 MHz solar flux corresponding to the period of the measurements. These linear relationships were interpolated at values of $100 \times 10^{-22} \text{ W m}^{-2} \text{ Hz}^{-1}$ and $200 \times 10^{-22} \text{ W m}^{-2} \text{ Hz}^{-1}$. It was assumed that the average value of the peak electron density corresponded to the average value of $f_p E_s$ and that the probability of occurrence of sporadic E corresponded to the probability that sporadic E was observed with a blanketing frequency exceeding 0.5 MHz. It was assumed that the probability distribution of the sporadic E peak electron density would exceed a value n as given by

$$P(N_{m E_s} > n) = 0.5 \text{ E SPROB} \left[1 - \text{erf} \left(\frac{\log \frac{n}{AVNES}}{\sqrt{2} \text{ SIGMA}} \right) \right]$$

where

ESPROB Is the probability of sporadic E occurring with a critical frequency exceeding 0.5 MHz.

AVNES is the average peak electron density of the sporadic E layer when it occurs.

and

SIGMA is the standard deviation about the mean value.

Values of SIGMA were chosen which provided the best fit to the data for the higher values of $f_b E_s$. For small values of n the probability is mainly controlled by ESPROB and in the region of AVNES by the average value of $f_b E_s$.

The variation for the blanketing sporadic E critical frequency assumed for a local time HL is

$$0 \text{ hours to } 4 \text{ hours} \quad f_b E_s = C_1 - C_2 \cos \frac{\pi(4-HL)}{20}$$

$$4 \text{ hours to } 8 \text{ hours} \quad f_b E_s = C_1 - C_2 \cos \frac{\pi(4-HL)}{4}$$

$$8 \text{ hours to } 24 \text{ hours} \quad f_b E_s = C_1 - C_2 \cos \frac{\pi(8-HL)}{20}$$

where C_1 and C_2 are derived from series of the form

$$C_1 = \sum_{n=0}^f C_{in} \left| \sin x \right|^n$$

4 values of both C_1 and C_2 are obtained for each value of $\left| \sin x \right|$ for winter and summer, at $\bar{S}_{10.7}$ values of 100 and 200. Values for the day and solar activity are calculated using the interpolation formula

$$C = \left(\frac{C_{w100} + C_{s100}}{2} \right) (2 - .01\bar{S}) + \left(\frac{C_{w200} + C_{s200}}{2} \right) (.01\bar{S} - 1) \\ + 1.570796 \alpha \left[\frac{(C_{w100} - C_{s100})}{2} (2 - .01\bar{S}) + \left(\frac{C_{w200} - C_{s200}}{2} \right) (.01\bar{S}) \right] \cos \frac{2\pi D}{365.25}$$

when α is ± 1 depending on the hemisphere. This sign change was used because the data for the southern and northern hemispheres were so sparse it was thought better to combine them and assume that conditions were similar at similar seasons for similar non-adjusted solar fluxes.

The average value of the peak electron density AVNES was then calculated using the relation

$$AVNES = 1.24 \times 10^4 (f_b E_s)^2$$

where

$$AVNES \text{ is in units } \text{cm}^{-3}$$

and

$$f_b E_s \text{ is in MHz}$$

The probability that the blanketing frequency of the sporadic E layer exceed 0.5 MHz was also determined in a similar manner. In this case the time variation was assumed to be

$$ESPROB = C_3 + C_4 \cos \left(\frac{2\pi (HL - C_5)}{24} \right)$$

Values of the probability of sporadic E occurrence for two three hour periods are shown in Figure 10 to give an indication of the diurnal and seasonal variation in this parameter and the degree to which the model fits the latitudinal variation.

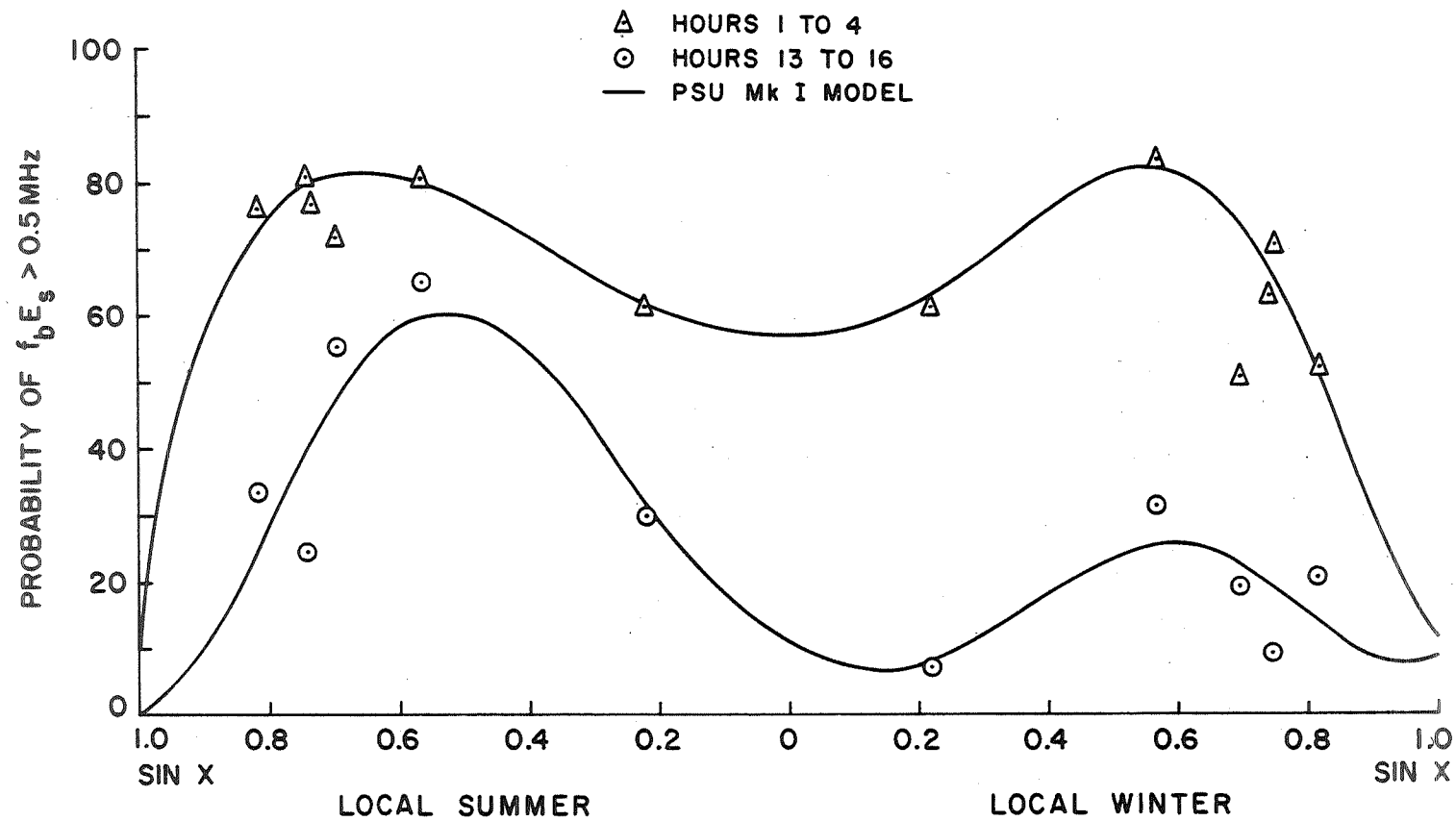


Figure 10 Six month average mid-winter and mid-summer probability of sporadic E with $f_b E_s > 0.5$ MHz, $\bar{S}_{10.7} = 100$.

The standard deviation SIGMA was derived from the formula

$$\text{SIGMA} = 0.01 \left[(S - 100) \left(0.55 + 0.15 \cos \frac{2\pi}{24} (HL + 2) \right) \right. \\ \left. + (200 - S) \left(0.6 + 0.1 \cos \frac{2\pi}{24} (HL + 2) \right) \right]$$

7. Comparisons of the model with data

A large number of comparisons of the model with experimental data are possible, only a few of which can be given here.

Of major interest is the behavior of the F1 region. In the Mk 1 model these densities are derived from solar flux values, CIRA neutral atmospheric densities and laboratory values of recombination rates. They are thus independent of any ionospheric electron density data except in the region of the peak where the boundary conditions take control. A major source of electron density data for comparison purposes is the series of mean monthly reduced ionograms produced by N.B.S. which served as the main source of $H_m F_2$. These were obtained as mean monthly profiles at times when the K_p index was less than 4.5 and thus they corresponded to quiet magnetic conditions. In the following comparisons the MK 1 models program was run for the 15th day of the month using the 2800 MHz solar flux averaged for 27 days about this time. Figures 11, 12, 13 and 14 show data for March 1959 ($\bar{S} = 103$) and March 1961 ($\bar{S} = 220$) for Grand Bahama Island and St. Johns Newfoundland. It would appear from these comparisons that the correction for solar activity has rather overestimated in the 150 - 250 km height range as the model electron densities are rather too low for $\bar{S} = 103$ and too high at $\bar{S} = 220$. Values at Grand Bahama Island are generally higher with respect to the model than for St. Johns. As would be expected, the divergence between the models and the measured data is greater at times close to sunrise and sunset than during the day. No attempt has been made to obtain a better fit to the experimental data by adjusting the solar flux values as the uncertainties in the reduced ionograms are probably of the order of the $\pm 20\%$ difference observed during the day.

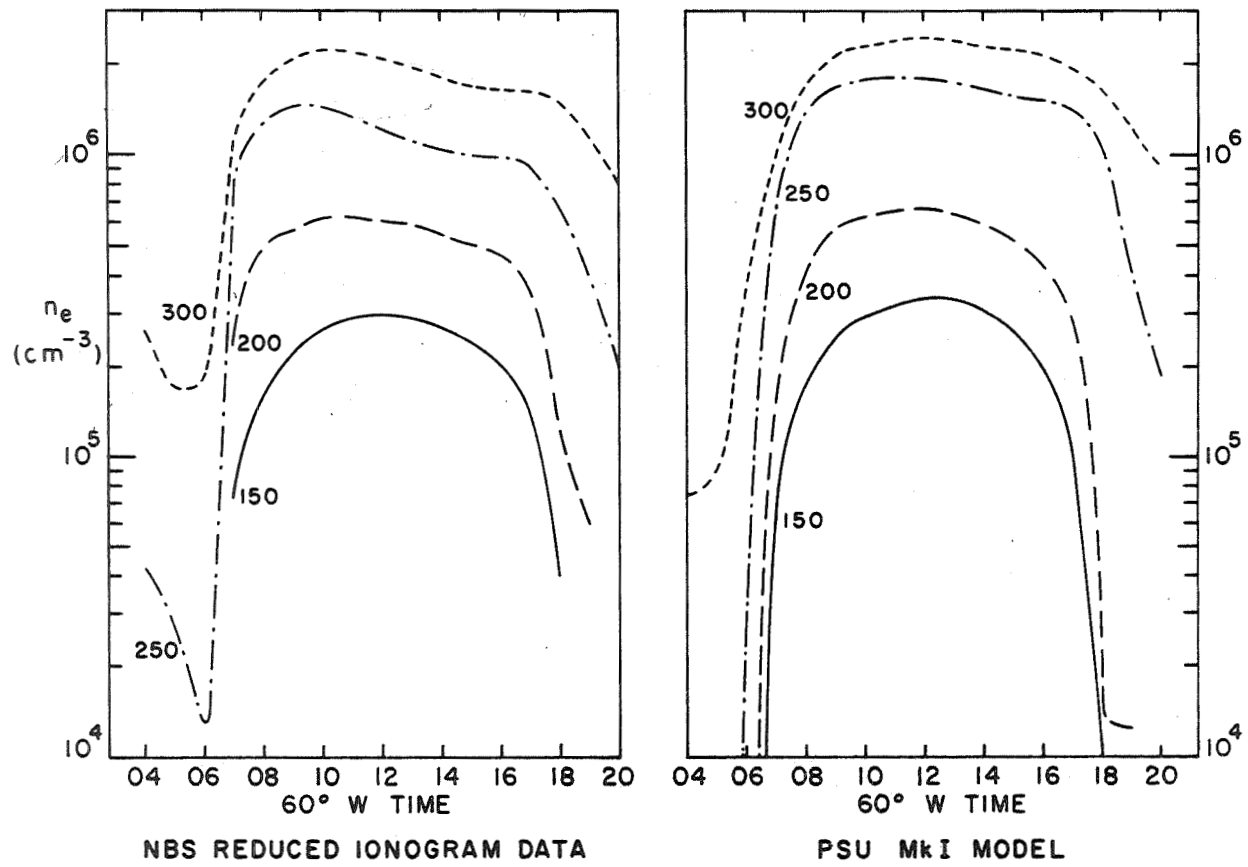


Figure 11 Electron densities for Grand Bahama Island, March 1959, $\bar{S}_{10.7} = 220$.

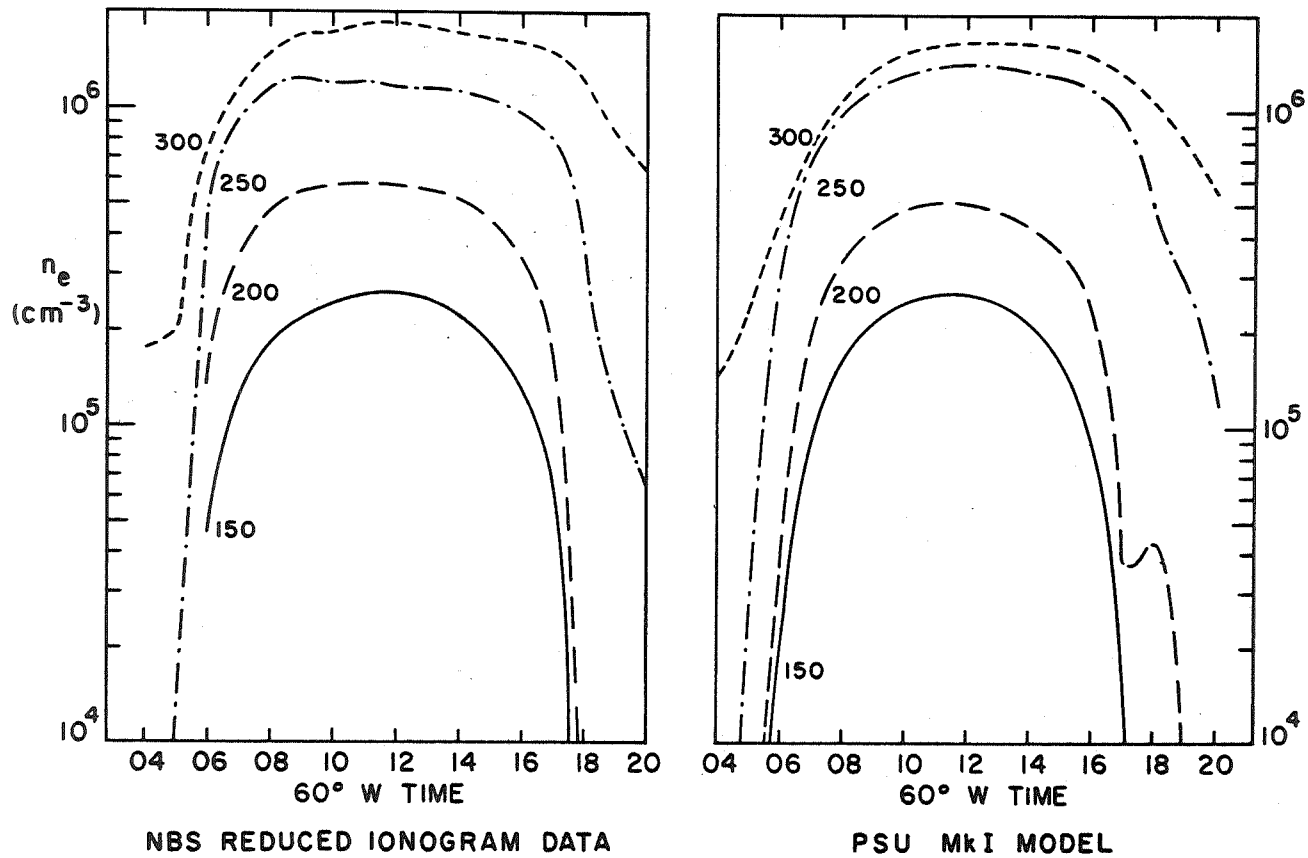


Figure 12 Electron densities for St. Johns, Newfoundland,
 March 1959, $\bar{S}_{10.7} = 220$.

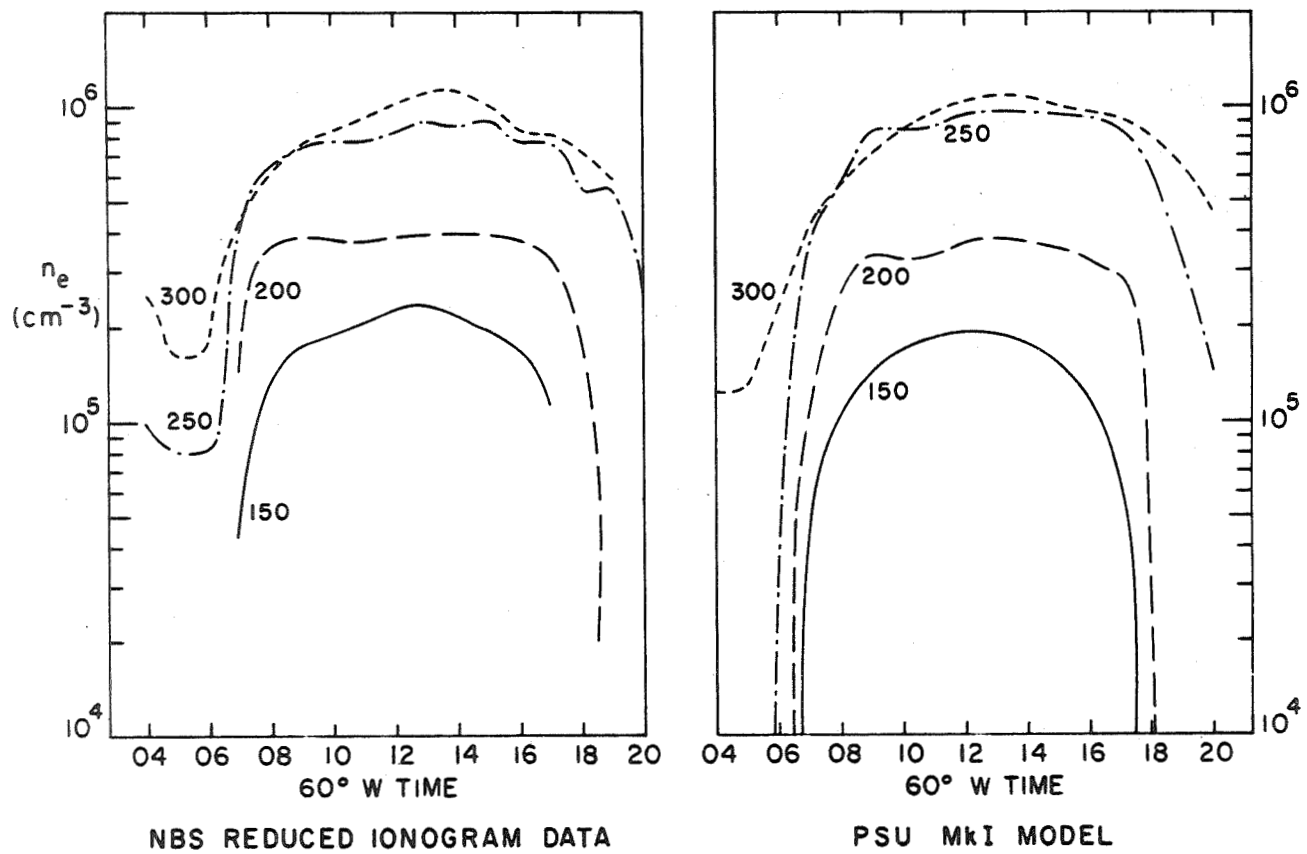


Figure 13 Electron densities for Grand Bahama Island, March 1961, $\bar{S}_{10.7} = 103$.

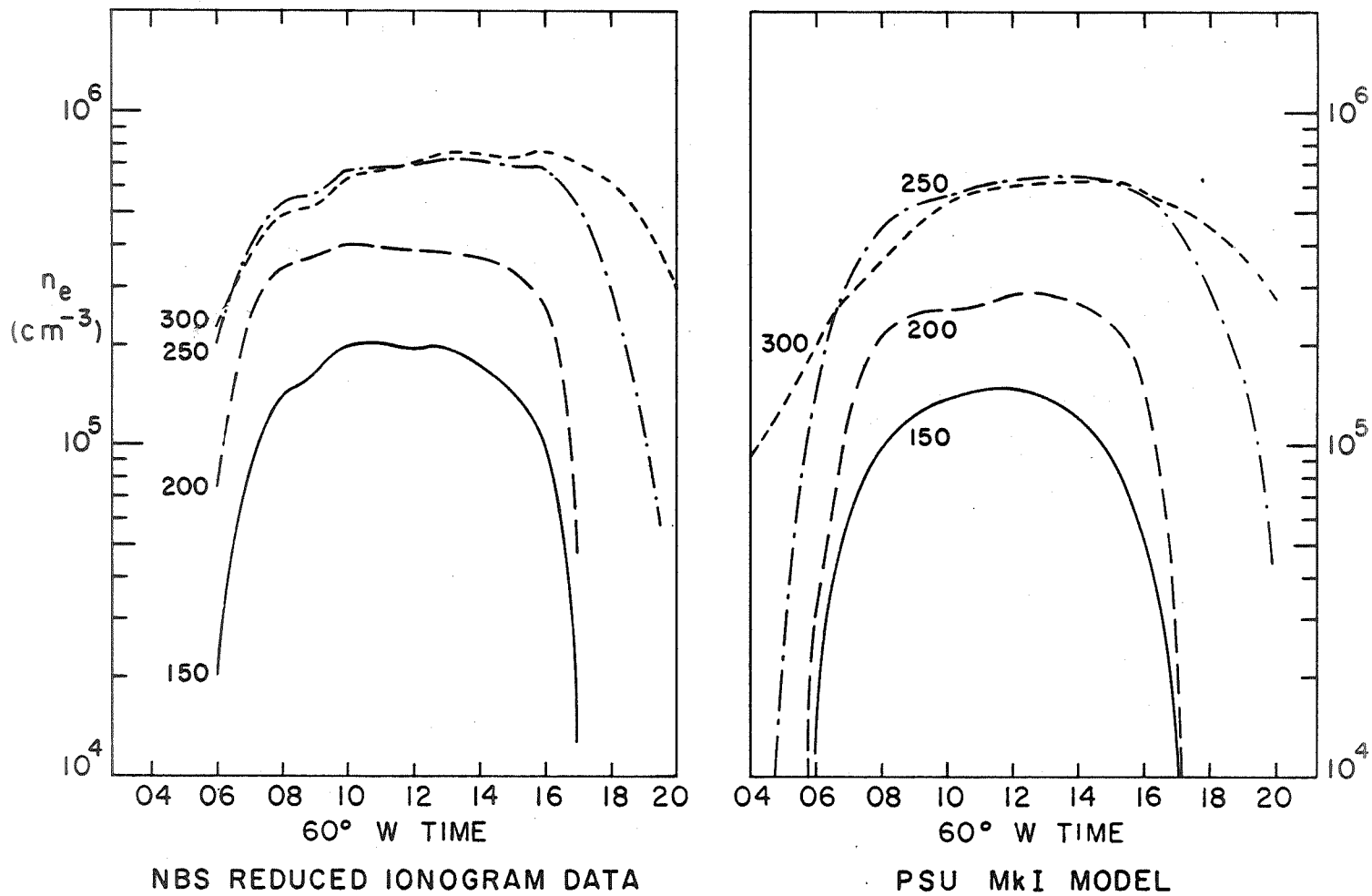


Figure 14 Electron densities for St. Johns, Newfoundland,
 March 1961, $\bar{S}_{10.7} = 103$.

Figures 15, 16, 17 and 18 show the comparisons for a medium level of solar activity for summer and winter. It is apparent that the densities in the 100 to 200 km range agree well in the summer at both St. Johns and Grand Bahama Island. The winter values are of the order of 15% too low at Grand Bahama Island and 25% too low at St. Johns when compared with the measured profiles. These differences are probably due to seasonal variations in the neutral atmosphere not taken into account in the C. I. R. A. model.

Two types of error are likely to arise in using models to establish boundary conditions. The first due to departures of the behavior on any given day from some average behavior observed at that location over an extended period and the second due to errors in the geographical interpolation procedure. The interpolation errors will increase at locations remote from stations for which data for the model were derived but will still be present even for stations included due to inexactness or smoothing inherent in the numerical model used to represent the parameter. To examine these types of error a comparison has been made in Figure 19 of peak electron densities measured at Arecibo for one summer and one winter day with two ionospheric models. The first is a model derived from all available data from the ionosonde at Puerto Rico for the year 1961 to 1962 for which the K_p index was less than 4.5. The mean monthly values observed at each hour for summer and winter months were fitted separately to linear relationships with the 2500 MHz solar flux, and these values were interpolated for the actual levels of solar activity on the days in question. The location of the ionosonde which made the measurements was only about 60 km. from the Arecibo Observatory so that differences in ionospheric conditions should be negligible. This

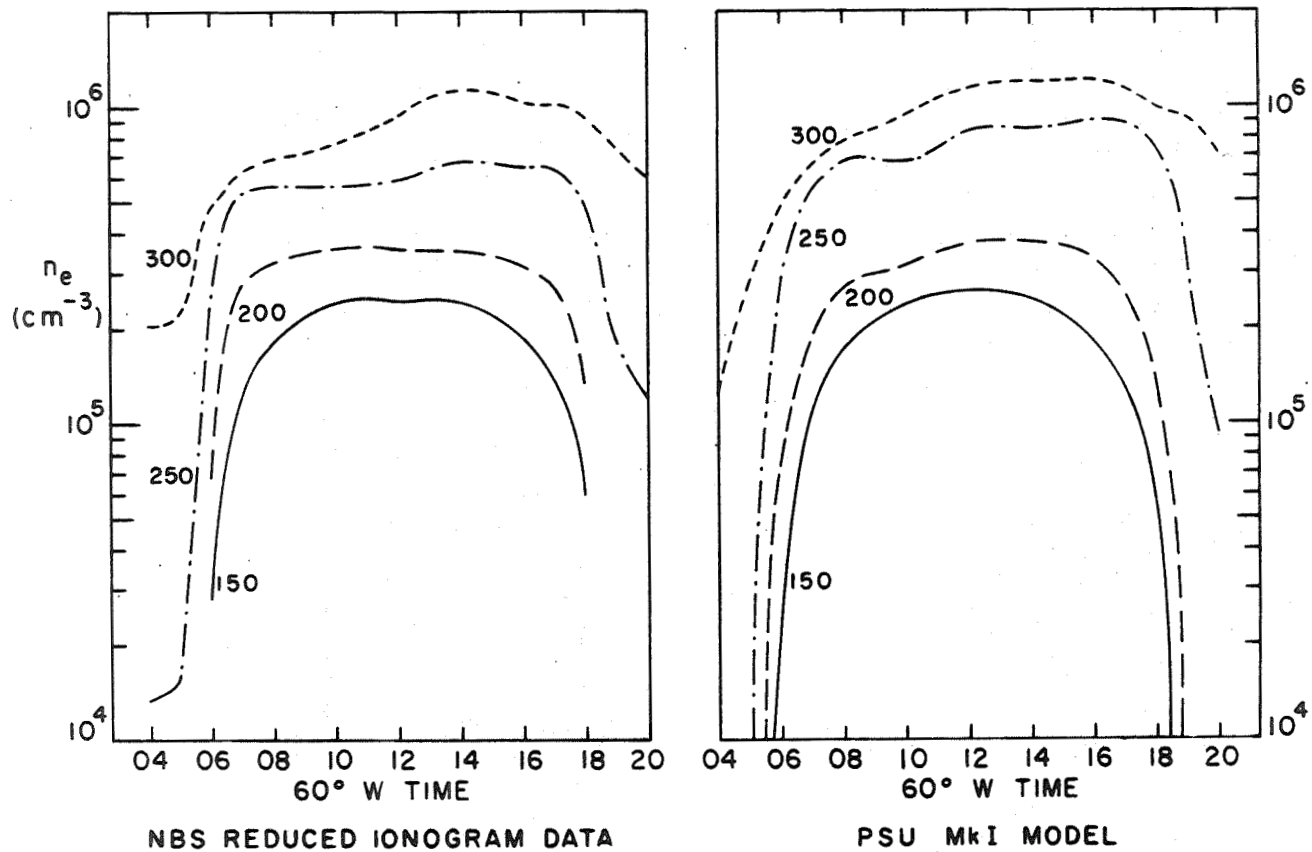


Figure 15 Electron densities for Grand Bahama Island, December 1960, $\bar{S}_{10.7} = 141$.

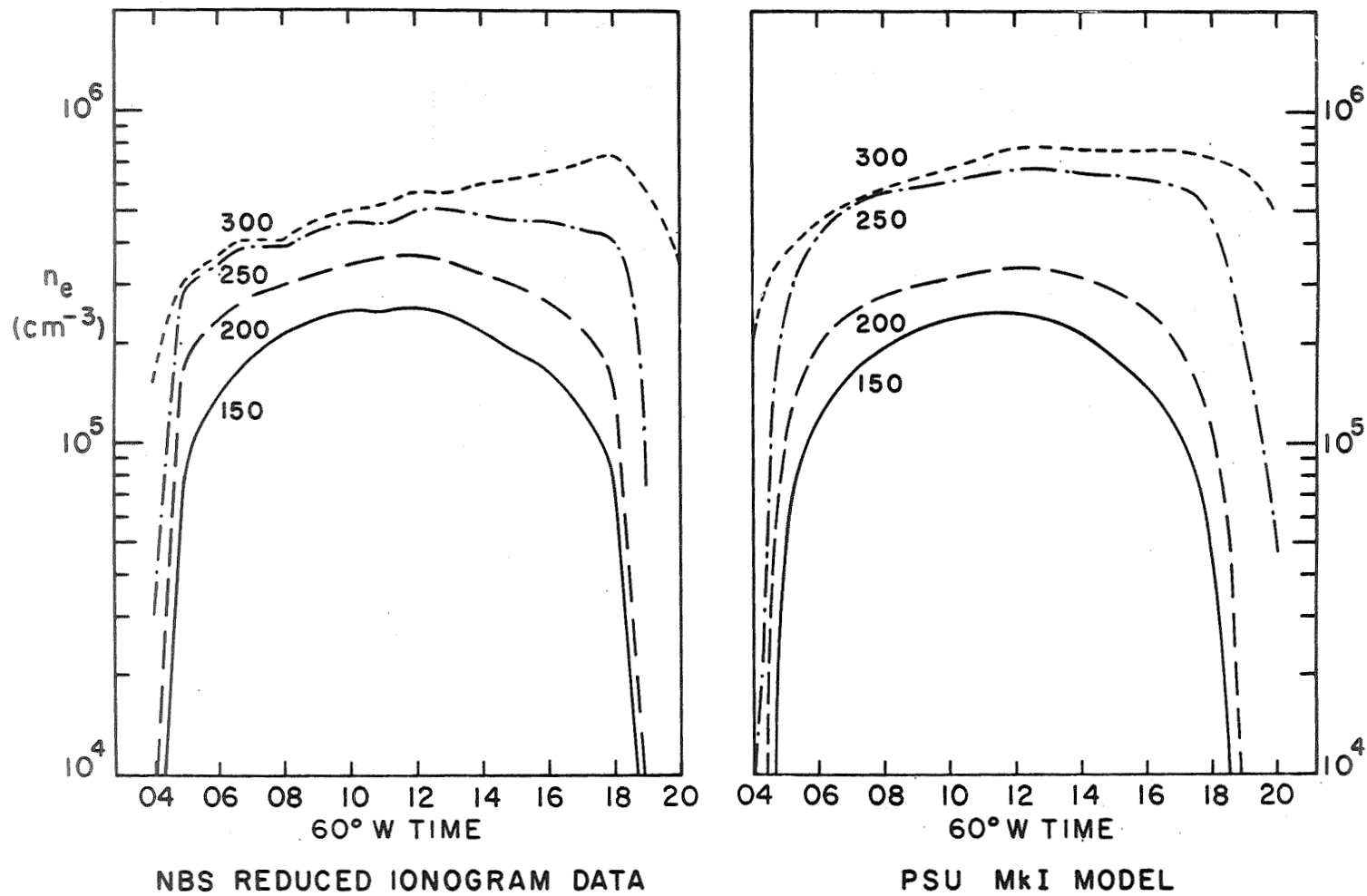


Figure 16 Electron densities for St. Johns, Newfoundland, May 1960, $\bar{S}_{10.7} = 161$.

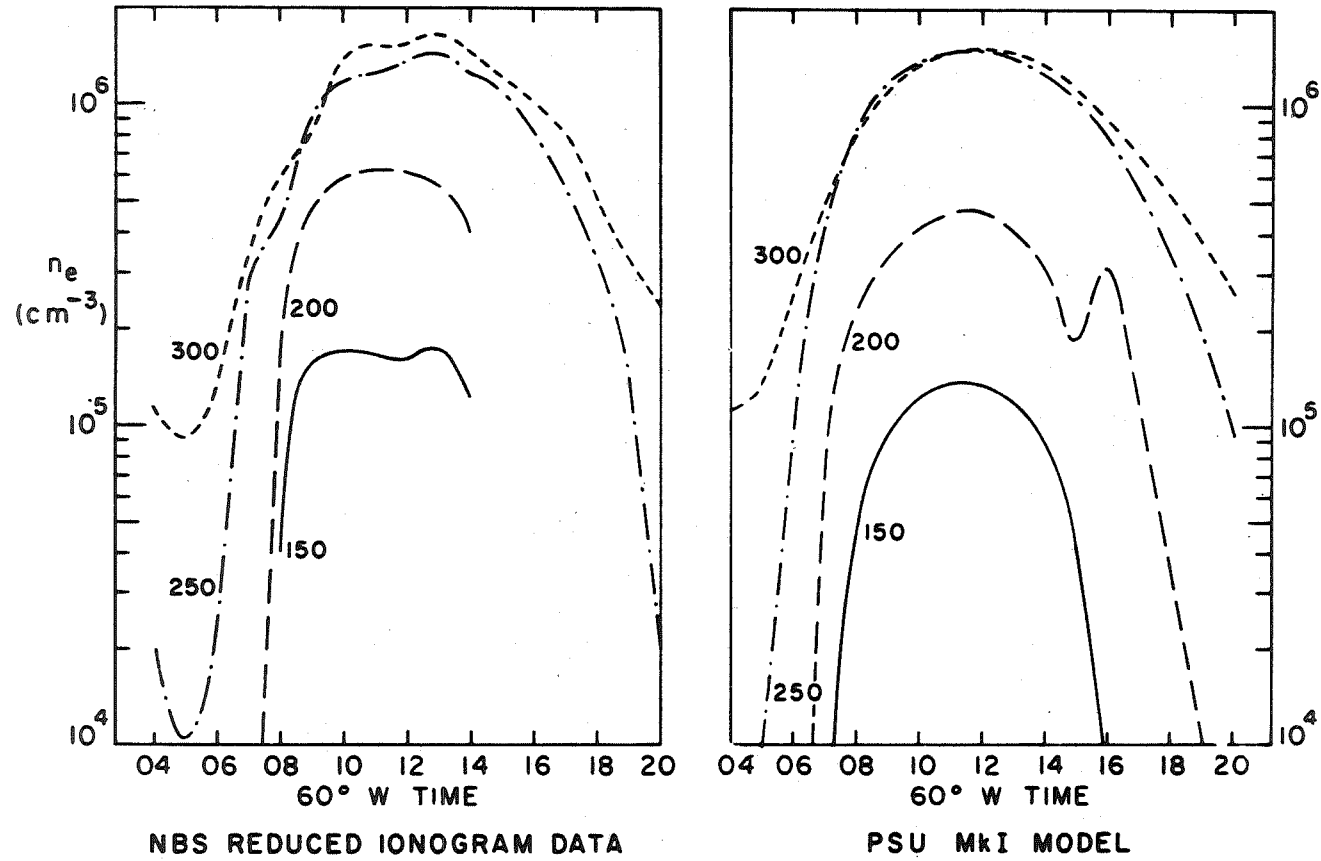


Figure 17 Electron densities for St. Johns, Newfoundland, November 1960, $\bar{S}_{10.7} = 146$.

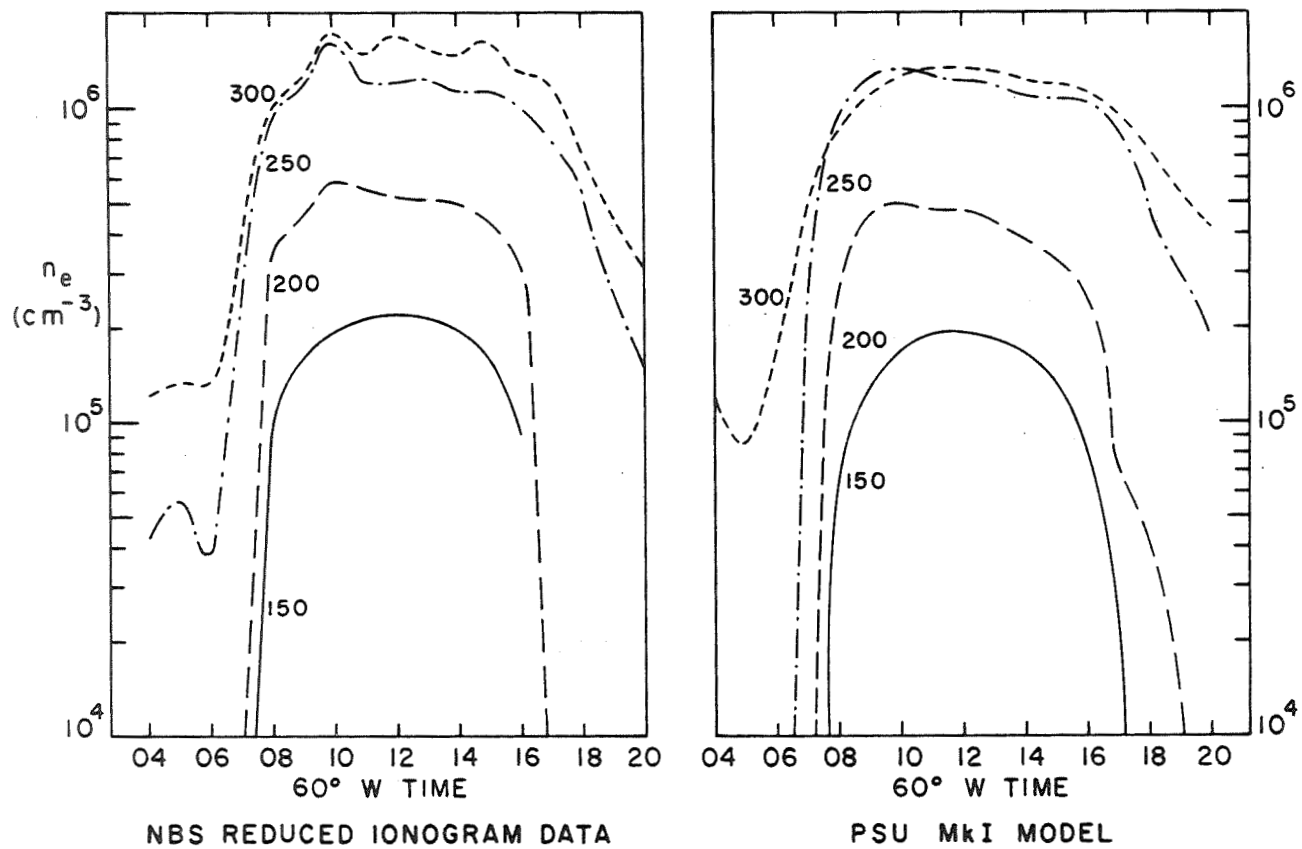


Figure 18 Electron densities for Grand Bahama Island, December 1960, $\bar{S}_{10.7} = 141$.

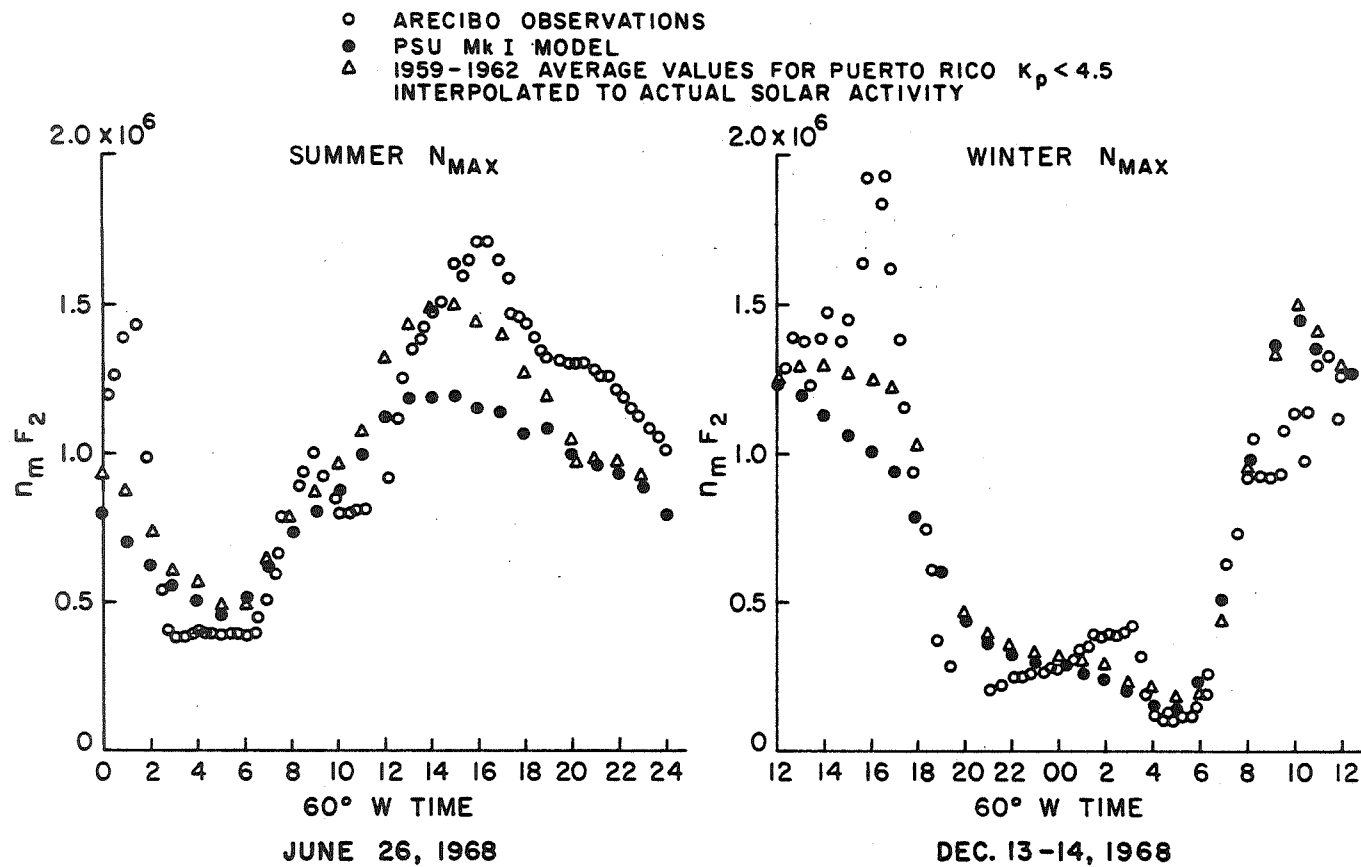


Figure 19 Comparison of Arecibo data with two models for F2 region peak electron density.

model should then represent quite accurately the average behavior at Arecibo. The second set of values are from the Penn State Mk 1 model which in the case of $N_m F_2$ means essentially the C. C. I. R. (1967) values with a slightly different method of interpretation for solar activity. As Puerto Rico was included in the data bank for the C. C. I. R. (1967) model differences between the two sets of values should represent mainly differences due to geographical fitting. It is apparent that the agreement in almost all cases is better for the model derived from Puerto Rican data alone. In particular the agreement is considerably closer on both days between 12 and 16 hours. Very large departures from both models are observed at around 16 hours on December 13, 1968. Similar large differences from average values are frequently observed at Arecibo and elsewhere and have been discussed in detail by Douppnik and Nisbet (1968).

Petrie and Lockwood (1969) have compared C. C. I. R. predictions with Alouette topside sounder measurements and found differences of as much as 0.7 MHz in monthly median values of $f_x F_2$. This would correspond to an error in the electron density of about 30%. A factor of considerable interest is the fluctuations in the electron density at one location. Based on their data it would appear that the daily values of $f_x F_2$ had a standard deviation of 0.55 MHz in June 1963 and 0.84 MHz in December 1963 about the mean monthly value. These would correspond to fluctuations in $N_m F_2$ having a standard deviation of 18% and 25% respectively.

Most of the data from which values of $H_m F_2$ were obtained were in the form of mean monthly profiles which had been averaged in the region of the peak by adding a Chapman function top with a scale height of 100 km. When the models based on these data were compared with incoherent scatter sounding measurements at Arecibo, Millstone

and Nançay it was discovered that the model values were usually higher by about 30 km. This error is surprisingly large compared with other estimates. It is known, however, that topside and bottomside profiles can differ by about 75 km. Jackson (1969) has shown that better agreement between electron content measurements from the ground trace and the reduced profiles can be obtained by reducing the virtual range by values ranging from zero to 40 km. The present results would indicate that similar errors may be present in ground based soundings. Comparisons of reduced ionograms and incoherent scatter sounding measurements at Arecibo by Doupnik and Nisbet (1966) and Smith (1970) did not show such errors. It would therefore seem that the errors may have been introduced in the averaging procedure used to obtain the mean profiles, in the method of fitting the relatively small amount of data to a global model, or in a systematic error such as occurs with topside sounders. Wright (1962) has shown that the standard deviation for values $H_m F_2$ was ~ 15 km at noon for both Newfoundland and Puerto Rico based on data from May 1959 to April 1960. Such variations must be taken into account when comparing data for individual days with a model.

Perhaps the most stringent comparison of the models with actual data is with the incoherent scatter soundings. Figures 20 and 21 show comparison of the mean monthly altitudes of constant plasma frequency at Millstone for one summer and one winter month. Figure 22 shows a comparison of a day's data at Nançay. Figures 23 and 24 show comparisons for the summer and winter day at Arecibo discussed previously with respect to Figure 19. In each case it is apparent that there is general agreement in the profiles although marked differences occur at sunrise and sunset and the percentage errors can be quite large at and above the F2 peak.

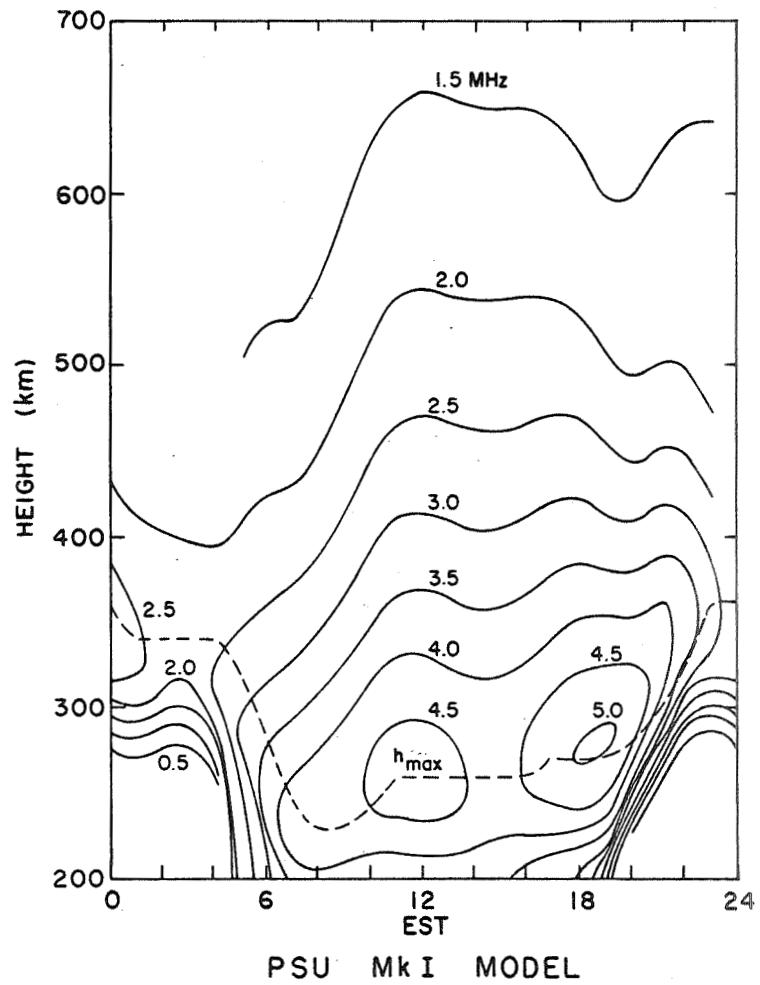
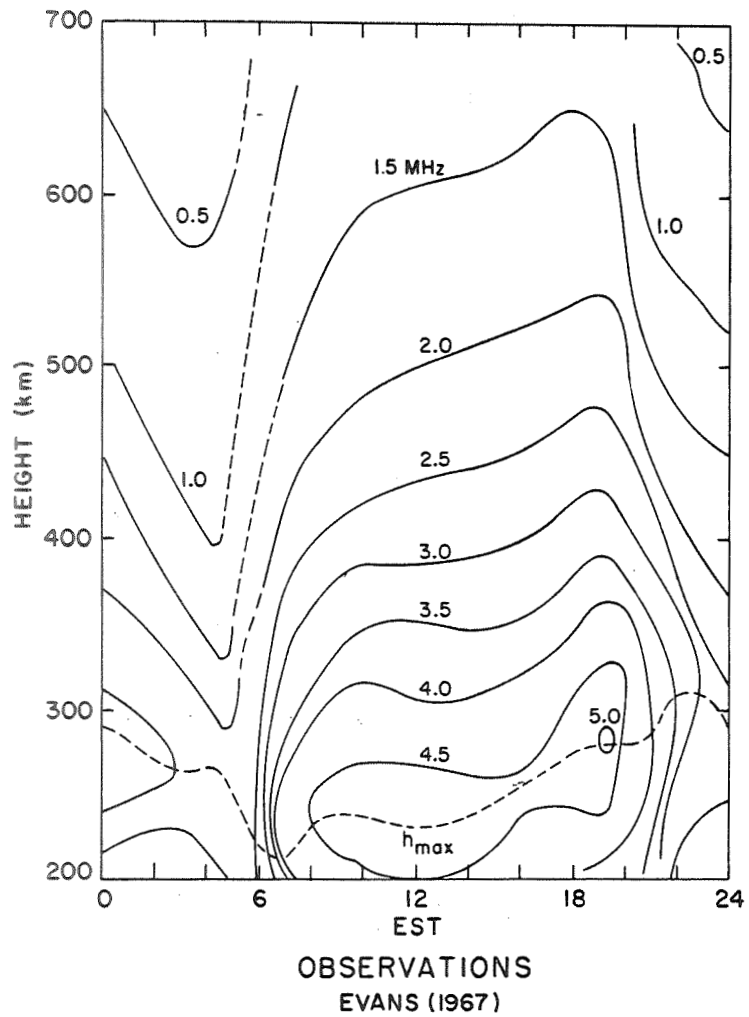


Figure 20 Plasma frequency Millstone Hill, July 1964, $\bar{S}_{10.7} = 68$.

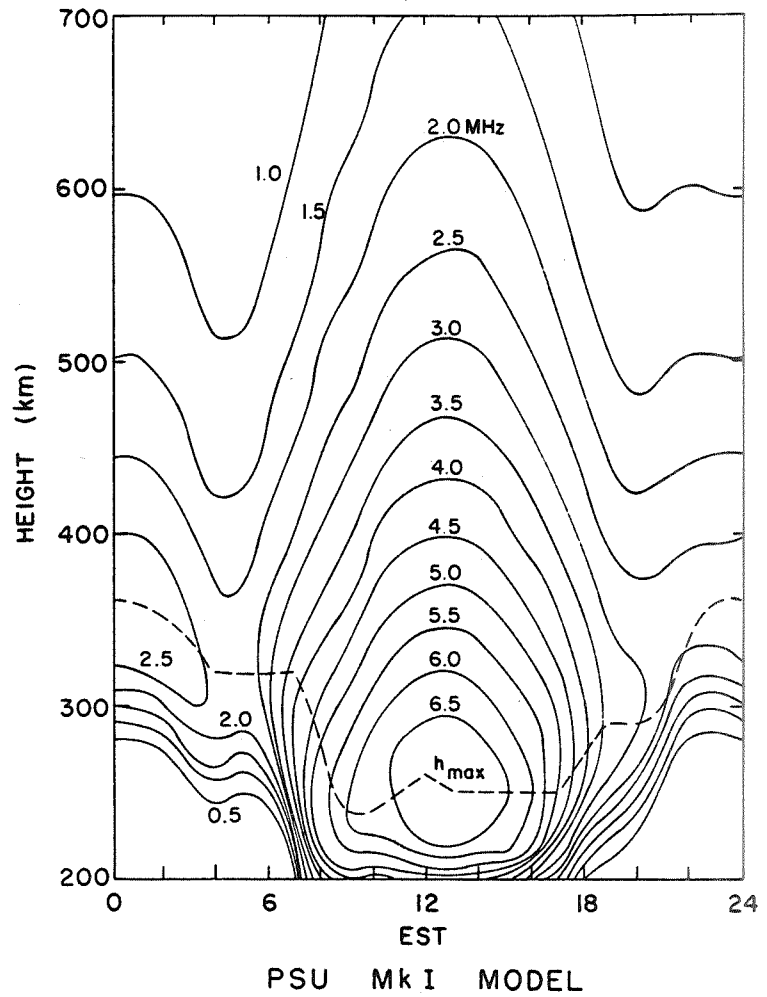
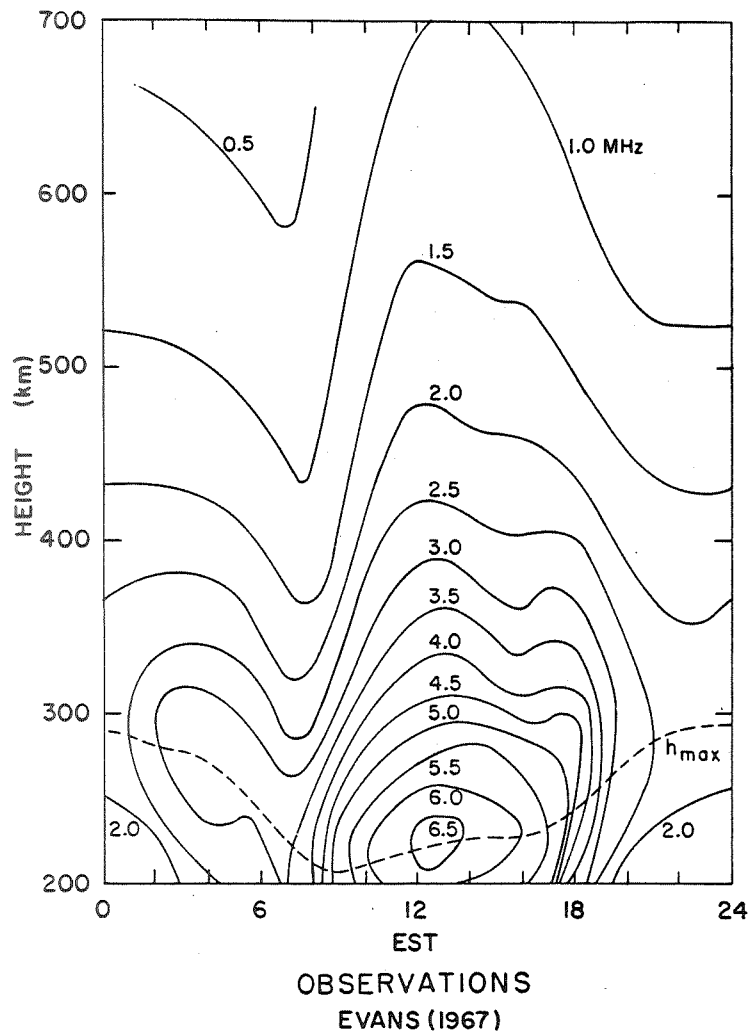
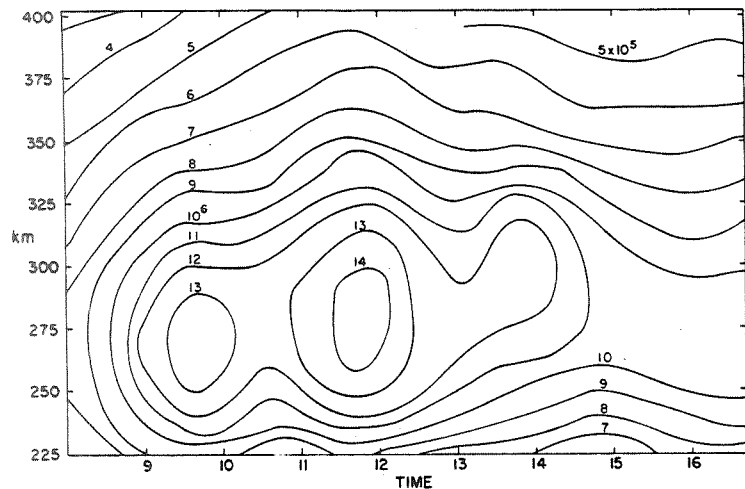
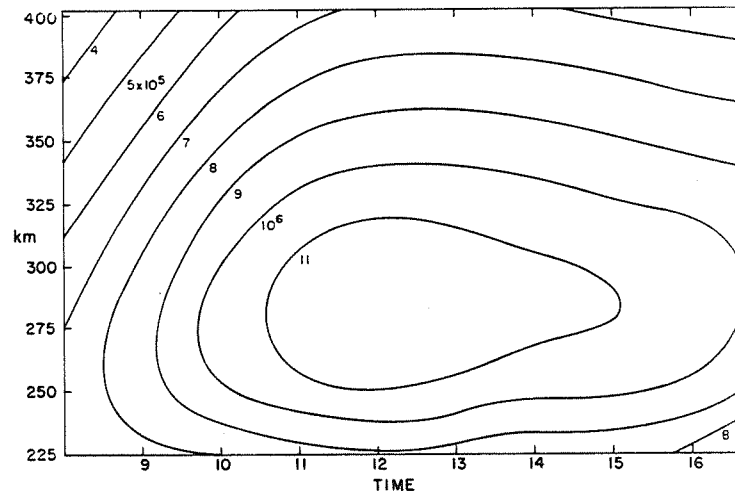


Figure 21 Plasma frequency Millstone Hill, November 1964, $\bar{S}_{10.7} = 73$.



INCOHERENT SCATTER OBSERVATIONS
VASSEUR AND WALDTEUFEL (1968)



P.S.U. MARK I MODEL

Figure 22 Plasma frequency, Nancay, March 12, 1967, $\bar{S}_{10.7} = 135.9$.

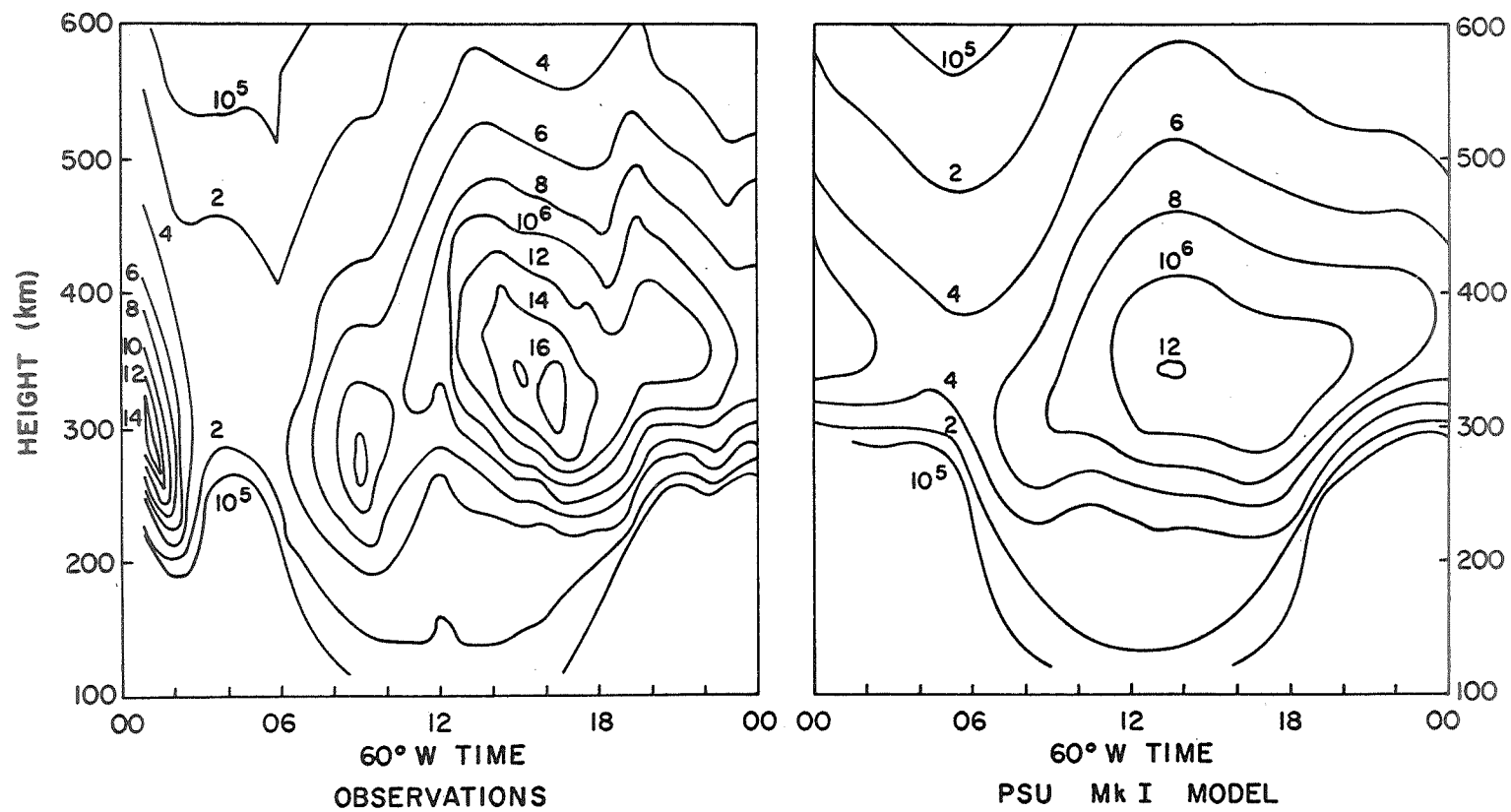


Figure 23 Plasma frequency, Arecibo Observatory, June 26, 1968, $S_{10.7} = 141.40$.

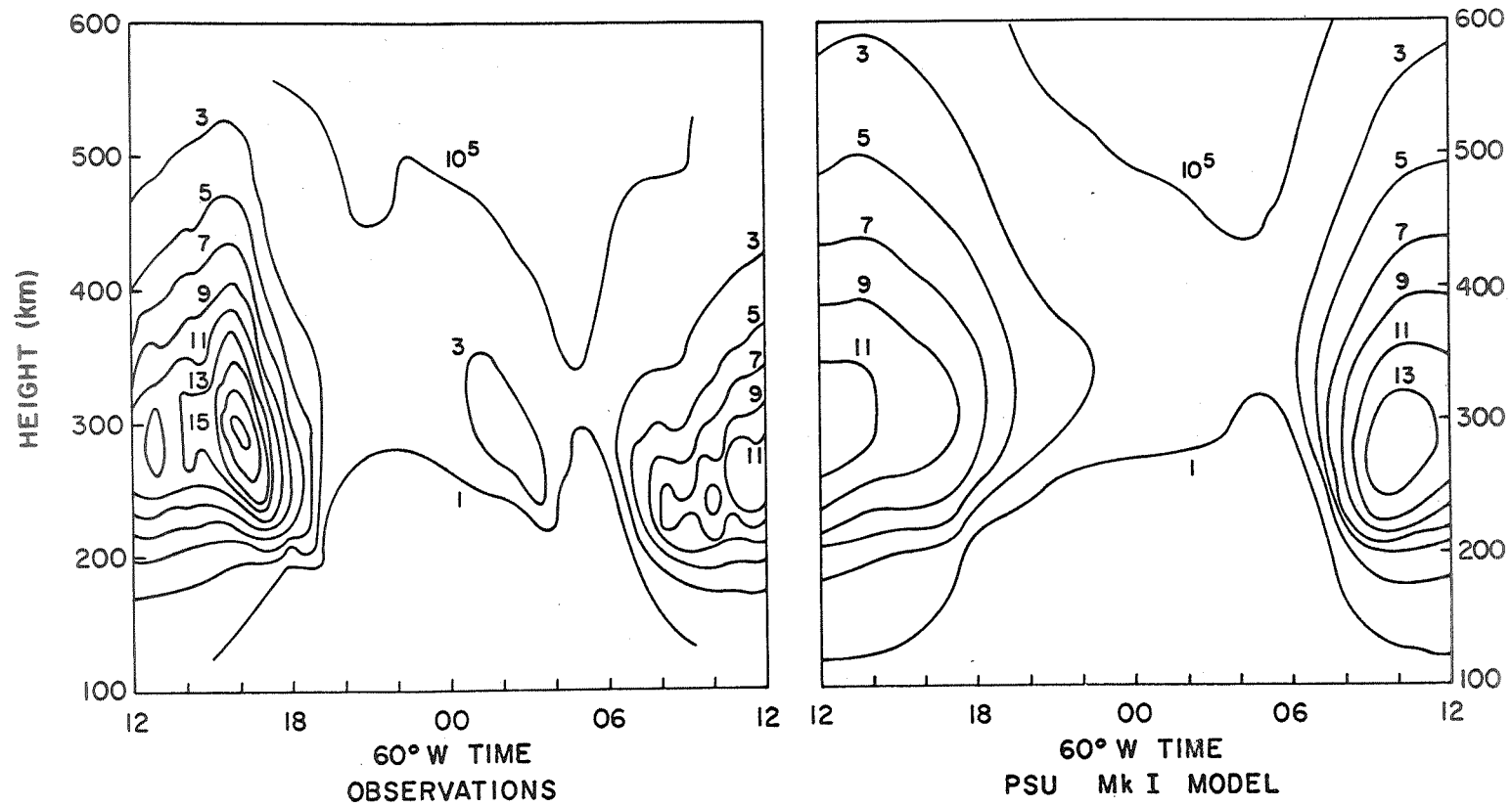


Figure 24 Plasma frequency, Arecibo Observatory, December 14, 1968, $S_{10.7} = 135.7/138.6$.

Figure 25 shows a comparison of the values reported by Reddy and Matsushita (1968) for the six month mean blanketing sporadic E critical frequency $F_b E_s$. Figure 26 gives the comparisons of the percentage of time the blanketing frequency exceeded given values in the time period 01-04 hours and Figure 27 gives similar results for 13 to 16 hours. In these graphs P1 corresponds to 0.5 MHz, P2 to 2 MHz, P4 to 4 MHz, P5 to 5 MHz and P6 to 6 MHz. The model values were calculated using the average value of the peak E_s electron density, the probability of observing E_s and the standard deviation for the middle of time period for the middle day of each month in the period from 1958 to 1968 using measured values of 10.7 cm solar flux. Six month running means were then computed for each of the required parameters. This is of course a self comparison but does provide an overall check of a rather complicated reduction procedure and a measure of the degree to which the assumed geographical, temporal and solar activity interpolation formulas fit the data. Considering the assumptions made it is perhaps not surprising that the agreement is poorest for Adak which is at a high geographic latitude and low magnetic latitude. Differences are also quite large for Kokobunji ($\sin x = .6935$), Port Stanley ($\sin x = -.7354$) and Grand Bahama Island ($\sin x = .7412$) because all of these stations had quite similar values for the magnitude of $\sin x$. As this parameter was used as the only geographic variable, the least squares fitting technique constrained the model to give similar results for these three stations apart from the seasonal reversal in the southern hemisphere.

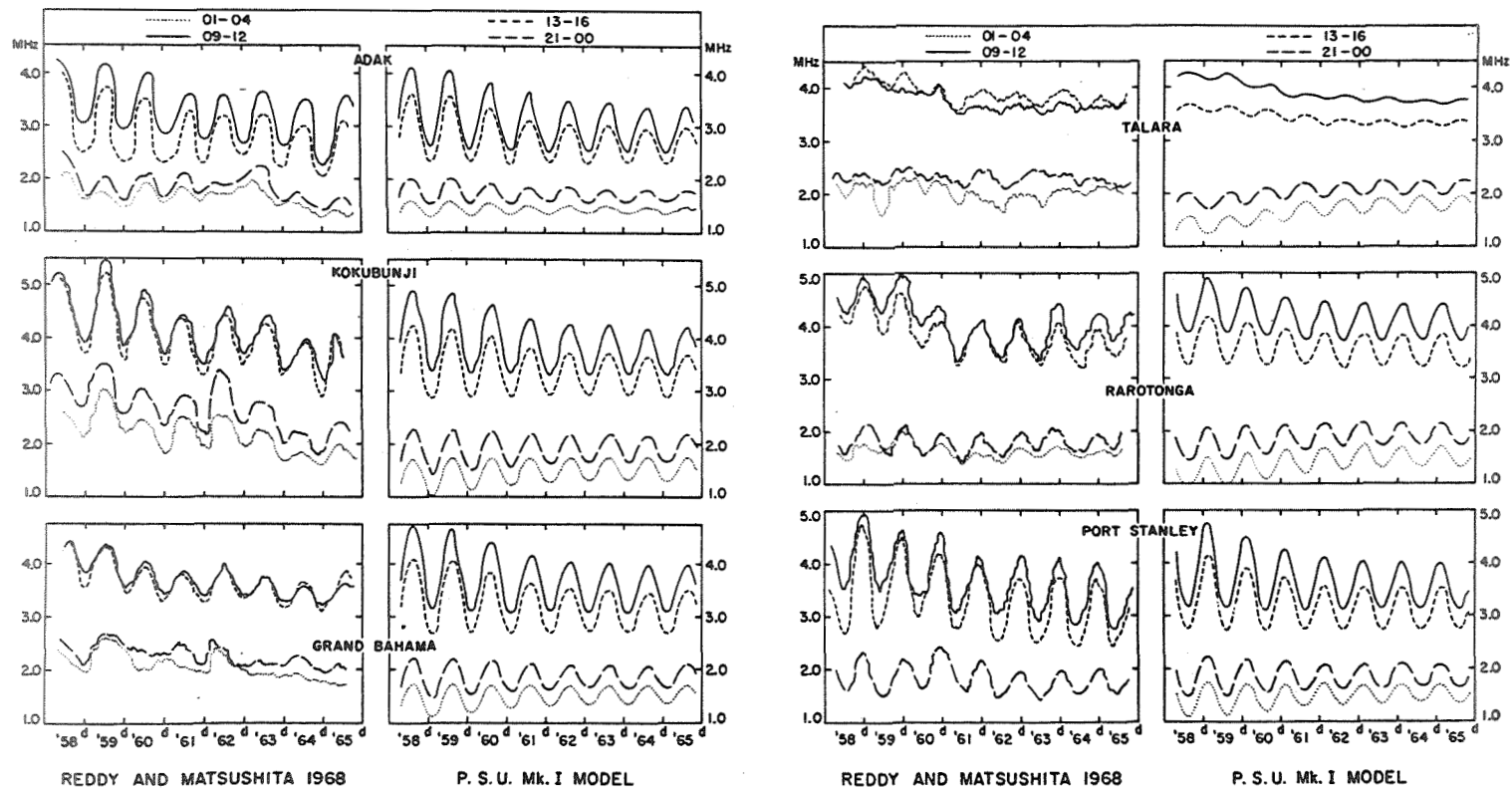


Figure 25 Six month running average of f_{pE_s} during 1958-1965; d indicates December of each year.

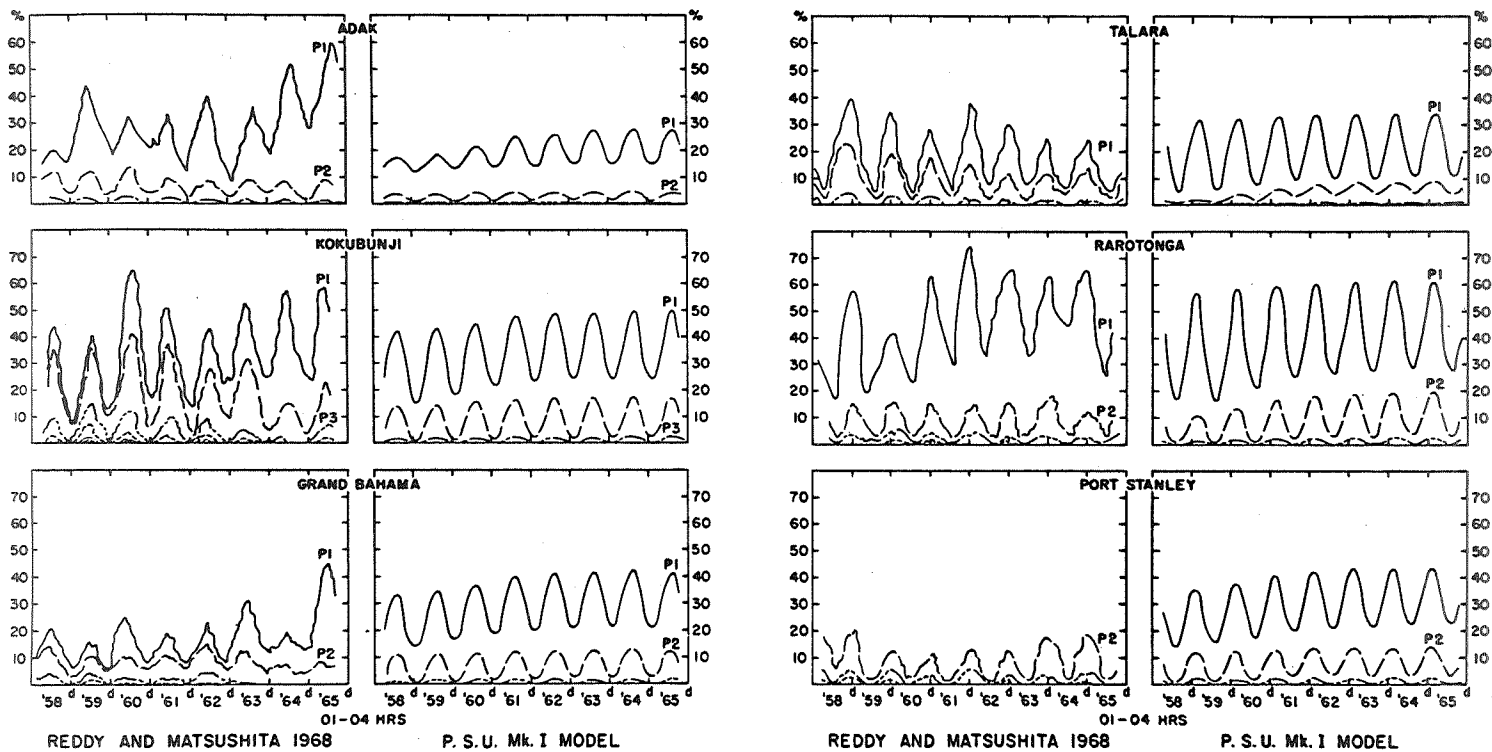


Figure 26

Six month running averages of P1, P2, P3, P4, P5 and P6 during 1958-1965; curves refer to the average P values in the post-midnight period of 01-04 hours. In the observed data P1 curve for Port Stanley is not shown because it is not reliable.

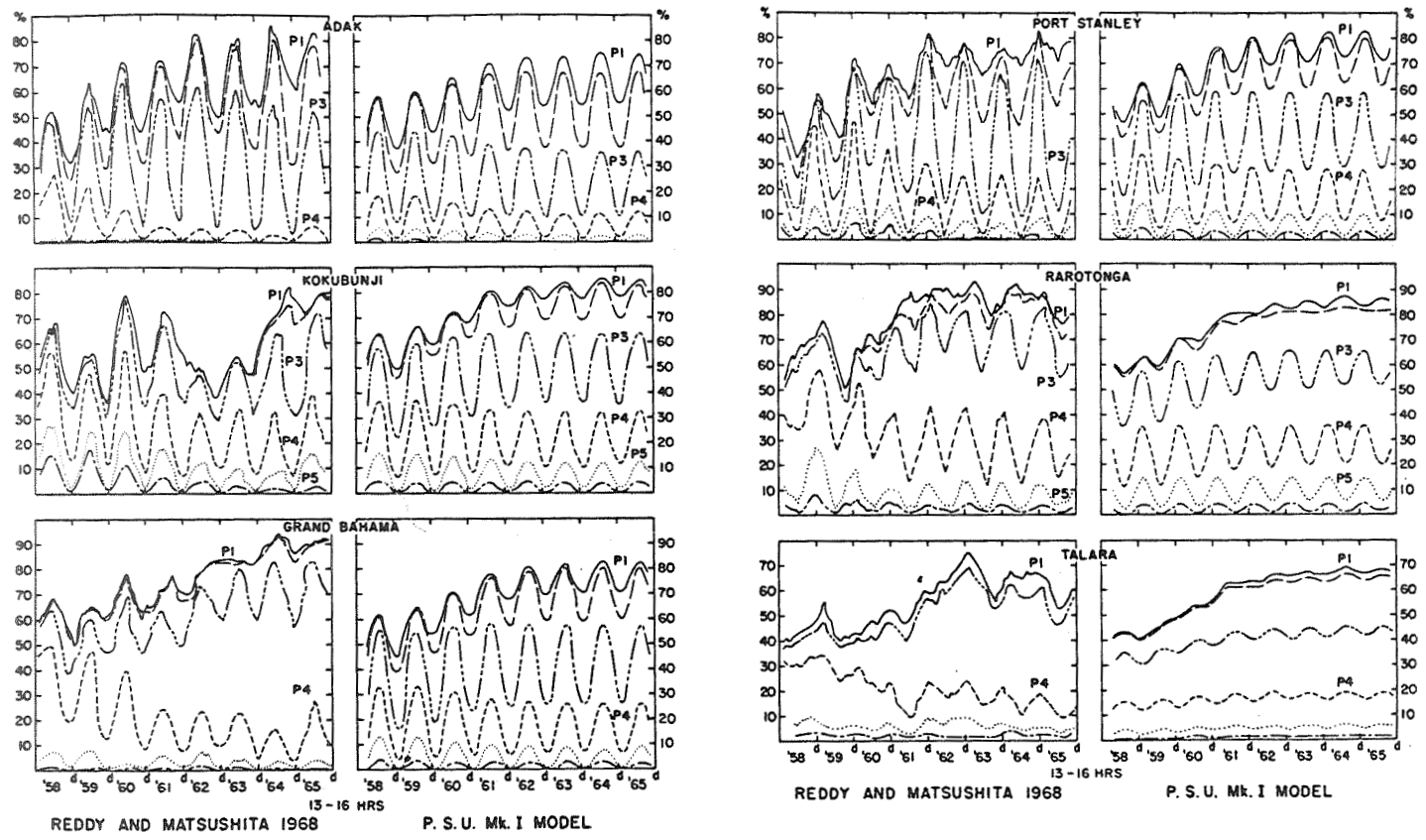


Figure 27 Six month running averages of P1, P2, P3, P4, P5 and P6 (top to bottom in that order) during 1958-1965); curves refer to the average P values in the afternoon 13-16 hours.

Conclusions

The model presented represents a very simplified picture of the ionosphere even as it is understood at present. Obvious extensions are the inclusion of a more complete theory of the F_2 region including drifts and electric fields possibly along the lines of the models of Sterling et al (1969), and of the electron and ion temperatures possibly along the lines of the work of Herman and Chandra (1969). The behavior of the helium and hydrogen ions has been treated in an over simplified manner and the use of equilibrium solutions for the F region neglects very important terms in the continuity equations. The effects of field line curvature have been neglected so that the equatorial ionosphere is undoubtedly poorly represented and effects such as particle precipitation which are of importance in the high latitude ionosphere were not considered.

The second major inadequacy is in the knowledge of the boundary conditions. While the data on the peak electron density incorporated in the C. C. I. R. model were based on all available data from some 134 stations for four years, the data on other parameters was based on from six to eight stations. It is regrettable that at this time after many years of ionospheric measurements that so little data is available on which to base a model. It would seem to be of considerable importance that the large body of data on ionospheric parameters be reduced in a consistent manner. In the measurement of most parameters it is desirable that the statistical distributions should be determined rather than such parameters as average values which may well be meaningless when the method of observation truncates the distribution. The parameters of the statistical distribution may then be correlated with better understood geophysical variables.

The model presented is thus a very preliminary attempt at the production of a comprehensive ionospheric model that will reproduce the main features of the geographical diurnal, seasonal, and solar cycle behavior of the midlatitude ionosphere under quiet conditions.

It is felt that the advantages of a computer model of the ionosphere have been demonstrated. The interaction of as many parameters as are necessary to give even the crudest picture of ionospheric behavior would require an unmanageable number of tables or graphs. A computer model is immediately comparable with data from any source, be it in the form of satellite electron content measurements, bottomside soundings, radio wave propagations, topside sounder satellite measurements or incoherent scatter soundings. A computer model can incorporate very complicated neutral atmospheric behavior, solar radiation data, absorption and ionization cross sections and boundary conditions. It is relatively simple to update the model as new data become available. The complexity of the model is only limited by the size of the computer, the time to perform the calculations, the knowledge of ionospheric theory, and the boundary conditions. The present program takes 18 seconds on an I. B. M. 360 model 67 computer to calculate the models for 24 hours for one station. This corresponds to a cost of about \$2.16 for 24 hours or 9 cents per model.

The model has already shown up several interesting anomalies and has been helpful in planning series of experiments. It is expected that with further development, its field of application will increase considerably.

While a computer model has the great advantage that an electron density profile can be obtained for any desired location and time in some

applications it is convenient to have data in tabular form for a number of locations, times and solar activities. For these purposes a set of tables has been prepared from the Penn State Mk I Ionospheric Model by Nisbet (1970) at intervals of 20° latitude from -60° to $+60^{\circ}$, of 90° longitude, 2 hours in time and for two levels of solar activity.

REFERENCES

- Bates, D. R. (1959), Some problems concerning the terrestrial atmosphere above about 100 km level, Proc. Roy. Soc. A253, 451-462.
- Brace, L. H., B. M. Reddy and H. G. Mayer (1967), Global behavior of the ionosphere at 1000-kilometers altitude, J. Geophys. Res., 72, 265-283.
- C.C.I.R. (1967), C.C.I.R. Report 340 Atlas of Ionospheric Characteristics, Union Internationale des telecommunications, Geneve.
- Chan, K. L. and L. Colin (1969), Global electron densities from topside soundings, Proc. I.E.E.E., 57, 990-1004.
- C.I.R.A. (1965), Cospar International Reference Atmosphere, Compiled by working group IV, COSPAR, North Holland, Amsterdam.
- Douppnik, J. and J. S. Nisbet (1966), Electron temperature and density fluctuations in the daytime ionosphere, in Electron Density Profiles in the Ionosphere and Exosphere, edited by J. Frihagen, 493-504, North Holland, Amsterdam.
- Douppnik, J. R. and J. S. Nisbet (1968), Fluctuations of electron density in the daytime F-region, J. Atmos. Terr. Phys., 30, 931-961.
- Evans, J. V. (1967), Millstone Hil Thomson scatter results for 1964, Planet. Space Sci. 15, 1387-1405 .
- Farley, D. T. Jr. (1966), Observations of the equatorial ionosphere using incoherent backscatter, in Electron Densities in the Ionosphere and Exosphere, edited by J. Frihagen, 446-469, North Holland, Amsterdam.
- Fite, W. L. (1969), Positive ion reactions, Canadian Journal of Chemistry 47, 1797-1807.
- Hall, L. A., J. E. Higgins, C. W. Chagnon and H. E. Hinteregger (1969), Solar-cycle variation of the extreme ultraviolet radiation, J. Geophys. Res., 74, 4181-4183.

- Herman, J. R. and S. Chandra (1969), The influence of varying solar flux on ionospheric temperatures and densities: A theoretical study, *Planet. Space Sci.*, 17, 815-840.
- Hinteregger, H. E., L. A. Hall and G. Schmidke (1965), Solar XUV radiation and neutral particle distribution in July 1963, in *Space Research V*, edited by D. G. King-Hele, P. Miller and G. Righini, 1175-1190, North-Holland, Amsterdam.
- Hinteregger, H. E. (1967), The effects of solar XUV radiation on the earth's atmosphere, IQSY-COSPAR Symposium, London, Paper III-1, *Annals of the IQSY* 5, 305- (1969).
- Jackson, J. E. (1969), Topside ionograms and electron density profiles, *Proc. I.E.E.E.*, 57, 960-976.
- Jelly, D. H. and L. E. Petrie (1969), The high-latitude ionosphere, *Proc. I.E.E.E.*, 57, 1005-1012.
- Kasner, W. H. and M. A. Biondi (1967), Electron-ion recombination studies in oxygen, *Bull. Am. Phys. Soc.*, 12, p. 218.
- Manson, J. E. (1967), The spectrum of the quiet sun between 30 and 128A for November 1965, *Astrophys. J.*, 147, 703-710.
- Manson, J. E. (1968), Instrumental recalibration and refinement of solar ultra-soft X-ray intensities, *Astrophys. J.*, 153, L 191.
- Matsushita, (1966), Sporadic E and ionospheric currents, *Radio Sci.*, 1, 204-211.
- Matuura, N. and T. Ondoh (1969), The structure of the topside ionosphere deduced from Alouette data, *Proc. I.E.E.E.*, 57, 1150-1153.
- Nisbet, J. S. (1963), Factors controlling the shape of the upper F region under daytime equilibrium conditions, *J. Geophys. Res.*, 68, 6099-6112.

- Nisbet, J. S. (1968), Photoelectron escape from the ionosphere, J. Atmos. Terr. Phys., 30, 1257-1278.
- Nisbet, J. S. (1970), Tables from the Penn State Mark I ionospheric model, Sci. Rpt. 362(E), Ionosphere Research Laboratory, The Pennsylvania State University, University Park, Pa. 16802.
- Petrie, L. E. and G. E. K. Lockwood (1969), On the prediction of F-layer penetration frequencies, Proc. I.E.E.E., 57, 1025-1028.
- Reddy, C. A. and S. Matsushita (1968), Solar cycle variation of blanketing sporadic E, J. Geophys. Res., 73, 1641-1660.
- Reddy, C. A. and M. M. Rao (1968), On the physical significance of the Es parameters fbEs, fEs and foEs, J. Geophys. Res., 73, 215-224.
- Schmerling, E. R. (1958a), Ionospheric electron densities for Washington D. C., Panama, Talara and Huancayo for July 1957, Sci. Rpt. 105, Ionosphere Research Laboratory, The Pennsylvania State University, University Park, Pa. 16802.
- Schmerling, E. R. (1958b), Ionospheric electron densities for Washington D. C., Panama, Talara and Huancayo for August 1957, Sci. Rpt. 108, Ionosphere Research Laboratory, The Pennsylvania State University, University Park, Pa. 16802.
- Schmerling, E. R. (1958c), Ionospheric electron densities for Washington D. C., Panama, Talara and Huancayo for September 1957, Sci. Rpt. 111, Ionosphere Research Laboratory, The Pennsylvania State University, University Park, Pa. 16802.
- Schmerling, E. R. (1959a), I.G.Y. true height electron density reports 4, 5, 6, Sci. Rpt. 118, Ionosphere Research Laboratory, The Pennsylvania State University, University Park, Pa. 16802.

- Schmerling, E. R. (1959b), Ionospheric electron densities for Washington D. C., Panama, Talara and Huancayo for April-May-June 1958, Sci. Rpt. 128, Ionosphere Research Laboratory, The Pennsylvania State University, University Park, Pa. 16802.
- Schmerling, E. R. (1960a), Ionospheric electron densities for Washington D. C., Panama, Talara and Huancayo for July-August-September 1958, Sci. Rpt. 130, Ionosphere Research Laboratory, The Pennsylvania State University, University Park, Pa. 16802.
- Schmerling, E. R. (1960b), Ionospheric electron densities for Washington, D. C., Panama, Talara and Huancayo for October-November-December 1958, Sci. Rpt. 137, August 1, Ionosphere Research Laboratory, The Pennsylvania State University, University Park, Pa. 16802.
- Smith, D. H. (1970), The comparison of electron density profiles obtained from backscatter observations and ionogram analysis, Radio Science, 5, 685-692.
- Stein, J. A. and J. C. G. Walker (1965), Models of the upper atmosphere for a wide range of boundary conditions, J. Atmos. Sci., 22, 11-17.
- Sterling, D. L., W. B. Hanson, R. J. Moffett and R. G. Baxter (1969), Influence of electromagnetic drifts and neutral air winds on some features of the F₂ region, Radio Science, 4, 1005-1023.
- Swartz, W. E. (1969), F-region ambient electron heating, paper presented at the 1969 Spring AGU meeting in Washington, D. C., April 25.
- Swider, W. (1964), The determination of the optical depth at large solar distance, Planet. Space. Sci., 12, 761-782.
- Young, J. M., G. R. Carruthers, J. C. Holmes, C. Y. Johnson and H. P. Patterson (1968), Detection of lyman- β and helium resonance radiation in the night sky, Science, 160, 990-991.

Vasseur, G. and P. Waldteufel (1968), Etude par diffusion de Thompson de la production et de la recombinaison dans la region-F de l'ionosphere diurne, J. Atmos. Terr. Phys. 30, 779-794.

Weller, C. S. and M. A. Biondi (1968), Temperature dependence of recombination of NO^+ ions and electrons, Bull. Am. Phys. Soc., 13, p. 199.

Wright, J. R. (1962), Diurnal and seasonal changes in the structure of the mid-latitude quiet ionosphere, NBS J. Research, Radio Propagation, 66D, 297-312.

APPENDIX

Fortran Program

```
C      PENN STATE MK I
C      IONOSPHERIC MODEL
C      13 MARCH 1970  VERSION 15.10
C      APPROVED FOR TESTING ONLY.
C      J. S. NISBET AND R. L. DIVANY
REAL*8  HEADER(10),DUMMY(10)
REAL*4  SINX(8),SINSQ(8),E(5,45),X(45),HMAX(24)
REAL*4  NE(45,24),U(13,76,2),FLAT(8),FLON(8),NMAX(24)
REAL*4  HL(24),H(24)
REAL*4  CONT(24) ,AVNES(24),ESPROB(24),SIGMA(24)
INTEGER CC1,CC2,CC3, KK(14,2),OM,NPTS/44/
REAL*4  PLOTOP(1336)
EQUIVALENCE (PLOTOP,CC1),(PLOTOP(2),NS),(PLOTOP(3),NT),
1(PLOTOP(4),NPTS),(PLOTOP(5),MONTH),(PLOTOP(6),D),(PLOTOP(7),SN),
2(PLOTOP(8),HEADER),(PLOTOP(28),IDENT),(PLOTOP(148),FLAT),
3(PLOTOP(156),FLON),(PLOTOP(164),HL),(PLOTOP(188),H),
4(PLOTOP(212),X),(PLOTOP(257),NE)
LOGICAL*1 IDENT(60,8)
DATA IREAD/5/,IPRINT/6/,IPUNCH/7/
OM=0
C      THIS FIRST CALL TO THE MODEL SUBROUTINE IS FOR INITIALIZATION ONLY
CALL MODEL1 (X)
C*****
C*
C*      DESCRIPTION OF NECESSARY INPUT DATA
C*
C*      THERE ARE FOUR TYPES OF DATA CARDS REQUIRED BY THIS PROGRAM:
C*      1.  HEADER CARD - THIS CARD MAY CONTAIN ANY ALPHANUMERIC
C*              INFORMATION DESIRED AND IS PRINTED AT THE TOP
C*              OF EACH PAGE PRODUCED BY THE MODEL PROGRAM.
C*****  NOTICE THAT ONLY ONE SUCH CARD MAY BE INCLUDED AND IT IS *****
C*****  READ ONLY ONCE AT THE BEGINNING OF THE RUN. *****
C*
C*      2.  PARAMETER CARD - THIS CARD CONTAINS FOUR NECESSARY
C*              PARAMETERS- CC1,CC3,NP, AND TIME.
C*              CC1 IS AN INTEGER AND IS PUNCHED IN COLUMN
C*              1.  IF CC1 .GT. 0,ONLY ONE U.T. WILL BE
C*              PROCESSED FOR 1-8 STATIONS.
C*              IF CC1=0 24 HOURS U.T. WILL BE PROCESSED FOR*
C*              1 STATION ONLY.
C*              CC3 IS AN INTEGER AND IS PUNCHED IN COLUMN
C*              3.  IF CC3 .GT. 0,A TAPE WILL BE WRITTEN FOR *
C*              A SEPARATE PLOTTING PROGRAM.
C*
```

C* NP IS AN INTEGER INDICATING THE NUMBER OF *
C* STATIONS TO PROCESS AND IS PUNCHED IN COLUMN*
C* 5. *
C* TIME IS A FLOATING POINT NUMBER INDICATING *
C* THE TIME (U.T.) DESIRED TO BE PROCESSED IF *
C* CCI .GT. 0 (IN COLS. 6-10) *
C* *

CONTINUE

C* *
C* 3. STATION CARD - THIS CARD CONTAINS LATITUDE IN DECIMAL DEGREES*
C* PUNCHED IN COLUMNS 1-10. *
C* EAST LONGITUDE IN DECIMAL DEGREES IS PUNCHED *
C* IN COLUMNS 11-20. *
C* STATION IDENTIFICATION IS ALPHANUMERIC AND IS *
C* PUNCHED IN COLUMNS 21-80. *
C* *
C* 4. THIS CARD CONTAINS SN, MONTH, IDAY. *
C* SN IS THE 10.7 CM. SOLAR INDEX FOR THE TIME REQUESTED AND IS *
C* PUNCHED FLOATING POINT IN COLUMNS 1-10. SN IS ASSUMED TO *
C* HAVE BEEN ADJUSTED TO 1 A.U. ONLY IF PREFIXED WITH A MINUS *
C* SIGN. *
C* MONTH IS THE INTEGER MONTH NUMBER IN COLUMNS 19-20. *
C* IDAY IS THE INTEGER DAY NUMBER IN COLUMNS 28-30 (OPTIONAL) *
C* *
C* REPEAT (2-4) AS MANY TIMES AS NECESSARY. *

C*****

READ (IREAD,20) HEADER
5 READ (IREAD,10,END=230) CC1,CC2,CC3,NP,TIME
10 FORMAT (3I1,12,F5.1)
NS=8
IF (NP.LE.8) NS=NP
15 FORMAT (2F10.5,60A1)
20 FORMAT (10A8)
READ (IREAD,15) (FLAT(N),FLON(N),(IDENT(I,N),I=1,60),N=1,NS)
IF (NP.GT.8) GO TO 220
25 READ (IREAD,30) SN,MONTH,IDAY
30 FORMAT (F10.5,2I10)
IF (MONTH.EQ.OM) GO TO 35
C READ FOURIER COEFFICIENTS FOR FINDING F2 PEAK ELECTRON DENSITY.
C (THIS IS ONLY DONE IF THE MONTH REQUESTED IS DIFFERENT FROM THE
C LAST MONTH PROCESSED)
CALL ATLAS (KK,U,MONTH)
OM=MONTH
C THE DAY NUMBER IS OPTIONAL AND IF OMITTED THE APPROXIMATE DAY
C NUMBER OF THE MIDDLE OF THE MONTH WILL BE USED.
35 D=IFIX((MONTH-1)*365.0/12.0+15.0)
IF (IDAY.GT.0) D=IDAY
C GET S 10.7 AND S 10.7 AT 1 A.U.
R=1.0-0.016716*COS((D-5.0)*6.283186/365.0)
IF (SN.GT.0.0) GO TO 40
SX=-SN
SN=-SN/(R*R)
GO TO 45
40 SX=SN*R*R

```
45 IF (CC1.GT.0) GO TO 160
C   CCI=0 PROCESS 24 HOURS U.T. FOR 1 STATION
   NP=1
   NT=24
C   COMPUTE F2 PEAK ELECTRON DENSITY FOR TIME OR TIMES DESIRED.
   CALL TIMES (NP,FLAT,FLON,KK,U,SX,NMAX,SINX,SINSQI)
   K=1
   DO 80 I=1,NT
   H(I)=I-1
C   CALCULATE LOCAL SOLAR TIME FOR STATION DESIRED.
   HL(I)=I-1.0+FLON(K)/15.0
   IF (HL(I).LT.0.0) HL(I)=HL(I)+24.0
   IF (HL(I).GT.24.0) HL(I)=HL(I)-24.0
C   GET ALTITUDE OF F2 PEAK ELECTRON DENSITY.
   IF (SINX(K).GT.0.0) GO TO 50
   CALL HITE2 (ABS(SINX(K)),HL(I),SN,D+182.625,HMAX(I))
   GO TO 55
50 CALL HITE2 (SINX(K),HL(I),SN,D,HMAX(I))
C   GET ELECTRON DENSITY AT 1000 KM.
55 CALL TOP2 (TOP,SN,D,HL(I),SINX(K),SIGN(1.0,FLAT(K)))
C   CALCULATE F REGION MODEL.
   CALL MODEL2 (-FLON(K),FLAT(K),SN,D,HL(I),NMAX(I),HMAX(I),SINSQI(K)
1     ,X,E, TOP)
   DO 60 J=1,44
60 NE(J,I)=E(5,J)/1000.0
C   COMPUTE ELECTRON CONTENT.
   SUM1=0.50*(NE(1,I)+NE(19,I))
   DO 65 J1=2,18
65 SUM1=SUM1+NE(J1,I)
   SUM1=SUM1*1.0E+09
   SUM2=0.50*(NE(19,I)+NE(29,I))
   DO 70 J1=20,28
70 SUM2=SUM2+NE(J1,I)
   SUM2=SUM2*2.0E+09
   SUM3=0.50*(NE(29,I)+NE(44,I))
   DO 75 J1=30,44
75 SUM3=SUM3+NE(J1,I)
   SUM3=SUM3*5.0E+09
   CONT(I)=SUM1+SUM2+SUM3
80 CONTINUE
C   WRITE OUTPUT TAPE FOR PLOT PROGRAM IF CC3>0
   IF(CC3 .GT. 0) WRITE(92) PLOTOP
   ASIGN=SIGN(1.0,FLAT(K))
   K1=1
   K2=24
C   DO SPORADIC E REGION CALCULATIONS.
   CALL SPORAD (SINX(K),HL,K1,K2,D,SN,AVNES,ESPROB,SIGMA,ASIGN)
   DO 85 J=1,24
85 AVNES(J)=AVNES(J)/1000.0
   K1=1
   K2=12
C   OUTPUT ALL INFORMATION.
90 WRITE (IPRINT,95) HEADER
95 FORMAT ('1',10A8)
```

```
WRITE (IPRINT,100) FLON(NP), FLAT(NP), (IDENT(I,NP), I=1,60)
100 FORMAT (' EAST LONGITUDE =',F8.2,5X,' LATITUDE =',F8.2,5X,60A1)
WRITE (IPRINT,105) SN,SX,D,MONTH
105 FORMAT (' S 10.7          =',F8.2,10X,' S 10.7 (1A.U.) =',F8.2,10X'D
1AY =',F8.2,10X'MONTH =',I3)
IF (ABS(SINX(K)).LT.0. .OR.ABS(SINX(K)).GT.0.82) WRITE (IPRINT,110
1)
110 FORMAT (' THE GEOMAGNETIC LATITUDE FOR THIS STATION IS BEYOND THE'
1,' RANGE OF THE MODEL')
WRITE (IPRINT,115) (H(KX),KX=K1,K2)
115 FORMAT ('0UNIVERSAL TIME =',7X,12F9.2)
WRITE (IPRINT,175) (HL(J),J=K1,K2)
WRITE (IPRINT,120)
120 FORMAT ('0ALTITUDE',14X'ELECTRON DENSITY      METERS -3 X10-9      ',
1'(CM. -3 X10-3)')
DO 125 L=1,44
125 WRITE (IPRINT,130) X(L),(NE(L,KX),KX=K1,K2)
130 FORMAT (' ',F8.2,15X,12F9.2)
WRITE (IPRINT,210) (CONT(KX),KX=K1,K2)
WRITE (IPRINT,135) (NMAX(KX),KX=K1,K2)
135 FORMAT (' PEAK ELECTRON DENSITY =',1P12E9.2)
WRITE (IPRINT,140) (HMAX(KX),KX=K1,K2)
140 FORMAT (' HEIGHT OF PEAK          =',12F9.2)
WRITE (IPRINT,145) (ESPROB(KX),KX=K1,K2)
145 FORMAT (' ESPROB PERCENT',8X'='',12F9.2)
WRITE (IPRINT,150) (AVNES(KX),KX=K1,K2)
150 FORMAT (' AVNES/1000. CM-3',6X,'='',12F9.2)
WRITE (IPRINT,155) (SIGMA(KX),KX=K1,K2)
155 FORMAT (' SIGMA ES',14X,'='',12F9.2)
IF (K1.EQ.13) GO TO 5
K1=13
K2=24
GO TO 90
C
CC1>0 USE ONLY ONE U.T. FOR 1-8 STATIONS
160 NT=1
H(1)=TIME
C
COMPUTE F2 PEAK ELECTRON DENSITY FOR TIME OR TIMES DESIRED.
CALL POINTS (NT,NP,FLAT,FLON,TIME,KK,U,SX,NMAX,SINX,SINSQI)
I=1
DO 200 K=1,NP
C
CALCULATE LOCAL SOLAR TIME FOR STATION DESIRED.
HL(K)=TIME+FLON(K)/15.0
IF (HL(K).LT.0.0) HL(K)=HL(K)+24.0
IF (HL(K).GT.24.0) HL(K)=HL(K)-24.0
C
GET ALTITUDE OF F2 PEAK ELECTRON DENSITY.
IF (SINX(K).GT.0.0) GO TO 165
CALL HITE2 (ABS(SINX(K)),HL(K),SN,D+182.625,HMAX(K))
GO TO 170
165 CALL HITE2 (SINX(K),HL(K),SN,D,HMAX(K))
C
GET ELECTRON DENSITY AT 1000 KM.
170 CALL TOP2 (TOP,SN,D,HL(K),SINX(K),SIGN(1.0,FLAT(K)))
175 FORMAT (' LOCAL TIME          =',7X,12F9.2)
C
CALCULATE F-REGION MODEL.
CALL MODEL2 (-FLON(K),FLAT(K),SN,D,HL(K),NMAX(K),HMAX(K),SINSQI(K))
```

```
1      ,X,E, TOP)
      ASIGN=SIGN(1.0, FLAT(K))
C      DO SPORADIC E REGION CALCULATIONS.
      CALL SPORAD (SINX(K), HL, K, K, D, SN, AVNES, ESPROB, SIGMA, ASIGN)
      AVNES(K)=AVNES(K)/1000.0
      DO 180 J=1, 44
180    NE(J, K)=E(5, J)/1000.0
C      COMPUTE ELECTRON CONTENT.
      SUM1=0.50*(NE(1, K)+NE(19, K))
      DO 185 J1=2, 18
185    SUM1=SUM1+NE(J1, K)
      SUM1=SUM1*1.0E+09
      SUM2=0.50*(NE(19, K)+NE(29, K))
      DO 190 J1=20, 28
190    SUM2=SUM2+NE(J1, K)
      SUM2=SUM2*2.0E+09
      SUM3=0.50*(NE(29, K)+NE(44, K))
      DO 195 J1=30, 44
195    SUM3=SUM3+NE(J1, K)
      SUM3=SUM3*5.0E+09
      CONT(K)=SUM1+SUM2+SUM3
200  CONTINUE
C      OUTPUT ALL INFORMATION.
C      WRITE OUTPUT TAPE FOR PLOT PROGRAM IF CC3>0
      IF(CC3 .GT. 0) WRITE (92) PLOTOP
      DO 215 J=1, NP
      WRITE (IPRINT, 95) HEADER
      WRITE (IPRINT, 100) FLON(J), FLAT(J), (IDENT(M, J), M=1, 60)
      WRITE (IPRINT, 105) SN, SX, D, MONTH
      IF (ABS(SINX(J)).LT.0. .OR. ABS(SINX(J)).GT.0.82) WRITE (IPRINT, 110
1)
      WRITE (IPRINT, 115) H(I)
      WRITE (IPRINT, 175) HL(J)
      WRITE (IPRINT, 120)
      DO 205 L=1, 44
205    WRITE (IPRINT, 130) X(L), NE(L, J)
      WRITE (IPRINT, 210) CONT(J)
210    FORMAT ('0ELECTRON CONTENT          ='1P12E9.2)
      WRITE (IPRINT, 135) NMAX(J)
      WRITE (IPRINT, 140) HMAX(J)
      WRITE (IPRINT, 145) ESPROB(J)
      WRITE (IPRINT, 150) AVNES(J)
215    WRITE (IPRINT, 155) SIGMA(J)
      GO TO 5
220  WRITE (IPRINT, 225)
225  FORMAT (///' TOO MANY STATIONS HAVE BEEN REQUESTED.(EIGHT IS', ' TH
1E MAXIMUM NUMBER)'///' ONLY THE FIRST 8 WILL BE PROCESSED')
      READ (IREAD, 20) (DUMMY, I=9, NP)
      NP=8
      GO TO 25
230  STOP
      END
      SUBROUTINE MODEL1 (X)
      REAL*4 X(45), DEN(3, 45), CN(3, 45), T(45), E(5, 45), DN(3), EM(3)
```

REAL*4 GAM(3), PROD(3), Z(45), OPTONE(45)
REAL PROD(45), SNK0(4), S1K(10), S2K(10), S3K(10), S4K(10), PRO(3)
REAL*4 ENE(45), VV(45), S1(45), S2(45), S3(45), S4(45)
REAL CC(45)

REAL*4 INT(62), P(62)

C C(1,1), C(2,1) AND C(3,1) ARE THE ABSORPTION CROSS SECTIONS
C FOR N2, O2, AND O RESPECTIVELY

REAL*4 C(3,62)/0.0,1.6,0.0,1.4,1.9,0.0,0.23,1.9,0.0,2.6,4.0,0.0,25
10.0,40.0,0.0,1.65,8.25,0.0,4.25,5.9,0.0,5.35,5.2,0.0,3.4,7.0,0.0,3
2.8,7.4,0.0,4.35,9.3,4.7,4.95,8.9,4.9,4.95,11.7,5.0,11.1,13.5,5.3,3
3.35,26.0,5.3,6.75,40.0,6.1,28.0,33.0,6.1,9.7,28.0,6.1,13.8,33.0,11
4.0,26.0,28.0,6.1,13.8,20.0,8.5,71.0,25.0,8.5,24.0,22.0,8.5,25.0,22
5.0,8.5,25.0,41.0,14.5,26.0,33.0,13.0,22.0,35.0,14.0,27.0,27.0,14.0
6,26.0,33.0,14.0,23.0,35.0,14.0,22.0,39.0,14.0,23.0,29.0,13.0,23.0,
727.0,12.9,26.0,30.0,13.0,26.0,29.0,13.0,25.0,28.0,13.0,25.0,27.0,1
82.9,24.0,26.0,12.1,22.0,25.0,10.5,20.0,24.0,12.5,18.5,23.0,11.1,16
9.5,22.0,10.3,16.5,22.0,10.0,15.5,22.0,9.3,14.6,21.0,8.7,13.4,20.0,
18.1,12.0,19.5,9.8,12.0,18.7,9.2,10.7,16.0,8.0,9.8,14.4,7.2,9.7,13.
24,6.7,8.3,11.2,5.6,7.2,9.4,4.7,6.0,8.0,4.0,4.7,6.8,3.4,3.9,5.7,2.9
3,2.8,4.2,2.1,1.75,2.2,1.1,0.8,1.4,0.7,0.6,0.8,0.4,0.25,0.44,0.22,0
4.07,0.2,0.1/

C CP(1,1), CP(2,1) AND CP(3,1) ARE THE IONIZATION CROSS SECTIONS
C FOR N2, O2, AND O RESPECTIVELY

REAL*4 CP(3,62)/0.0,0.9,0.0,0.0,0.76,0.0,0.0,0.76,0.0,0.0,1.6,0.0,
10.0,18.0,0.0,0.0,4.15,0.0,0.0,3.0,0.0,0.0,2.9,0.0,0.0,4.2,0.0,0.0,
24.8,0.0,0.0,7.9,4.7,0.0,6.2,4.9,0.0,5.3,5.0,0.0,5.4,5.3,0.0,9.1,5.
33,0.0,14.0,6.1,14.0,13.4,6.1,4.9,11.2,6.1,7.6,16.8,11.0,14.3,13.9,
46.1,8.3,10.2,8.5,49.0,13.9,8.5,14.5,11.2,8.5,17.7,13.0,8.5,17.4,29
5.0,14.5,23.0,23.0,13.0,20.0,25.0,14.0,24.0,22.0,14.0,25.0,31.0,14.
60,23.0,33.0,14.0,22.0,37.0,14.0,21.0,28.0,13.0,21.0,25.0,12.9,22.0
7,26.0,13.0,23.0,26.0,13.0,22.0,25.0,13.0,21.0,24.0,12.9,21.0,23.0,
812.1,19.8,23.0,10.5,20.0,24.0,12.5,18.5,23.0,11.1,16.5,22.0,10.3,1
96.5,22.0,10.0,15.5,22.0,9.3,14.6,21.0,8.7,13.4,20.0,8.1,12.0,19.5,
19.8,12.0,18.7,9.2,10.7,16.0,8.0,9.8,14.4,7.2,9.7,13.4,6.7,8.3,11.2
2,5.6,7.2,9.4,4.7,6.0,8.0,4.0,4.7,6.8,3.4,3.9,5.7,2.9,2.8,4.2,2.1,1
3.75,2.2,1.1,0.8,1.4,0.7,0.6,0.8,0.4,0.25,0.44,0.22,0.07,0.2,0.1/

C PCONS(1) ARE THE PHOTON FLUXES IN EACH OF THE I GROUPS OF SOLAR
C RADIATION FOR A 10.7 CM FLUX VALUE OF 150

REAL*4 PCONS(62)/2.7,0.4,1.5,4.0,0.65,0.6,0.35,0.2,0.7,0.8,4.0,3.8
1,1.8,0.65,1.6,0.7,0.36,0.28,0.16,0.5,0.32,0.23,0.6,0.4,0.15,0.20,0
2.35,.7,.35,1.2,.8,.6072,.25,.8,.5,.5,.6,.4,.35,.6,.4,.4
3,0.7,0.6,0.4,0.4,4.0,0.8,0.5,0.3,0.4,0.4,0.3,1.6,2.2,3.2,0.4,0.071
4,0.16,0.16,0.09,0.03/

REAL*4 EXPON(62)/0.5,0.5,0.0,0.5,0.5,0.0,0.5,0.5,0.0,0.0,0.0,0.0,0.5
1.0,0.0,0.0,0.0,1.0,1.0,1.0,0.0,1.0,1.0,0.0,0.0,0.0,1.0,0.0,0.0,0.5
2,0.5,0.5,1.0,0.5,0.5,0.5,0.5,0.5,0.5,0.5,0.5,0.5,1.0,0.5,0.5,0.5,0
3.5,0.5,0.5,2.0,2.0,2.0,2.0,2.0,2.0,2.0,2.0,2.0,2.0,2.0,2.0,2.0,2.0
4/

INTEGER CC1, CC2, CC3

C RR3 AND RR4 ARE THE RATES FOR THE DISSOCIATIVE RECOMBINATION
C REACTIONS OF NO+ AND O2+ MULTIPLIED BY TEMP IN K

RR3=1.44E-4

RR4=6.6E-5

C X IS INDEX OF ALTITUDE LOWER BOUNDARY AT 120 KM


```
X(1)=120.00
DO 5 N=2,19
5 X(N)=X(N-1)+10.0
DO 10 N=20,29
10 X(N)=X(N-1)+20.0
DO 15 N=30,44
15 X(N)=X(N-1)+50.0
C Z(N) IS THE INDEX OF GEOPOTENTIAL ALTITUDE
DO 20 N=1,44
20 Z(N)=(X(N)-120.0)*6493.0/(6373.0+X(N))
C EM(1), EM(2) AND EM(3) ARE THE MOLECULAR MASSES OF N2, O2 AND O
EM(1)=28.0
EM(2)=32.0
EM(3)=16.0
BX=1.87
CX=1.0
C TEMP AT 120 KM
TZERO=355.0
TINF=0.0
C DN(1), DN(2), DN(3) ARE BOUNDARY DENSITIES OF N2, O2 AND O
DN(1)=4.00E+11
DN(2)=7.50E+10
DN(3)=7.60E+10
V=0.700
RETURN
ENTRY MODEL2 (W,G,SN,D,HL,EMAX,HITE,SINSQI,X,E, TOP)
C DENSITY AT F2 PEAK
E(5,45)=EMAX
C HEIGHT OF F2 PEAK
X(45)=HITE
TIN=TINF
C CALCULATES GEOPOTENTIAL ALTITUDE OF F2 PEAK
Z(45)=(X(45)-120.0)*6493.0/(6373.0+X(45))
C SETS ELECTRON DENSITIES AT PEAK TO MODEL
ENE(45)=E(5,45)
C ADJUSTS PHOTON FLUXES USING ASSUMED SOLAR VARIATION WITH
C 10.7 CM SOLAR FLUX
DO 25 I=1,62
DIV=75.9
IF (I.GT.57) DIV=81.0
25 P(I)=PCONS(I)*1.0E+09*(SN/DIV)**EXPON(I)
C CALCULATES EXOSPHERIC TEMPERATURES TIN FOR HOUR AND SOLAR ACTIVITY
C AND SEASON
30 DELTAT=((0.39+0.15*SIN(6.283187*(D-172.0)/365.0))*SIN(12.56637*(D-
180.0)/365.0)-0.30)*SN
S =SN+DELTAT/3.4
C0= 5.443538E+02+4.328897E+00*S
C1=-1.179819E+02-6.495360E-01*S
C2= 3.115091E+01-4.766818E-02*S
C3= 4.069323E+00+4.154682E-02*S
C4=-6.389061E+00+1.415760E-02*S
C5= 1.045482E+00-1.995652E-02*S
Z1=-1.138663E+01-7.298749E-01*S
Z2= 1.359668E+01+2.815729E-03*S
```

```
Z3= 9.859158E-01+8.138881E-02*S
Z4= 7.061132E-01-1.151708E-02*S
Z5=-2.925315E-01-4.625236E-02*S
O=3.141593*HL/12.
TIN =C0+C1*COS(O)+C2*COS(2.*O)+C3*COS(3.*O)
A  +C4*COS(4.*O)+C5*COS(5.*O)
1    +Z1*SIN(O)+Z2*SIN(2.*O)+Z3*SIN(3.*O)
B  +Z4*SIN(4.*O)+Z5*SIN(5.*O)
C    CALCULATES SCALE HEIGHT
HT=0.8734*TIN
CON=1.0-TZERO/TIN
C    DEL IS THE SOLAR DECLINATION
DEL=-0.40915*COS((D+8.0)*(2.0*3.141593/365.25))
C    Y = SECANT SOLAR ZENITH ANGLE
Y=1.0/(SIN(0.017453*G)*SIN(DEL)+COS(0.017453*G)*COS(DEL)*COS(0.261
18*(HL-12.0)))
IF(Y .GT. 0.0 .AND. Y .LT. 59.3) GO TO 33
DO 32 I=1,62
32  P(I)=0.0
    P(1)=.93E+06*SQRT(S)
    P(32)=.80E+04*S
    P(47)=.46E+06*SQRT(S)
    Y=1.0
C    CONVERTS HOURS LOCAL TIME TO DEGREES
33  CCON=3.141593*HL/12.0
C    CALCULATES FOURIER COEFFICIENTS FOR TEMPERATURE GRADIENT FACTOR
A0= 2.210156E-02-1.970030E-05*S
A1= 6.712358E-03-1.181107E-05*S
A2= 2.748180E-04+3.390522E-07*S
A3=-5.663477E-04+8.669016E-07*S
A4=-4.652258E-05+2.322930E-07*S
A5= 8.984354E-05-1.128157E-07*S
B1=-3.407398E-03+1.900959E-05*S
B2=-5.428597E-04+4.101313E-06*S
B3=-2.518983E-04-5.341112E-07*S
B4=-1.380845E-04+2.075324E-07*S
B5= 1.358994E-04+3.931811E-07*S
C    TEMPERATURE GRADIENT FACTOR
    B =A0+A1*COS(O)+A2*COS(2.*O)+A3*COS(3.*O)
A  +A4*COS(4.*O)+A5*COS(5.*O)
1    +B1*SIN(O)+B2*SIN(2.*O)+B3*SIN(3.*O)
B    +B4*SIN(4.*O)+B5*SIN(5.*O)
DO 35 M=1,3
35  GAM(M)=EM(M)/(HT*B)
    N=45
    BZ=B*Z(N)
    IF (BZ.GT.20.0) BZ=20.0
C    NEUTRAL TEMPERATURES AT EACH HEIGHT
T(N)=TIN*(1.0-CON*EXP(-BZ))
TEMP=(1.0-CON)/(EXP(BZ)-CON)
DO 40 M=1,3
C    DEN(1,N), DEN(2,N) AND DEN(3,N) ARE DENSITIES OF N2, O2 AND O AT
C    ALTITUDE INDEX N
DEN(M,N)=EXP(BZ)*DN(M)*(TEMP)**(1.0+GAM(M))
```

```
C   CN(M,N) ARE THE COLUMN CONTENTS OF CONSTITUENTS M ABOVE
C   ALTITUDE INDEX N
40  CN(M,N)=DEN(M,N)*HT*T(N)*1.0E+05/(TIN*EM(M))
    DO 50  I=1,62
C   FACT(I) IS THE OPTICAL DEPTH AT GROUPS
    FACT=(CN(1,N)*C(1,I)+CN(2,N)*C(2,I)+CN(3,N)*C(3,I))*Y*1.0E-18
    IF (FACT.GT.20.0) GO TO 45
C   INT(I) ARE THE PHOTON FLUXES
    INT(I)=P(I)*EXP(-FACT)
    GO TO 50
45  INT(I)=0.0
50  CONTINUE
    DO 60  M=1,3
    SUM=0.0
    DO 55  I=1,62
55  SUM=SUM+INT(I)*CP(M,I)
C   PROD(M) IS THE TOTAL PRODUCTION OF IONS FROM NEUTRAL SPECIES M
60  PROD(M)=DEN(M,N)*SUM*1.0E-18
C   PRODT(N) IS THE TOTAL PRODUCTION OF POSITIVE IONS AT ALTITUDE N
    PRODT(N)=PROD(1)+PROD(2)+PROD(3)
C   RR1 IS THE REACTION RATE OF O+ + N2 TO NO+ + N
    RR1=0.70*PROD(3)/(ENE(45)*(DEN(1,45)+10.0*DEN(2,45)))
    IF(Y .EQ. 1.0) RR1=2.0E-11
C   RR2 IS THE REACTION RATE OF O+ + O2 TO O2+ + O
    RR2=10.0*RR1
C   E(2,N) IS PE O+ DENSITY
    E(2,N)=PROD(3)/(RR1*DEN(1,N)+RR2*DEN(2,N))
C   E(1,N) IS PE NE DENSITY
    E(1,N)=0.5*(E(2,N)+SORT(E(2,N)**2+4.0*T(N)*((RR1*DEN(1,N)*E(2,N)+P
1  ROD(1))/RR3+(RR2*DEN(2,N)*E(2,N)+PROD(2))/RR4)))
C   E(3,N) IS PE NO+ DENSITY
    E(3,N)=T(N)*(PROD(1)+E(2,N)*RR1*DEN(1,N))/(RR3*E(1,N))
C   E(4,N) IS PE O2+ DENSITY
    E(4,N)=T(N)*(PROD(2)+E(2,N)*RR2*DEN(2,N))/(RR4*E(1,N))
    DO 65  N=1,44
    BZ=B*Z(N)
    IF (BZ.GT.20.0) BZ=20.0
    T(N)=TIN*(1.0-CON*EXP(-BZ))
    TEMP=(1.0-CON)/(EXP(BZ)-CON)
    DO 65  M=1,3
    DEN(M,N)=EXP(BZ)*DN(M)*(TEMP)**(1.0+GAM(M))
65  CN(M,N)=DEN(M,N)*HT*T(N)*1.0E+05/(TIN*EM(M))
    DO 90  N=1,44
    DO 75  I=1,62
    FACT=(CN(1,N)*C(1,I)+CN(2,N)*C(2,I)+CN(3,N)*C(3,I))*Y*1.0E-18
    IF (FACT.GT.20.0) GO TO 70
    INT(I)=P(I)*EXP(-FACT)
    GO TO 75
70  INT(I)=0.0
75  CONTINUE
    DO 85  M=1,3
    SUM=0.0
    DO 80  I=1,62
80  SUM=SUM+INT(I)*CP(M,I)
```

```
85 PROD(M)=DEN(M,N)*SUM*1.0E-18
   PRODT(N)=PROD(1)+PROD(2)+PROD(3)
   E(2,N)=PROD(3)/(RR1*DEN(1,N)+RR2*DEN(2,N))
   E(1,N)=0.5*(E(2,N)+SQRT(E(2,N)**2+4.0*T(N)*((RR1*DEN(1,N)*E(2,N)+P
90 1ROD(1))/RR3+(RR2*DEN(2,N)*E(2,N)+PROD(2))/RR4)))
   OPTONE(N)=E(2,N)/E(1,N)
   IF(Y .EQ. 1.0) GO TO 205
   DO 100 M=1,3
   SUM=0.0
   DO 95 I=1,62
95 SUM=SUM+P(I)*CP(M,I)
C   PRO(M) IS PRODUCTION OF M ION AT F2 PEAK NEGLECTING ABSORPTION
100 PRO(M)=DEN(M,45)*SUM*1.0E-18
C   PROT IS PRODUCTION AT PEAK NEGLECTING ABSORPTION
   PROT=PRO(1)+PRO(2)+PRO(3)
C   ZOH IS NUMBER OF SCALE HEIGHTS OF O. 190KM IS BELOW PEAK
   ZOH=(Z(7)-Z(45))/(5.25E-02*T(7))
C   ALPHA IS FRACTIONAL UNABSORBED FLUX AT PEAK
   ALPHA=1.0-PRODT(45)/PROT
   IF (ALPHA.GT.0.025) GO TO 105
   A=1.0+ALOG(ALPHA/(1.0-PRODT(45)*EXP(ZOH)/PROT))/ZOH
   GO TO 110
105 ALPHA=0.025
   A=2.4
110 N=45
C   ROUTINE TO SOLVE FOR TE
   TE=2000.0
   DELT=500.0
   CALL LOSS (N,PRODT,DEN,TE,T,E,QE1,VO2,FO,VN2,RO2,RN2,Q)
   ERR=1.0-(RO2+RN2+FO+VO2+VN2+QE1)/Q
   TSIGN=SIGN(1.0,ERR)
115 CALL LOSS (N,PRODT,DEN,TE,T,E,QE1,VO2,FO,VN2,RO2,RN2,Q)
   ERR=1.0-(RO2+RN2+FO+VO2+VN2+QE1)/Q
   IF (ABS(ERR).GT.0.001) GO TO 125
C   IF TE AT PEAK IS CALCULATED GREATER THAN 3TN IT IS SET TO 3TN
120 IF (TE.LE.3.0*T(N)) GO TO 135
   TE=3.0*T(N)
   DX=0.25
   GO TO 140
125 IF (DELT.LT.0.1) GO TO 120
   IF (TSIGN.EQ.SIGN(1.0,ERR)) GO TO 130
   TSIGN=-1.0*TSIGN
   DELT=0.499*DELT
130 TE=TE+TSIGN*DELT
   GO TO 115
135 DX=1.0/(TE/T(N)+1.0)
140 IF (TE.LT.T(N)) TE=T(N)
C   CALCULATES SCALE HEIGHT OF O AT THE PEAK
   SCHT=1.294795E-09*((6373.0+X(N))**2)*T(N)
C   CHECK NEGATIVE ABOVE PEAK
   CHECK=Z(N)-SCHT
   BPCOH=(BX+CX)/SCHT
C   DM IS DIFFUSION COEFF OF O+ IN O AT PEAK
   DM=(2.156E+17*SINSOI*SQRT(T(N)))/DEN(3,N)
```

```
C      BM IS LOSS RATE OF O+ IONS AT PEAK
      BM=RR1*DEN(1,N)+RR2*DEN(2,N)
      TCON=(TOP/E(5,N))*(1.0/DX)
      CALL BOUND (A,BX,CX,DX,V,ALPHA,SNK0,S1K,S2K,S3K,S4K,B1C,BAPC,BC,BD
1,ENY)
C      CALCULATES TERMS IN EXPONENTIAL SERIES
      DO 155 N=1,44
      ZZ=Z(45)-Z(N)
      AAA=TCON*EXP(-ZZ/(16.0*SCHT))
      S1CON=1.0
      IF (X(N).GE.X(45)) S1CON=(1.0-AAA+AAA*EXP(-15.0*ZZ/(16.0*SCHT)))*
1DX
      VV(N)=V*EXP(BPCOH*(ZZ))
      S1(N)=SNK0(1)*S1CON
      S2(N)=SNK0(2)
      S3(N)=SNK0(3)
      S4(N)=SNK0(4)
C      SUMS SERIES
      DO 145 KK=1,7
      VCON=VV(N)**KK
      IF (VCON.LT.1.0E-60) GO TO 150
      S1(N)=S1(N)+S1K(KK)*VCON
      S2(N)=S2(N)+S2K(KK)*VCON
      S3(N)=S3(N)+S3K(KK)*VCON
145 S4(N)=S4(N)+S4K(KK)*VCON
150 S1(N)=S1(N)*EXP(DX*ZZ/SCHT)
      S2(N)=S2(N)*EXP(CX*ZZ/SCHT)
      S3(N)=S3(N)*EXP((1.0+CX)*ZZ/SCHT)
      S4(N)=S4(N)*EXP((A+CX)*ZZ/SCHT)
C      NORMALIZES SERIES MODEL TO NE AT PEAK
155 ENE(N)=ENE(45)/ENY*(BD*S1(N)+B1C*S3(N)+BC*S2(N)+BAPC*S4(N))
      J=1
160 IF (X(J).LT.200.0) GO TO 165
      E(5,J)=E(1,J)
      IF (E(1,J).GE.ENE(J)) GO TO 180
      J=J+1
      E(5,J)=0.50*(E(1,J)+ENE(J))
      J=J+1
      GO TO 190
165 E(5,J)=E(1,J)
      J=J+1
      GO TO 160
170 IF (ENE(J).GT.E(1,J)) GO TO 185
      IF (Z(J).GE.CHECK) GO TO 190
175 E(5,J)=E(1,J)
180 J=J+1
      IF (J.LT.45) GO TO 170
      GO TO 200
185 IF (ENE(J+1).GT.ENE(J)) GO TO 190
      GO TO 175
190 DO 195 JJ=J,44
      E(2,JJ)=0.0
      E(3,JJ)=0.0
      E(4,JJ)=0.0
```

```
195 E(5,JJ)=ENE(JJ)
200 RETURN
C LISTED BELOW ARE THE CALCULATIONS NECESSARY FOR THE NIGHT PROGRAM
C SCALE HEIGHT OF O
205 SCHT=1.294795E-09*((6373.0+X(45))**2)*T(45)
TCON=(TOP/E(5,45))**2
DO 215 N=1,44
ZDIF=Z(45)-Z(N)
C CC(N)=NUMBER OF SCALE HEIGHTS OF O BELOW PEAK
CC(N)=ZDIF/SCHT
AAA=TCON*EXP(-ZDIF/(16.0*SCHT))
IF (ABS(CC(N)).GT.20.0) GO TO 210
C EMPIRICAL FORMULA FOR NIGHT DENSITIES
E(5,N)=ENE(45)*1.32019*EXP(0.5*CC(N)-0.277778*EXP(CC(N)*1.8))
IF (ZDIF.LE.0.0) E(5,N)=E(5,N)*SQRT(1.0-AAA+AAA*EXP(-ZDIF*15.0/(16
1.0*SCHT)))
GO TO 215
210 E(5,N)=TOP*EXP((774.968-Z(N))/(32.0*SCHT))
215 CONTINUE
J=1
216 IF(E(5,J).GT.E(1,J).OR. J.EQ.45) GO TO 220
E(5,J)=E(1,J)
J=J+1
GO TO 216
220 RETURN
END
C FIFTE 09/25/69 -- FIFT * VERSION 2.11 *
SUBROUTINE LOSS (N,PRODT,DEN,TE,T,E,QE1,VO2,FO,VN2,RO2,RN2,Q)
C THIS SUBROUTINE CALCULATES ELECTRON THERMAL LOSS RATES AT PEAK.
REAL*4 DEN(3,45),T(45),E(5,45),PRODT(45)
REAL*4 COEF(7)/-1.528787E+01,-9.297430E+00,-1.244620E-01,3.485308E
1-01,5.106051E-02,2.794473E-03,5.425251E-05/
D=E(5,N)*(TE-T(N))
C RN2 IS ROTATIONAL LOSS FOR N2
RN2=2.9E-14*D*DEN(1,N)/SQRT(TE)
C RO2 IS ROTATIONAL LOSS FOR O2
RO2=6.9E-14*D*DEN(2,N)/SQRT(TE)
DEBYE=6.9*SQRT(TE*T(N)/(E(5,N)*(TE+T(N))))
AL=ALOG(1.8E+03*DEBYE*TE)
C QE1 IS ELECTRON ION LOSS
QE1=3.20E-08*E(5,N)*(AL/TE**1.5)*E(5,N)*(TE-T(N))
PLOT=8.29E-18*TE**2-6.98E-15*TE+1.39E-12
C VO2 IS VIBRATIONAL LOSS TO O2
VO2=PLOT*DEN(2,N)*E(5,N)
VPLOT=(2.1529E+05-5.7891E+02*TE+0.47555*TE**2-1.327E-04*TE**3)*(
1-3.0271E-04-1.4793E-07*T(N))*(TE-T(N))*1.0E-13/TE
C FO IS LOSS TO FINE STRUCTURE OF O
FO=3.4E-12*D*DEN(3,N)*(1.0-7.0E-05*TE)/T(N)
C VN2 IS VIBRATIONAL LOSS TO N2
VN2=VPLOT*DEN(1,N)*E(5,N)
C Q IS HEAT INPUT TO ELECTRONS BASED ON CALCULATED HEATING EFFICIENCY
R=ALOG(E(5,N)/(DEN(1,N)+DEN(2,N)+DEN(3,N)))
SUM=0.0
X=1.0
```

```
DO 5 I=1,7
SUM=SUM+COEF(I)*X
5 X=X*R
Q=SUM*PRODT(N)
RETURN
END
C FIFTED 09/25/69 -- FIFT * VERSION 2.11 *
SUBROUTINE BOUND (A,B,C,D,V,YALF,SNK0,S1K,S2K,S3K,S4K,B1C,BAPC,BC,
1BD,ENY)
C THIS PROGRAM USES VALUES OF A,B,C,D, AND H SQUARED BETAM OVER DM
C = V TO CALCULATE VALUES OF BD,BC,B1C, AND BAPC THAT SATISFY THE
C BOUNDARY CONDITIONS J.S.N. 14 FEB. 1969
C THE NOTATIONS FOLLOW NISBET JS J.G.R. V68 NOV 15 1963
C THE PROCEDURE USED IS TO CALCULATE BC AND BD FOR THE ACTUAL
C CONDITIONS.
REAL*4 S1K(10),S2K(10),S3K(10),S4K(10),S5K(10),S6K(10),S7K(10)
REAL*4 S8K(10),SNK0(4)
EQUIVALENCE (S1,S1K0),(S2,S2K0),(S3,S3K0),(S4,S4K0),(S5,S5K0)
EQUIVALENCE (S6,S6K0),(S7,S7K0),(S8,S8K0)
CALL GAM (A,B,C,D,R1,R2,R3,T,U,W)
BPC=B+C
BPC2=BPC*BPC
CMD=C-D
DMC=D-C
APC=A+C
APCMD=APC-D
S1K0=1.0
S1K(1)=1.0/(BPC2*(1.0+DMC/BPC))
DO 5 N=2,7
M=N-1
5 S1K(N)=S1K(M)/(BPC2*N*(N+DMC/BPC))
S5K0=D
DO 10 N=1,7
10 S5K(N)=S1K(N)*(D+N*BPC)
S2K0=1.0
S2K(1)=1.0/(BPC2*(1.0+CMD/BPC))
DO 15 N=2,7
M=N-1
15 S2K(N)=S2K(M)/(BPC2*N*(N+CMD/BPC))
S6K0=S2K0*C
DO 20 N=1,7
20 S6K(N)=S2K(N)*(C+N*BPC)
S3K0=1.0
S3K(1)=1.0/(BPC2*(1.0+(1.0+CMD)/BPC)*(1.0+1.0/BPC))
DO 25 N=2,7
M=N-1
25 S3K(N)=S3K(M)/(BPC2*(N+(1.0+CMD)/BPC)*(N+1.0/BPC))
S7K0=S3K0*(1.0+C)
DO 30 N=1,7
30 S7K(N)=S3K(N)*(1.0+C+N*BPC)
S4K0=1.0
S4K(1)=1.0/((1.0+APCMD/BPC)*(1.0+A/BPC)*BPC2)
DO 35 N=2,7
M=N-1
```

```
35 S4K(N)=S4K(M)/((N+APCMD/BPC)*(N+A/BPC)*BPC2)
S8K0=S4K0*APC
DO 40 N=1,7
40 S8K(N)=S4K(N)*(A+C+N*BPC)
B1C=-1.0/(1.0+C-D)
BAPC=YALF/(A*APCMD)
SNK0(1)=S1
SNK0(2)=S2
SNK0(3)=S3
SNK0(4)=S4
DO 45 N=1,7
VTTN=V**N
S1=S1+S1K(N)*(VTTN)
S2=S2+S2K(N)*(VTTN)
S3=S3+S3K(N)*(VTTN)
S4=S4+S4K(N)*(VTTN)
S5=S5+S5K(N)*(VTTN)
S6=S6+S6K(N)*(VTTN)
S7=S7+S7K(N)*(VTTN)
45 S8=S8+S8K(N)*(VTTN)
BC=-(B1C*(R2*V**U-S7/S5)+BAPC*(R3*V**W-S8/S5))/(R1*V**T-S6/S5)
BD=-(BC*S6+B1C*S7+BAPC*S8)/S5
ENY=BD*S1+B1C*S3+BC*S2+BAPC*S4
RETURN
END
```

```
C FIFTED 09/25/69 -- FIFT * VERSION 2.11 *
SUBROUTINE GAM (A,B,C,D,R1,R2,R3,T,U,W)
REAL*4 P(6),GOFP(6),G(6)
GAMMAF(X)=X**X*EXP(-X)*SQRT(6.283186*X)*(1.0+1.0/(12.0*X)+1.0/(288
1.0*X*X)-139.0/(51840.0*X*X*X)-571.0/(2488320.0*X**4))
P(1)=(C-D)/(B+C)+1.0
P(2)=(B+D)/(B+C)
P(3)=(C+1.0-D)/(B+C)+1.0
P(4)=1.0/(B+C)+1.0
P(5)=(A+B+2.0*C-D)/(B+C)
P(6)=(A+B+C)/(B+C)
DO 10 I=1,6
X=P(I)+5.0
G(I)=GAMMAF(X)
DENOM=P(I)
DO 5 K=1,5
5 DENOM=DENOM*(P(I)+K)
10 GOFP(I)=G(I)/DENOM
R1=(GOFP(1)/GOFP(2))*(B+C)**((2.0*(C-D))/(B+C))
R2=(GOFP(3)*GOFP(4)/GOFP(2))*((B+C)**((2.0*(1.0+C-D))/(B+C)))
R3=(GOFP(5)*GOFP(6)/GOFP(2))*((B+C)**((2.0*(A+C-D))/(B+C)))
T=-(P(1)-1.0)
U=-(P(3)-1.0)
W=-(A+C-D)/(B+C)
RETURN
END
```

```
C FIFTED 09/25/69 -- FIFT * VERSION 2.11 *
SUBROUTINE ATLAS (K,U,MONTH)
C THIS SUBROUTINE CALCULATES NE AT F2-MAXIMUM USING
```



```
C C.C.I.R. NOTE 340 MODELS
REAL*4 U(13,76,2),P(3),C(3),COM(3),G(78,2),DF(76,2),AF(9,2)
REAL*4 BF(9,2),OMEG(24,2),OMEGA(2),FLON(8),FLAT(8),COT(8)
REAL*4 SIT(8),FOF2(2),NMAX(24),SINSQI(8),SINX(8)
REAL*4 DR/1.745329E-02/,RD/57.29578/
DATA P(3)/3.0E+05/
INTEGER*4 NFF(2),K(14,2)
CALL RT (K,U,MONTH)
NFF(1)=K(9,1)+1
NFF(2)=K(9,2)+1
RETURN
ENTRY TIMES (NP,FLAT,FLON,K,U,SN,NMAX,SINX,SINSQI)
C THIS PROGRAM SEGMENT IS USED WHEN 24 HOURS AT ONE STATION ARE
C REQUIRED
DO 35 N=1,NP
P(1)=FLAT(N)
P(2)=FLON(N)
CALL MAGFIN (P,COM)
TMP=COM(2)*COM(2)+COM(3)*COM(3)
C(1)=RD*ATAN(ATAN(-COM(1)/SQRT(TMP))/SQRT(COS(DR*P(1))))
SINX(N)=SIN(DR*C(1))
SINSQI(N)=SIN(ATAN(-COM(1)/SQRT(TMP)))**2
C(2)=FLON(N)
C(3)=P(1)
DO 5 J=1,2
CALL GK (J,K,C,G)
5 CALL AJBJ (J,K(10,J),NFF(J),U,G,AF,BF)
T=-180.0
15 DO 25 I=1,24
I8=8
CALL SICOJT (I8,COT,SIT,T)
DO 20 J=1,2
CALL ABSICO (J,K(10,J),AF,BF,COT,SIT,FOF2(J))
20 OMEG(I,J)=1.24E+04*FOF2(J)*FOF2(J)
25 T=T+15.0
DO 30 I=1,24
30 NMAX(I )=((SN-60.0)*OMEG(I,2)+(136.0-SN)*OMEG(I,1))/76.0
35 CONTINUE
RETURN
ENTRY POINTS (NT,NP,FLAT,FLON,TIME,K,U,SN,NMAX,SINX,SINSQI)
C THIS PROGRAM SEGMENT CALCULATES NE AT F2 MAX FOR SEVERAL STATIONS
C AT ONE VALUE OF U.T.
DO 50 I=1,NT
T=15.0*TIME-180.0
I8=8
CALL SICOJT (I8,COT,SIT,T)
DO 40 J=1,2
40 CALL DKSICO (J,NFF(J),K(10,J),U,SIT,COT,DF)
DO 50 N=1,NP
P(1)=FLAT(N)
P(2)=FLON(N)
CALL MAGFIN (P,COM)
TMP=COM(2)*COM(2)+COM(3)*COM(3)
C(2)=FLON(N)
```

```
C(3)=P(1)
C(1)=RD*ATAN(ATAN(-COM(1)/SQRT(TMP))/SQRT(COS(DR*P(1))))
SINX(N)=SIN(DR*C(1))
SINSQI(N)=SIN(ATAN(-COM(1)/SQRT(TMP)))**2
DO 45 J=1,2
CALL GK (J,K,C,G)
CALL DKGK (J,NFF(J),G,DF,OMEGA(J))
OMEGA(J)=1.24E+04*OMEGA(J)*OMEGA(J)
45 CONTINUE
50 NMAX(N)=((SN-60.0)*OMEGA(2)+(136.0-SN)*OMEGA(1))/76.0
RETURN
END
```

```
C FIFTED 09/25/69 -- FIFT * VERSION 2.11 *
SUBROUTINE RT (K,U,M)
C SUBROUTINE TO READ FOURIER COEFFICIENTS FROM TAPE
REAL*8 CARD(10,2)
INTEGER*4 K(14,2)
REAL*4 U(13,76,2)
DO 5 I=1,M
5 READ (91) CARD,K,U
REWIND 91
RETURN
END
```

```
C FIFTED 09/25/69 -- FIFT * VERSION 2.11 *
SUBROUTINE MAGFIN (POS,UNE)
```

```
C COMPUTE NASA MAGNETIC FIELD COMPONENTS
REAL*4 P(7,7),DP(7,7),CP(7),AOR(7),SP(7),POS(3),UNE(3)
REAL*4 CT(7,7)/0.0,0.0,3.33333E-01,2.66667E-01,2.57143E-01,2.53968
1E-01,2.52525E-01,0.0,0.0,0.0,2.00000E-01,2.28571E-01,2.38095E-01,2
2.42424E-01,0.0,0.0,0.0,0.0,1.42857E-01,1.90476E-01,2.12121E-01,0.0
3,0.0,0.0,0.0,0.0,1.11111E-01,1.61616E-01,0.0,0.0,0.0,0.0,0.0,0.0,9
4.09091E-02,0.0,0.0,0.0,0.0,0.0,0.0,0.0,0.0,0.0,0.0,0.0,0.0,0.0,0.0
5/
REAL*4 GE(7,7)/0.0,3.04112E-01,2.40350E-02,-3.15180E-02,-4.17940E-
102,1.62560E-02,-1.95230E-02,0.0,2.14740E-02,-5.12530E-02,6.21300E-
202,-4.52980E-02,-3.44070E-02,-4.85300E-03,0.0,0.0,-1.33810E-02,-2.
348980E-02,-2.17950E-02,-1.94470E-02,3.21200E-03,0.0,0.0,0.0,-6.496
400E-03,7.00800E-03,-6.08000E-04,2.14130E-02,0.0,0.0,0.0,0.0,-2.044
500E-03,2.77500E-03,1.05100E-03,0.0,0.0,0.0,0.0,0.0,6.97000E-04,2.2
67000E-03,0.0,0.0,0.0,0.0,0.0,0.0,1.11500E-03/
REAL*4 H(7,7)/0.0,0.0,0.0,0.0,0.0,0.0,0.0,0.0,0.0,-5.79890E-02,3.31240
1E-02,1.48700E-02,-1.18250E-02,-7.96000E-04,-5.75800E-03,0.0,0.0,-1
2.57900E-03,-4.07500E-03,1.00060E-02,-2.00000E-03,-8.73500E-03,0.0,
30.0,0.0,2.10000E-04,4.30000E-04,4.59700E-03,-3.40600E-03,0.0,0.0,0
4.0,0.0,1.38500E-03,2.42100E-03,-1.18000E-04,0.0,0.0,0.0,0.0,0.0,-1
5.21800E-03,-1.11600E-03,0.0,0.0,0.0,0.0,0.0,0.0,-3.25000E-04/
DATA P(1,1)/1.0/,DP(1,1)/0.0/,HC/6371200.0/,RD/57.295780/
DATA CP(1)/1.0/,SP(1)/0.0/
P1=POS(1)
P2=POS(2)
IF (P1.LT.89.9) GO TO 5
IF (P1.EQ.89.9) GO TO 10
P1=89.9
P2=0.0
```

```
GO TO 10
5 IF (P1+89. .GE.0) GO TO 10
  P1=-89.9
  P2=0.0
10 PHI=P2/RD
  AR=HC/(HC+POS(3))
  C=SIN(P1/RD)
  S=SQRT(CP(1)-C*C)
  SP(2)=SIN(PHI)
  CP(2)=COS(PHI)
  AOR(1)=AR*AR
  AOR(2)=AOR(1)*AR
  DO 15 M=3,7
  SP(M)=SP(2)*CP(M-1)+CP(2)*SP(M-1)
  CP(M)=CP(2)*CP(M-1)-SP(2)*SP(M-1)
15 AOR(M)=AR*AOR(M-1)
  BV=0.0
  BN=BV
  BPHI=BV
  DO 40 N=2,7
  FN=N
  SUMR=0.0
  SUMT=SUMR
  SUMP=SUMT
  DO 35 M=1,N
  IF (N.EQ.M) GO TO 20
  IF (N.NE.M-1) GO TO 25
  P(N,M)=C*P(N-1,M)
  DP(N,M)=C*DP(N-1,M)-S*P(N-1,M)
  GO TO 30
20 P(N,N)=S*P(N-1,N-1)
  DP(N,N)=S*DP(N-1,N-1)+C*P(N-1,N-1)
  GO TO 30
25 P(N,M)=C*P(N-1,M)-CT(N,M)*P(N-2,M)
  DP(N,M)=C*DP(N-1,M)-S*P(N-1,M)-CT(N,M)*DP(N-2,M)
30 FM=M-1
  TS=GE(N,M)*CP(M)+H(N,M)*SP(M)
  SUMR=SUMR+P(N,M)*TS
  SUMT=SUMT+DP(N,M)*TS
35 SUMP=SUMP+FM*P(N,M)*(-GE(N,M)*SP(M)+H(N,M)*CP(M))
  BV=BV+AOR(N)*FN*SUMR
  BN=BN-AOR(N)*SUMT
40 BPHI=BPHI-AOR(N)*SUMP
  UNE(1)=-BV
  UNE(2)=BN
  UNE(3)=-BPHI/S
  RETURN
  END
C FIFTE 09/25/69 -- FIFT * VERSION 2.11 *
C SUBROUTINE GK (JR,K,C,G)
C COMPUTE COORDINATE FUNCTIONS, G(I),I=1,.....K+1
C C(1)=MODIFIED LATITUDE.C(2),C(3)==GEOG.LAT.,LONGITUDE RESPECTIVELY
C DIMENSION K(14,2),C(1),G(78,2)
C DR=0.017453293
```

```
N=8
X=DR*C(1)
Y=C(2)*DR
Z=DR*C(3)
K0=K(1, JR)
SX=SIN(X)
G(1, JR)=1.0
G(2, JR)=SX
IF (K0.EQ.1) GO TO 10
DO 5 I=2, K0
5 G(I+1, JR)=SX*G(I, JR)
10 KDIF=K(2, JR)-K0
IF (KDIF.EQ.0) GO TO 30
J=1
CX1=COS(Z)
CX=CX1
T=Y
15 KC=K(J, JR)+4
G(KC-2, JR)=CX*COS(T)
G(KC-1, JR)=CX*SIN(T)
IF (KDIF.EQ.2) GO TO 25
KN=K(J+1, JR)
DO 20 I=KC, KN, 2
G(I, JR)=SX*G(I-2, JR)
20 G(I+1, JR)=SX*G(I-1, JR)
25 IF (J.EQ.N) GO TO 30
KDIF=K(J+2, JR)-KN
IF (KDIF.EQ.0) GO TO 30
CX=CX*CX1
J=J+1
FJ=J
T=FJ*Y
GO TO 15
30 RETURN
```

```
END
C FIFTED 09/25/69 -- FIFT * VERSION 2.11 *
C SUBROUTINE AJBJ (JR, LH, MX, D, G, ASTAR, BSTAR)
C PART OF SUBROUTINE TO CALCULATE NMAX F2
C COMPUTE COEFFICIENTS FOR A FIXED GEOGRAPHIC POINT
C DIMENSION D(13, 76, 2), G(78, 2), ASTAR(9, 2), BSTAR(9, 2)
C N=LH+1
```

```
DO 5 J=1, N
  ASTAR(J, JR)=0.0
  DO 5 K=1, MX
    5 ASTAR(J, JR)=ASTAR(J, JR)+D(2*J-1, K, JR)*G(K, JR)
  DO 10 J=2, N
    BSTAR(J, JR)=0.0
    DO 10 K=1, MX
      10 BSTAR(J, JR)=BSTAR(J, JR)+D(2*J-2, K, JR)*G(K, JR)
  RETURN
```

```
END
C FIFTED 09/25/69 -- FIFT * VERSION 2.11 *
C SUBROUTINE SICOJT (L, C, S, A)
C PART OF SUBROUTINE TO CALCULATE NMAX F2 TIME SERIES
```

```
C      COMPUTE SIN(JT),COS(JT),J=1,.....,L FOR ANGLE A
      DIMENSION C(1),S(1)
      T=0.01745329*A
      C(1)=COS(T)
      S(1)=SIN(T)
      DO 5 I=2,L
      C(I)=C(1)*C(I-1)-S(1)*S(I-1)
5     S(I)=C(1)*S(I-1)+S(1)*C(I-1)
      RETURN
      END

C      FIFTED 09/25/69 -- FIFT * VERSION 2.11 *
      SUBROUTINE ABSICO (JR,LH,ASTAR,BSTAR,COTIME,SITIME,OMEGA)
C      PART OF SUBROUTINE TO CALCULATE NMAXF2
C      COMPUTE OMEGA, SUMMING THE FOURIER SERIES
      DIMENSION COTIME(1),SITIME(1),ASTAR(9,2),BSTAR(9,2)
      OMEGA=ASTAR(1,JR)
      DO 5 J=1,LH
5     OMEGA=OMEGA+ASTAR(J+1,JR)*COTIME(J)+BSTAR(J+1,JR)*SITIME(J)
      RETURN
      END

C      FIFTED 09/25/69 -- FIFT * VERSION 2.11 *
      SUBROUTINE DKSICO (JR,MX,LH,D,SITIME,COTIME,DK)
C      PART OF SUBROUTINE TO CALCULATE NMAX F2
C      COMPUTE D SUB K, COEFFICIENTS FOR A FIXED TIME
      DIMENSION D(13,76,2),COTIME(1),SITIME(1),DK(76,2)
      DO 5 K=1,MX
      DK(K,JR)=D(1,K,JR)
      DO 5 L=1,LH
5     DK(K,JR)=DK(K,JR)+D(2*L,K,JR)*SITIME(L)+D(2*L+1,K,JR)*COTIME(L)
      RETURN
      END

C      FIFTED 09/25/69 -- FIFT * VERSION 2.11 *
      SUBROUTINE DKGK (JR,MX,G,DKSTAR,OMEGA)
C      PART OF SUBROUTINE TO CALCULATE NMAX F2
C      COMPUTE OMEGA, SUMMING THE GEOGRAPHIC SERIES
      DIMENSION G(78,2),DKSTAR(76,2)
      OMEGA=G(1,JR)*DKSTAR(1,JR)
      DO 5 K=2,MX
5     OMEGA=OMEGA+DKSTAR(K,JR)*G(K,JR)
      RETURN
      END

C      FIFTED 09/25/69 -- FIFT * VERSION 2.11 *
      SUBROUTINE SPORAD (SINX,HL,K1,K2,D,SN,AVNES,ESPROB,SIGMA,SIGN)
C      SUBROUTINE TO DO CALCULATIONS FOR SPORADIC E REGION.
      REAL*4 HL(24),AVNES(24),ESPROB(24),SIGMA1(24),SIGMA2(24)
      REAL*4 SIGMA(24),SUM(4,2,2),X(4),FBES(24)
      REAL*4 NQ2(8,5,2)/5.71241E01,4.66262E-01,1.43563E02,6.31522E01,-2.
130748E02,-2.43734E02,4.05788E01,1.80855E02,1.10385E01,-5.85146E01,
22.34711E02,9.30981E01,-5.10016E02,-1.10094E01,2.68515E02,-1.96195E
301,2.79192E00,7.36763E-01,-4.32670E-02,-7.37663E00,1.80668E00,1.30
4589E01,-4.45583E00,-6.60764E00,9.34586E-01,-3.20100E-01,3.67608E00
5,1.45866E00,-8.23541E00,-3.67285E00,3.78421E00,2.41967E00,1.46718E
601,-6.78199E00,5.09177E00,0.0,0.0,0.0,0.0,0.0,0.0,3.99023E01,5.55076E0
70,1.63753E02,-2.80688E01,-3.19521E02,-1.67921E01,1.48742E02,2.7027
```

```
81E01,9.36711E00,-6.09021E01,2.15444E02,5.16341E01,-4.84376E02,1.27
9245E02,2.63851E02,-1.15005E02,2.85327E00,8.33655E-01,-8.20516E-01,
1-8.21058E00,4.30828E00,1.26893E01,-6.18656E00,-5.08563E00,1.25431E
200,-2.33585E-01,3.18651E00,1.09609E00,-7.49261E00,-4.04376E00,3.13
3777E00,3.15937E00,0.0,0.0,0.0,0.0,0.0,0.0,0.0,0.0/
```

```
PSINX=ABS(SINX)
```

```
PSINX2=PSINX*PSINX
```

```
PSINX4=PSINX2*PSINX2
```

```
C K IS THE S# SUBSCRIPT
```

```
C I=1 FOR MAX,2 FOR MIN,3 FOR A, AND 4 FOR B
```

```
DO 5 K=1,2
```

```
DO 5 I=1,4
```

```
SUM(I,1,K)=NQ2(1,I,K)+NQ2(3,I,K)*PSINX2+NQ2(5,I,K)*PSINX4+NQ2(7,I,
1K)*PSINX4*PSINX2
```

```
5 SUM(I,2,K)=NQ2(2,I,K)*PSINX+NQ2(4,I,K)*PSINX2*PSINX+NQ2(6,I,K)*PSI
1NX4*PSINX+NQ2(8,I,K)*PSINX4*PSINX2*PSINX
```

```
PHI=NQ2(1,5,1)+NQ2(2,5,1)*PSINX2+NQ2(3,5,1)*PSINX4
```

```
CON1=2.0-0.010*SN
```

```
CON2=0.010*SN-1.0
```

```
DO 10 I=1,4
```

```
10 X(I)=CON1*SUM(I,1,1)+CON2*SUM(I,1,2)+1.570796*(CON1*SUM(I,2,1)+CON
12*SUM(I,2,2))*COS(1.720242E-02*D)*SIGN
```

```
EAMP=(X(1)-X(2))/(COS((14.5-PHI)*.2617991)-COS((2.5-PHI)*.261799
11))
```

```
EBAR=X(2)-EAMP*COS((2.5-PHI)*.2617991)
```

```
DO 30 J=K1,K2
```

```
ESPROB(J)=EBAR+EAMP*COS((HL(J)-PHI)*.2617991)
```

```
IF (HL(J).GE.8.0) GO TO 20
```

```
IF (HL(J).GT.4.0) GO TO 15
```

```
FBES(J)=X(3)-X(4)*COS((4.0-HL(J))/20.0*3.141593)
```

```
GO TO 25
```

```
15 FBES(J)=X(3)-X(4)*COS((HL(J)-4.0)/4.0*3.141593)
```

```
GO TO 25
```

```
20 FBES(J)=X(3)+X(4)*COS((HL(J)-8.0)/20.0*3.141593)
```

```
25 AVNES(J)=1.24E+04*FBES(J)*FBES(J)
```

```
SIGMA1(J)=(0.6+0.1*COS((HL(J)+2)*.2617991))
```

```
SIGMA2(J)=(0.55+0.15*COS((HL(J)+2)*.2617991))
```

```
30 SIGMA(J)=((SN-100.0)*SIGMA2(J)+(200-SN)*SIGMA1(J))/100.0
```

```
RETURN
```

```
END
```

```
C FIFTED 09/25/69 -- FIFT * VERSION 2.11 *
```

```
SUBROUTINE TOP2 (ED1000,SN,D,HL,SINX,SIGN)
```

```
C SUBROUTINE TO CALCULATE ELECTRON DENSITY AT 1000 KM.
```

```
REAL*4 SUM(2,2),COEF(8,2)
```

```
REAL*4 A(8,2)/1.50805E04,-2.36039E03,-2.80918E04,5.15285E04,5.2348
12E04,-1.10782E05,-8.04468E04,2.19078E04,1.94670E04,-8.98602E03,-6.
241293E04,7.91004E04,3.40314E05,-9.46900E04,-3.76804E05,-4.46713E04
3/
```

```
REAL*4 B(8,2)/1.92940E02,-1.30600E01,1.67090E02,-7.45390E02,-8.368
130E02,1.61762E03,9.78260E02,-5.89490E02,-4.74500E01,7.54800E01,6.3
27260E02,-5.92840E02,-2.11143E03,9.84360E02,1.81220E03,-3.40810E02/
```

```
PHI=ABS(SINX)
```

```
CON=COS(6.283185/360.0*D)
```

```
T=HL-16.0
```

```
DO 5 I=1,8
COEF(1,1)=A(I,1)+B(I,1)*SN
5 COEF(1,2)=A(I,2)+B(I,2)*SN
DO 10 J=1,2
SUM(1,J)=COEF(1,J)+COEF(3,J)*PHI*PHI+COEF(5,J)*PHI**4+COEF(7,J)*PHI**6
10 SUM(2,J)=COEF(2,J)*PHI+COEF(4,J)*PHI*PHI*PHI+COEF(6,J)*PHI**5+COEF(8,J)*PHI**7
EDD=SUM(1,1)+SUM(2,1)*CON*SIGN
EDN=SUM(1,2)+SUM(2,2)*CON*SIGN
ED1000=0.5*(EDN+EDD)+0.5*(EDD-EDN)*COS(6.283185/24.0*T)
IF (ED1000.LT.500.0) ED1000=500.0
RETURN
END
```

```
C FIFTE 09/25/69 -- FIFT * VERSION 2.11 *
C SUBROUTINE HITE2 (SINX,HL,SN,D,HMAX)
C CALCULATES THE HEIGHT OF THE F2 LAYER PEAK
C REAL*4 XHMAX(2),HS(2,2),A(7,2),B(7,2)
C THE 4-DIMENSIONAL ARRAY PCOEF CONTAINS COEFFICIENTS FOR A 4TH
C DEGREE POLYNOMIAL IN SINX WHICH YIELDS A SET OF FOURIER
C COEFFICIENTS FOR HMAX.
C THE FIRST SUBSCRIPT OF PCOEF IS FOR THE 5 POLYNOMIAL COEFFICIENTS.
C THE SECOND SUBSCRIPT OF PCOEF IS FOR 7 COSINE COEFFICIENTS AND 6
C SIN COEFFICIENTS.
C THE THIRD SUBSCRIPT OF PCOEF IS FOR S 10.7 = 100 AND 200.
C THE FOURTH SUBSCRIPT OF PCOEF IS FOR SUMMER AND WINTER VALUES.
REAL*4 PCOEF(5,13,2,2)/3.17050E02,3.32740E02,-1.18970E03,1.22870E0
13,-3.71860E02,-3.60660E00,3.18590E01,-1.07500E03,2.80630E03,-1.759
230E03,1.18810E01,8.92120E01,-6.30580E02,1.07570E03,-5.47130E02,-6.
338520E00,1.37810E02,-7.54120E02,1.17180E03,-5.48780E02,-8.95760E-0
41,6.85960E01,-4.56220E02,8.56370E02,-4.67840E02,3.34960E00,-1.0212
50E02,5.22970E02,-8.05990E02,3.80700E02,1.97930E00,-9.82640E01,5.00
6900E02,-8.29380E02,4.24910E02,-5.92410E01,-1.11600E02,7.28590E02,-
78.14000E02,2.56320E02,-2.01420E01,4.35410E01,2.62040E02,-6.10470E0
82,3.26240E02,-2.38300E00,-5.36600E00,3.07770E01,-1.07190E02,8.4173
90E01,2.24230E00,3.55500E01,-2.54230E02,3.92970E02,-1.76220E02,4.39
1700E00,4.48930E01,-2.43520E02,3.80970E02,-1.86800E02,1.97340E-01,-
22.78970E01,2.27730E02,-4.11160E02,2.10520E02/
REAL*4 PART2(65),PART3(65),PART4(65)
EQUIVALENCE (PCOEF(1,1,2,1),PART2),(PCOEF(1,1,1,2),PART3)
EQUIVALENCE (PCOEF(1,1,2,2),PART4)
DATA PART2/4.32560E02,-8.32270E00,-2.54090E02,-7.01670E00,1.64740E
102,-7.23350E00,-1.34110E02,-2.66670E02,1.53380E03,-1.12530E03,2.34
2170E01,6.86050E01,-7.87340E02,1.40060E03,-7.05670E02,-9.38360E00,1
3.17900E02,-7.49840E02,1.25160E03,-6.09910E02,-6.51560E00,1.08370E0
42,-4.98710E02,8.30650E02,-4.34090E02,5.62320E-01,-3.43280E01,2.096
590E02,-3.19190E02,1.42740E02,4.94140E00,-1.27990E02,5.86250E02,-9.
607160E02,4.44000E02,-1.02180E02,-1.20640E02,1.21950E03,-1.63880E03
7,6.41870E02,-3.36250E01,9.89440E01,1.87220E02,-4.59420E02,2.06780E
802,-5.39760E00,6.51540E01,-3.11860E02,4.17130E02,-1.64450E02,3.481
920E00,1.10380E02,-6.42740E02,9.64140E02,-4.34530E02,6.08420E00,7.7
19020E01,-4.40910E02,6.94960E02,-3.37700E02,-2.53250E00,3.88820E01,
2-6.93890E01,3.75620E01,-5.02540E00/
DATA PART3/3.19980E02,9.85260E00,4.58980E02,-1.17540E03,6.95130E02
```

```
1,-2.68430E01,1.74130E02,-1.51350E03,3.34570E03,-1.97850E03,-1.1297
20E01,3.01400E01,-1.38420E02,4.48890E02,-3.29980E02,-9.70990E00,-3.
323770E01,1.15020E02,-1.41960E02,6.85950E01,6.70140E00,-7.92430E01,
43.47510E02,-5.48500E02,2.72800E02,3.47910E00,9.06750E00,4.83810E01
5,-1.58070E02,9.68150E01,-3.83610E00,1.01700E02,-4.20080E02,5.77800
6E02,-2.55170E02,-3.71900E01,-3.56190E02,1.56800E03,-1.99770E03,8.2
71920E02,-2.55070E00,4.90540E01,-4.10150E02,8.26980E02,-4.62770E02,
8-1.15070E00,1.44450E02,-6.17890E02,8.46860E02,-3.71460E02,2.73010E
900,7.31720E00,5.08620E01,-2.44680E02,1.83950E02,5.03110E00,-5.6539
10E00,1.37070E02,-3.53400E02,2.16970E02,1.52320E00,-3.90230E01,1.95
2910E02,-3.10920E02,1.52320E02/
DATA PART4/3.86080E02,1.05190E02,1.85700E02,-9.87380E02,6.59840E02
1,-3.36780E01,6.77200E01,-1.05510E03,2.75600E03,-1.73340E03,-1.7639
20E01,7.01420E01,-3.09890E02,7.13490E02,-4.56180E02,-1.59110E01,-1.
343350E01,-4.43580E01,1.80030E02,-1.05320E02,1.00600E01,-6.91870E01
4,2.37760E02,-3.76430E02,1.97880E02,3.73960E00,5.72020E01,-1.73530E
502,1.78040E02,-6.55600E01,-6.15030E00,1.49820E02,-6.50650E02,9.541
670E02,-4.47190E02,-5.33100E01,-5.03370E02,2.17530E03,-2.73810E03,1
7.11820E03,-5.38190E00,2.32310E01,-3.06030E02,6.98960E02,-4.10350E0
82,-2.69520E00,2.09640E02,-8.07790E02,1.04460E03,-4.43350E02,2.0211
90E00,7.48770E01,-3.04040E02,3.42870E02,-1.15380E02,6.46240E00,1.96
1980E01,6.05660E01,-3.01550E02,2.15160E02,1.39500E00,-5.38580E01,2.
293500E02,-4.76030E02,2.34550E02/
INTEGER*4 IP1/5/
HLR=(15.0*HL)*0.01745329
DO 35 L=1,2
DO 30 I=1,2
B(1,I)=0.0
DO 10 J=1,7
SUM=PCOEF(1,J,I,L)
CONST=SINX
DO 5 K=2,IP1
SUM=SUM+PCOEF(K,J,I,L)*CONST
5 CONST=CONST*SINX
10 A(J,I)=SUM
DO 20 J=8,13
SUM=PCOEF(1,J,I,L)
CONST=SINX
DO 15 K=2,IP1
SUM=SUM+PCOEF(K,J,I,L)*CONST
15 CONST=CONST*SINX
20 B(J-6,I)=SUM
CON2=HLR
TOT=A(1,I)
DO 25 J=2,7
TOT=TOT+A(J,I)*COS(CON2)+B(J,I)*SIN(CON2)
25 CON2=CON2+HLR
30 HS(I,L)=TOT
35 XHMAX(L)=((SN-100.0)*HS(2,L)+(200.0-SN)*HS(1,L))/100.0
COSTH=COS(.0172042*(D+8))
HMAX=XHMAX(1)*(0.5+0.565*COSTH)+XHMAX(2)*(0.5-0.565*COSTH)
RETURN
END
```